CHAPTER 2: *IN SITU* OXYGEN ISOTOPE GEOCHEMISTRY BY ION MICROPROBE

John W. Valley & Noriko T. Kita,
WiscSIMS Laboratory
Department of Geology and Geophysics
University of Wisconsin
Madison, WI 53706 U.S.A.
valley@geology.wisc.edu

INTRODUCTION

High precision and accuracy with *in situ* analysis has been a "holy grail" for generations of stable isotope geochemists who employed a range of strategies for separation of heterogeneous samples and for interpretation of data from mixed samples. However, *in situ* techniques have in the past suffered from relatively poor precision and accuracy. Recent advances by ion microprobe have improved precision and accuracy, and make these time-consuming, uncertain approaches unnecessary. *In situ* analyses can be correlated with textures and imaging, offering the promise of new and fundamental information about patterns of isotope distribution.

The importance of stable isotope geochemistry is well established in many disciplines (see Clark and Fritz 1997, Griffiths 1998, Kendall & McDonnell 1998, Criss 1999, Ambrose & Katzenberg 2000, Valley and Cole 2001, Unkovich *et al*. 2001, Hoefs 2004, De Groot 2004, Johnson *et al*. 2004, Sharp 2007). Many seminal studies are included in these reviews. However, the conventional analytical techniques employed in these studies require homogenization of bulk samples that are larger than the scale of zonation in a wide range of samples. Important information has been lost by analysis of powders.

The ion microprobe's ability to analyze isotope ratios with high precision and accuracy from micrometre-scale spots in natural samples (as well as experimental products) *in situ* from a microscope slide reduces sample size by factors of ten thousand to one billion, and allows isotopic data to be correlated with other geochemical information in spatial context with textures and imaging (Fig. 2-1). The accuracy of these data now approaches that of conventional techniques that require far larger samples. These advantages are revolutionizing stable isotope geochemistry, just as the electron microprobe revolutionized *in situ* chemical analysis and the SHRIMP (ion probe) revolutionized zircon geochronology (Ireland 1995, Hinton *et al*. 1995, Ireland & Williams 2003).

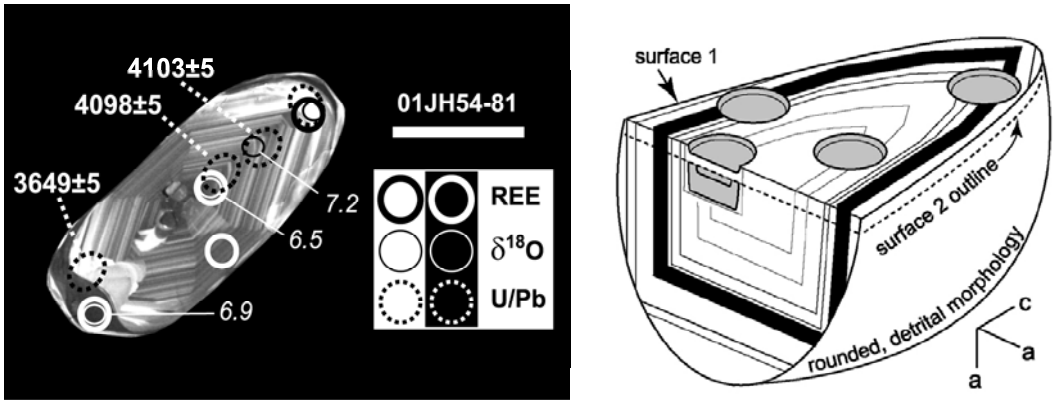

FIG. 2-1. Correlated ion microprobe analysis of $\delta^{18}O$, U-Pb, and trace elements in zircon. **Left:** CL image of a detrital zircon from the Jack Hills metaconglomerate, Australia, showing a concentrically zoned igneous core dated at 4.1 Ga and thin overgrowths that are younger than 3.7 Ga. Analysis pit locations are shown for $\delta^{18}O$, U-Pb, and REEs. Scale bar = 100 μm. **Right:** Cartoon of a zoned detrital zircon showing a strategy for three successive analyses from a domain <20 μm in diameter: U-Pb (surface 1), $\delta^{18}O$, and trace elements (surface 2, after repolishing). Note that zoning is finer than spot size; sub-μm analysis will be discussed below (from Cavosie *et al.* 2006).

Mineralogical Association of Canada Short Course 41, Toronto, May 2009, p. 19-63

This chapter discusses procedures for high precision and accuracy of ion microprobe analysis of oxygen isotope ratios, and reviews recent studies that have applied these techniques to Earth Science. It is beyond the scope of this chapter to discuss all of the earlier pioneering studies; additional references can be found in papers that are cited. Strategies for ion microprobe analysis vary according to trade-offs in instrument tuning, sample preparation, and analysis. Because of improved data quality at smaller spot sizes, applications discussed here emphasize results from the newest large-radius, multi-collector ion microprobe, IMS1280. These studies provide detailed records of zonation in samples including diagenetic cements, speleothems, foraminifera, otoliths, gems, zircon grains, and meteorites, which were previously inaccessible to analysis. In many cases, understanding the true scale and patterns of isotope variation provides new insight for processes as varied as diagenesis, paleoclimate, biomineralization, metamorphism, magma genesis, crustal evolution, and formation of the Solar System.

HIGH PRECISION *IN SITU* ANALYSIS OF OXYGEN ISOTOPE RATIOS

Analytical precision for analysis of $\delta^{18}O$ by ion microprobe has improved steadily over the past three decades due to development of new instrumentation and refinements in technique (Fig. 2-2): ±20‰ (2SD, IMS3f without electron-flood gun); ±2‰ (IMS4f, high mass resolution); ±1.0‰ (IMS4f, high energy offset); ± 0.6‰ (IMS1270, multi-collector); ± 0.3‰ (IMS1280) (Giletti *et al.* 1978, McKeegan 1987, Valley & Graham 1991, Hervig *et al.* 1992, Riciputi & Patterson 1994, Cavosie *et al.* 2005, Kelly *et al.* 2007, Kita *et al.* 2009). Precision is emphasized in this section before discussion of accuracy. Accuracy equal to precision can be attained in many samples by detailed monitoring of instrumental conditions, careful sample preparation, and use of appropriate standards. While ion microprobe precision for $\delta^{18}O$ has improved by an order of magnitude every 15 years since the first analyses were published (Giletti *et al.* 1978), and sample sizes have been reduced, this progress is reaching a plateau. Recent studies come close to the physical limit imposed by the number of atoms in spot sizes of 10 μm and below (Page *et al.* 2007a).

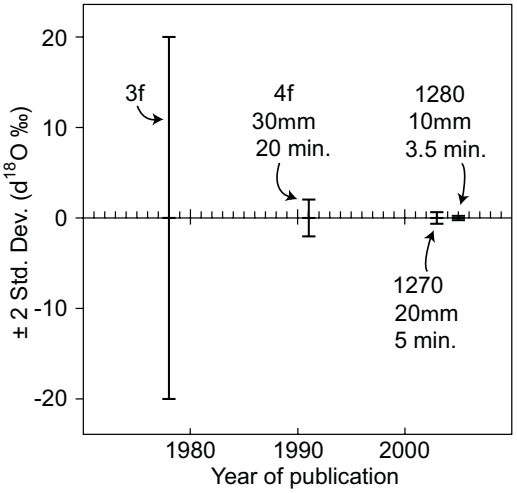

FIG. 2-2. The precision of ion microprobe analyses for $\delta^{18}O$ has improved from ±20‰ in 1978 to ±0.3‰ (2 SD) today due to the development of new instruments (IMS3f to IMS1280) and refinements in technique (see text). At the same time, accuracy, spot size, and speed of analysis have also improved.

The following figures present large data sets for $\delta^{18}O$ from 10, 3, and <1-μm diameter spots, and $\delta^{17}O$ from 15, 2, and 1 μm spots. A number of factors affect data quality. In general, there is a trade-off of precision, which may be limited by the number of ions counted, and spot size.

Figure 2-3 shows $\delta^{18}O$ values from 3.5-minute analyses of 10 μm diameter spots in quartz. Over 650 spot analyses were made in 48 hours from 12 different sample mounts. A quartz standard was analyzed four times every 10-20 sample spots. The sample data vary by over 40‰, revealing exciting trends in magmatic hydrothermal systems, but the standard data are constant with precision of ±0.3‰ (2 SD, standard deviation; ±0.02‰, 2 SE, standard error, N = 173). The repeated analysis of an appropriate standard and a well-prepared sample ensures that accuracy matches spot-to-spot precision.

Careful tuning of the instrument, sample preparation, and standardization are critical for obtaining results such as shown in Figure 2-3. Pertinent analytical details will be discussed in subsequent sections of this paper. Attention to detail pays off and it is important to note that not all ion microprobe data are of comparable quality. Procedures for reporting accuracy and precision vary, and the interested readers may want to evaluate precision and accuracy for themselves from the published tables of standard data. In general, this requires that standard analyses bracket samples and that data be published in chronological order of analysis.

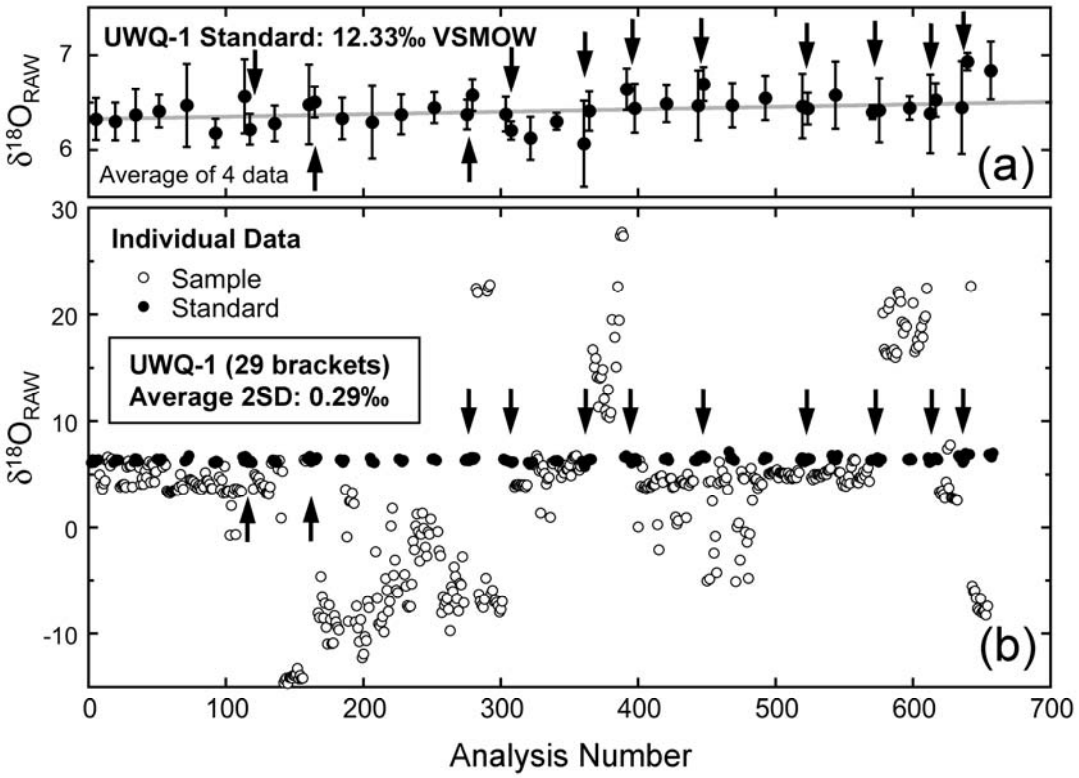

FIG. 2-3. Results from 48 hours of analysis of $\delta^{18}O$ in quartz from 12 sample mounts by IMS1280 at WiscSIMS. Data are from Rusk *et al.* (2007). The 658 spots analyzed include 173 from the quartz standard, UWQ-1 (solid dots). Grains of standard were cast in each mount. **(a)** Average value with 2 SD error bars for each group of 4 bracketing standard analyses. Arrows indicate sample changes. The spot-to-spot precision for each group of 8 standard analyses varies from 0.14 to 0.38 and averages 0.29‰ (2 SD; ±0.10‰ 2SE). **(b)** The 485 analyses of hydrothermal quartz samples (open circles) vary by 40‰ (from Kita *et al.* 2009).

Analysis of $\delta^{17}O$ in oxygen three-isotope studies is more challenging because of the ~5x lower natural abundance of ^{17}O than ^{18}O. Figure 2-4 shows $\delta^{18}O$ and $\delta^{17}O$ in an olivine standard, and samples of meteoritic olivine measured from 15 μm spots using an IMS1280 and three Faraday Cup detectors (Kita *et al.* 2008). Sample analyses are bracketed by analyses of standard in the same mount. The average values of precision for each group of eight bracketing standard analyses are 0.31‰ and 0.37‰ (2 SD) for $\delta^{18}O$ and $\delta^{17}O$, respectively (Kita *et al.* 2009).

Spot size is variable for ion microprobe analysis. The Cs beam, used for oxygen isotopes, can be focused to a diameter of 250 nm on the IMS1280 instrument, and 50 nm on the nanoSIMS. However, the primary beam current and the resulting signal varies with spot size, and the beam is generally defocused to a larger diameter in order to generate more secondary ions for analysis. At WiscSIMS, typical values for the 2 SD reproducibility of $\delta^{18}O$ for multiple analyses of a homogeneous material are ± 0.3‰ at 10 μm (Fig. 2-3), ± 0.7‰ at 3 μm (Fig. 2-5), and ± 2‰ at <1 μm (Fig. 2-6).

MULTI-COLLECTOR ION MICROPROBES

A number of ion microprobe instruments have been used for stable isotope analysis. Early workers used single-collector (detector) instruments such as the IMS4f. More recently, multicollector instruments have demonstrated key advantages. At present, the IMS1270/1280 series has proven best for the high precision needed for natural isotope abundances and sub-permil accuracy, but the multicollector nanoSIMS and SHRIMP II have also been employed, as have single channel instruments.

The first commercial ion microprobe multi-collector system was installed on an IMS1270 in 1998. This development led to major improvements in stable isotope performance, analogous to the

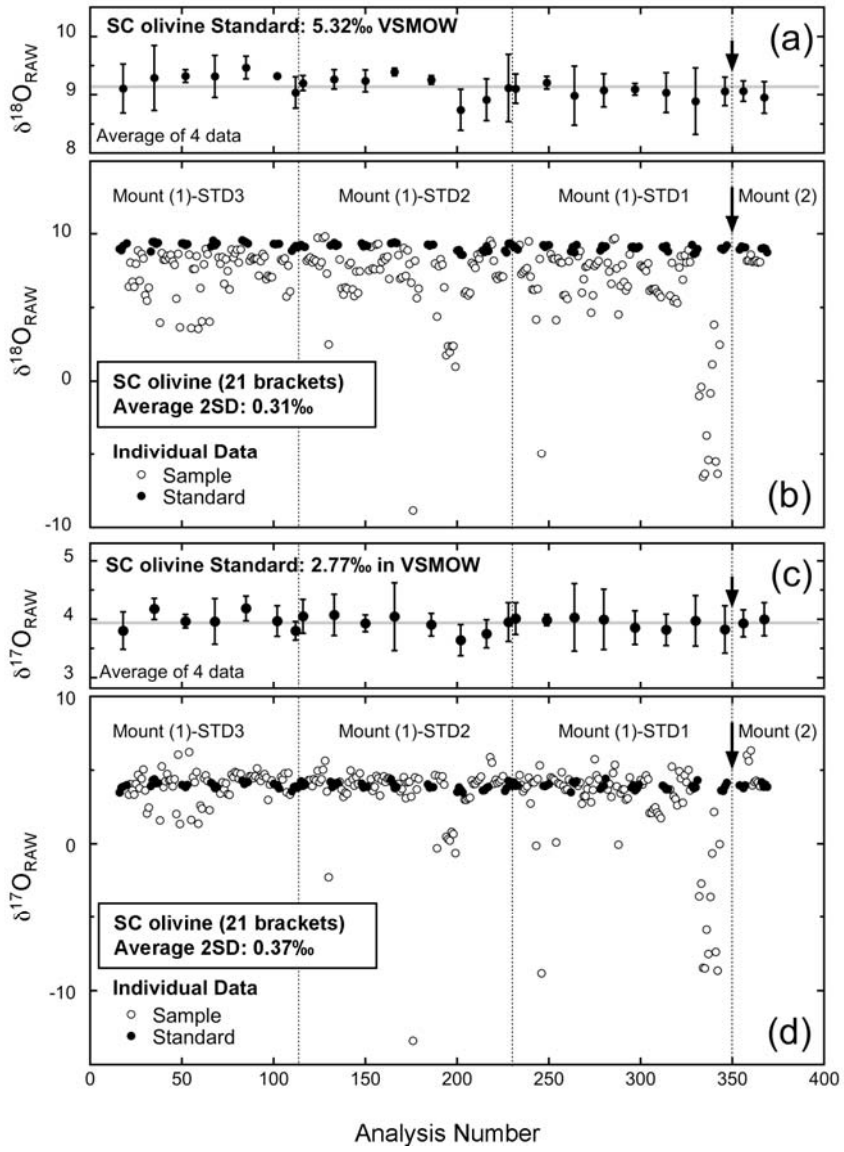

FIG. 2-4. Analyses of $\delta^{18}O$ and $\delta^{17}O$ in San Carlos olivine standard (SC, solid dots) and meteoritic olivine (open circles) using an IMS1280 at WiscSIMS (uncorrected data, Kita *et al.* 2008). 343 analyses were made in 56 hours including 103 standards.
(a) Average $\delta^{18}O$ and 2 SD values of groups of four standard analyses.
(b) Values of $\delta^{18}O$ for samples and standards.
(c) Average $\delta^{17}O$ and 2 SD values of each group of four standard analyses.
(d) Values of $\delta^{17}O$ for samples and standards.
Arrows indicate sample change. The average values of 2 SD for each group of eight bracketing standard analyses are 0.31‰ and 0.37‰ for $\delta^{18}O$ and $\delta^{17}O$, respectively (error bars in (a) and (c) are 2 SD) (from Kita *et al.* 2009).

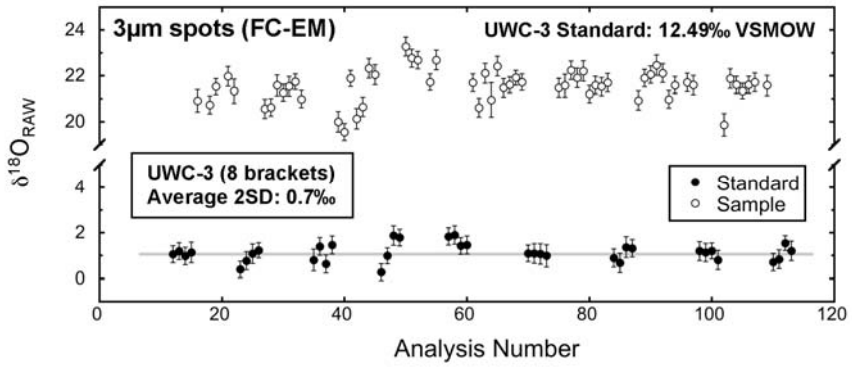

FIG. 2-5. Analyses of $\delta^{18}O$ in single foraminifera (open circles) and calcite standard, UWC-3 (solid dots), with a 3 μm diameter spot at WiscSIMS. Data are from Kozdon *et al.* (2009). A total of 94 analyses including 36 standard analyses were made in 48 hours. The average value of 2 SD for bracketing standard analyses is 0.7‰ (from Kita *et al.* 2009).

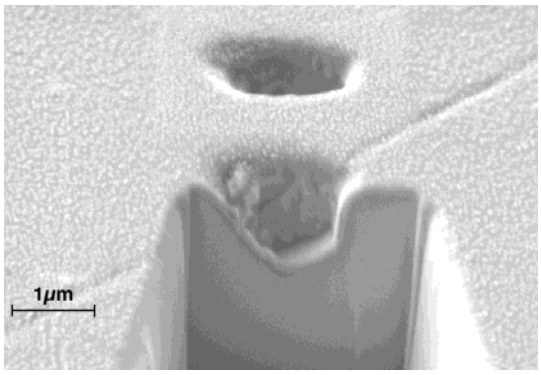

FIG. 2-6. SEM view of sub-micron pits from analysis of $\delta^{18}O$ in zircon (see Fig. 2-28). The pit in foreground was dissected by FIB (focused ion beam) revealing that dimensions are ~1 x 0.5 x 1 μm. Volume is ~ 0.5 μm^3 and weight is ~10^{-12} g per analysis (*vs*. 10^{-2}–10^{-3} g for conventional analyses). Spot-to-spot precision is degraded to ~2‰ (2 SD) for these analyses due to small sample size (from Page *et al.* 2007a).

advent of the double collector gas-source mass-spectrometer (Nier 1947). On an ion microprobe, simultaneous analysis of all isotopes of interest has many advantages including normalization of beam instability and drift, more rapid analysis, and efficient use of samples. The IMS1270/1280 multicollector system typically has a total of 11 detectors: 10 Electron Multipliers (EM) and Faraday Cups (FC), and a channel plate (Fig. 2-7). There is a trade-off in choice of EM *versus* FC detector. A FC is favored at high count rates where the relatively high background is not important. An EM has a much lower background signal, but is limited to lower count rates by deadtime, quasi-simultaneous arrivals (QSA), and aging. In practice, up to 5 detectors can be used simultaneously. The maximum dispersion is 17.3% in mass, sufficient for ^{6}Li and ^{7}Li. The minimum spacing of detectors permits adjacent isotopes of Pb to be analyzed. Significantly greater mass dispersion exists in nanoSIMS instruments offering the potential to analyze multiple isotope systems simultaneously (*i.e.*, C and O), but this requires compromises; such data are less accurate, but may be useful in certain studies.

For oxygen isotopes, the dynamic range problem (*i.e.*, $^{18}O/^{16}O$ ~1/500, $^{17}O/^{16}O$ ~1/2500) is solved by IMS1280 using either: 1) 3 FCs with high count rates (>10^6 cps) and 10 μm spots; or 2) for smaller spots with low count rates, sensitive, low background EMs for minor isotopes (^{17}O and ^{18}O) and a high count rate FC for the major isotope (^{16}O). Multiple collectors permit count rates of >10^9 cps for ^{16}O (by FC) such that counting precision of 0.1‰ for ^{18}O that takes many hours with a single EM (<2000 cps) is obtained in a few minutes (>10^6 cps). The use of 3 FCs avoids many difficulties associated with EMs (*e.g.*, deadtime, asymmetric pulse height distribution, focusing on the first dynode, aging of the detector, and QSA; Slodzian *et al*. 2001, Slodzian 2004, Schuhmacher *et al.* 2004), but the use of EMs is necessary for smaller spot size, or for analysis of minor or trace isotopes.

IMS1280

The IMS1280 features many improvements to the pioneering 1270 design that led to better precision and accuracy of isotope ratios, including: new primary beam ion optics; direct measurement of primary beam current to permit better correction of QSA (Slodzian *et al*. 2001, Slodzian 2004); automatic centering of the secondary beam to correct for small variability in sample geometry; NMR magnet control with long-term stability; control of stray magnetic fields; and a six-sample airlock chamber. Many of these features are available as upgrades and have been installed on earlier 1270 instruments.

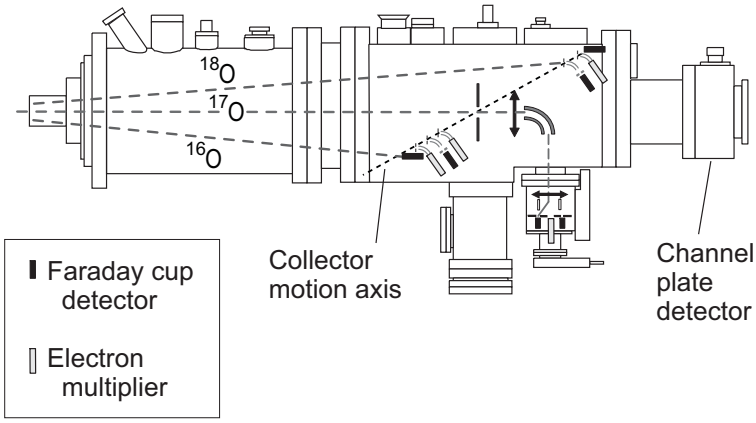

FIG. 2-7. The IMS1280 multicollector block at WiscSIMS has 11 detectors (4 electron multipliers, 6 Faraday cups, and a channel plate) including a fixed axial detector system and five independently movable trolleys. Alignment is shown for simultaneous analysis of three oxygen isotopes employing 3 FCs.

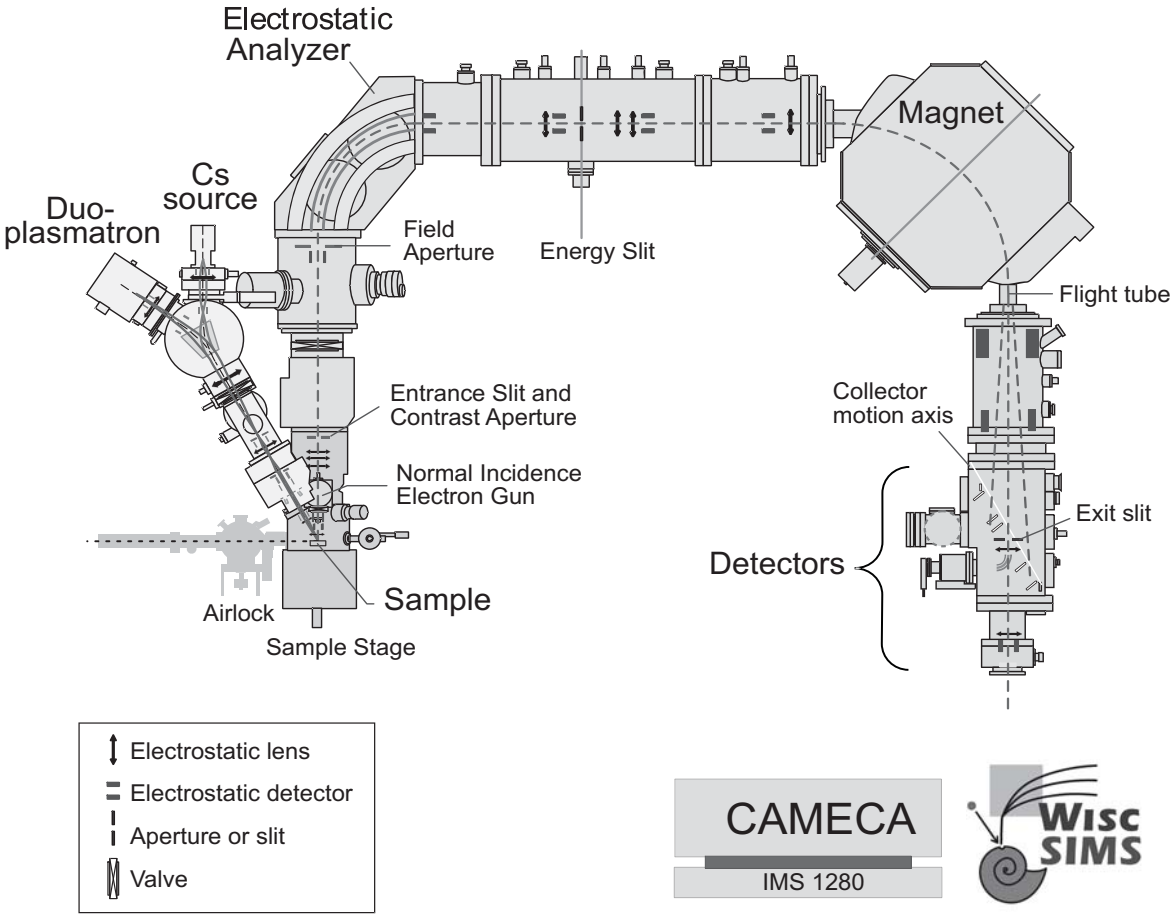

*FIG. 2-8. Schematic of the IMS1280, large radius, high resolution, multicollecting ion microprobe/ SIMS. For color version, see http://www.mineralogicalassociation.ca/index.php?p=160

Figure 2-8 shows a simplified diagram of the IMS1280. This instrument is variously referred to as an ion microprobe, a secondary-ion mass spectrometer (SIMS), or a double-focusing mass spectrometer. The name Ion Microprobe refers to the primary ion beam that is focused to a small spot on the sample surface. The primary beam is selected for efficient sputtering and ionization of the sample. For analysis of oxygen isotopes and many other elements, the Cs-source is used ($^{133}Cs^{+}$) necessitating charge compensation by conductive coatings and a normal incidence electron flood gun. Alternatively, the Duoplasmatron generates primary ions of $^{16}O^{+}$ or $^{16}O^{-}$, and other sources are available. The ion microprobe analyzes secondary ions that are sputtered from the sample surface and thus is one type of Secondary-Ion Mass Spectrometer. Some SIMS instruments have larger primary beam spots and hence are not ion microprobes. The secondary ions in a Double-Focusing Mass Spectrometer are sorted by the sector magnet according to mass and charge [turning radius is proportional to $(M/e)^{0.5}$], and at the same time focused in kinetic energy by the electrostatic analyzer such that high mass-resolving power can be obtained for secondary ions that are sputtered with a significant range of initial kinetic energy.

Instrument Bias and Use of Standards

Attaining high accuracy and precision by ion microprobe/SIMS requires the careful use of appropriate standards. SIMS analysis causes bias in isotope ratio and elemental composition. The bias (sometimes called instrumental mass fractionation or IMF) originates during the sputtering, transmission, and detection of secondary ions, but the details of this process are not well understood (Slodzian 1980, 1982, 2004, Lorin *et al.* 1981, Shimizu & Hart 1982, Gnaser & Hutcheon 1988, Zinner 1989, Ireland 1995). The magnitude of bias varies with the chemistry and crystal structure of the

target. It has been shown that bias also varies with crystal orientation for magnetite (Lyon *et al.* 1998, Huberty *et al.* 2009). This complication has been ruled out for many minerals by analysis of multiple grains of a homogeneous sample in known (or random) orientations. However, many minerals have not yet been tested (see below). To date, there is no theoretical basis upon which to make a correction for bias, as exists, for instance, for electron microprobe data. For some minerals, the magnitude of bias for $\delta^{18}O$ by IMS1270/1280 operated at higher mass resolution ($M/\Delta M = 2500$, Kita *et al.* 2009) is more than 10 times smaller than for IMS4f instruments operated at high energy offset (Hervig *et al.* 1992, Riciputi & Patterson 1994, Eiler *et al.* 1997, Valley *et al.* 1998, Riciputi *et al.* 1998). In all cases, accurate and precise analysis requires bracketing sample analyses with appropriate standards.

The best accuracy for stable isotope analysis is obtained for minerals showing limited solid solution where the standard is well calibrated, homogeneous, and has the same chemical composition and crystal structure as the sample. At WiscSIMS, this is routine for minerals such as quartz, calcite, and zircon. The recommended procedure is to place grains of standard in the center of each sample mount (Fig. 2-9, inset), and to repeatedly analyze the standard, bracketing sample data. This achieves two goals, calibration of instrument bias, and monitoring any drift or change in instrument parameters during the course of analysis. Typically, monitoring drift entails four analyses of standards before and after each group of 10–20 sample analyses. Standard data bracket all samples and comprise 25% or more of all analyses. This large effort is justified by the high precision that results. As seen in Figure 2-3 for 658 consecutive analyses of quartz, the standard data (solid dots) are homogeneous on the first 11 sample mounts (~600 analyses over 44 hours), but shift up by 0.47‰ for the last sample mount. This 0.47‰ difference is statistically significant at over 9 times the standard error for groups of 8 standard analyses (2 SD = 0.29; $SE = SD/N^{0.5}$; $2\ SE = 0.29‰/8^{0.5} = 0.1‰$, N=8). Thus, repeated standardization can detect subtle changes that would otherwise go unnoticed. Such changes can occur, even after long periods of stable operation, due to a number of instrumental factors including variability of tuning, small changes in room or cooling water temperature (<1°C), baseline drift of the ^{18}O FC, or real differences among different mounts of the standard. Improvement of data can result from correcting to individual groups of 8 bracketing standard analyses rather than the global average for an entire analysis session, although the two procedures often lead to identical results.

Minerals that show a range of solid solution present special constraints as no single standard will be appropriate. For oxygen isotope ratios, a number of approximate empirical correlations have been demonstrated for large groups of minerals, but no master variable has been found to correlate closely to bias either by IMS4f with a single EM detector at high energy offset (Hervig *et al.* 1992, Riciputi & Patterson 1994, Eiler *et al.* 1997, Riciputi *et al.* 1998) or by IMS1280 with multiple FC detectors at low energy offset and high MRP (Fig. 2-10A). Thus, accurate analysis requires a suite of standards that spans the composition range of samples. The elemental composition and mineral identification of each ion microprobe spot should be known to determine the bias correction.

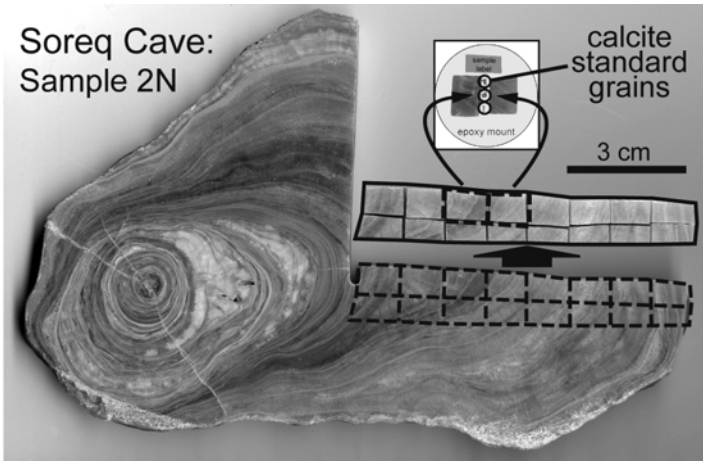

*FIG. 2-9. Annually banded speleothem from Soreq Cave, Israel dated by U-series geochronology to span 22.0–1.3 ka (Bar-Matthews *et al.* 2003). Long dimension = 168 mm. Inset: 10 mm-size chips cut from speleothem; two pieces were cast with calcite standard in 25 mm diameter epoxy mount for SIMS analysis. This mounting geometry allows efficient analysis of traverses along each sample piece with sample analyses regularly bracketed by standards. Note that all analysis spots are within 5 mm of the center of the mount (from Ian Orland).

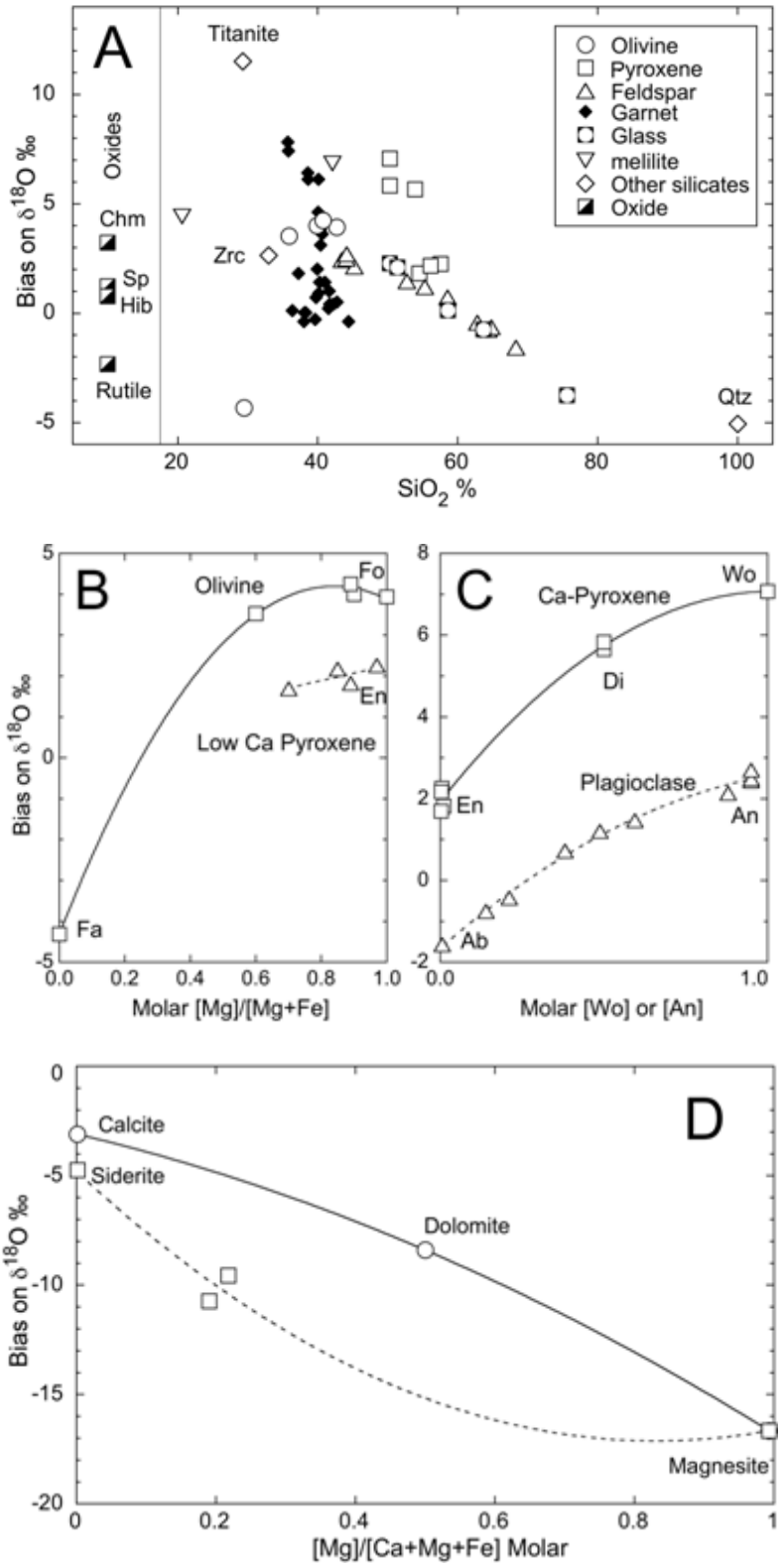

FIG. 2-10. Instrument bias for *in situ* analysis of oxygen isotope ratio by IMS1280 using dual FC detectors at WiscSIMS.
(A) Silicates and oxides plotted *vs*. wt.% SiO_2.
(B) Olivine and low Ca pyroxene *vs*. X_{Mg}.
(C) Pyroxene and plagioclase *vs*. X_{Ca}.
(D) Carbonates *vs*. X_{Mg} for Ca-Mg (solid line) and Fe-Mg (dashes).

Bias varies by up to 25‰ depending on chemical composition and crystal structure, and no master variable correlates well with bias. Accurate analysis is possible by construction of working curves for binary solid solutions within mineral groups such as plagioclase, carbonate minerals, olivine, or pyroxene. Sources of data: Kita *et al.* 2006, 2007b, 2009, Valley *et al.* 2007, Page *et al.* 2009.

The correlation of bias to mineral chemistry is considerably more accurate and precise if standards and samples all come from a binary solid solution within the same group of minerals such as the carbonate group (Fig. 2-10D; Valley *et al.* 1997, 2007, Eiler *et al.* 2002, Bowman *et al.* 2009); olivine or pyroxene (Fig. 2-10B,C; Kita *et al.* 2006, Downes *et al.* 2008); plagioclase (Fig. 2-10C; Kita *et al.* 2007b); garnet (Fig. 2-10A; Vielzeuf *et al.* 2005a, Lancaster *et al.* 2009, Page *et al.* 2009); or glasses (Fig. 2-10A; Eiler *et al.* 1998, 2007, Kita *et al.* 2007a,b). While Figure 2-10 shows nonlinear variations of bias up to 8‰ for $\delta^{18}O$ in silicates (olivine or garnet) and 14‰ for Ca-Mg carbonate, working curves fit the data well when multiple standards are available (*e.g.*, plagioclase, Fig. 2-10C). Thus, precise and accurate corrections of raw SIMS data can be achieved if sufficiently different standards are calibrated.

Page *et al.* (2009) expanded the sample set of Vielzeuf *et al.* (2005a) from 12 to 27 garnet compositions (Ca, Mg, Mn, Fe^{2+}, Al, Fe^{3+}) using an IMS1280 and standard operating procedures at WiscSIMS (see also Lancaster *et al.* 2009). They found that bias varies systematically by about 2‰ among the Mg, Mn, Fe^{2+} garnet compositions, but that Ca solid solution (grossular-andradite) extends the range of bias to 8‰. Fig. 2-10 shows that many Ca minerals have higher bias within their group (anorthite, calcite, wollastonite, and titanite). For garnet, Page *et al.* (2009) recommend mounting of a single garnet standard such as UWG-2 in each sample mount and constructing a working curve based on calibration of a group of garnet standards with compositions bracketing the unknowns. If the appropriate garnet standards are analyzed along with UWG-2 in the same analytical session as samples to calibrate bias, then the accuracy of this approach is indicated to be better than ±0.4‰, which is comparable to analytical precision.

Accuracy vs. Precision

It is important to distinguish accuracy from precision (Fig. 2-11). Confusion arises because of different definitions of "precision" and "accuracy". A critical observer may want to examine the data. In oxygen isotope geochemistry, isotope ratios are expressed on the $\delta^{18}O$-scale, normalized to V-SMOW, Vienna Standard Mean Ocean Water, or V-PDB, Peedee Belemnite (see O'Neil 1986). Accuracy is thus not expressed in absolute terms, but is actually the precision of comparisons to a standard. While the absolute abundances of oxygen

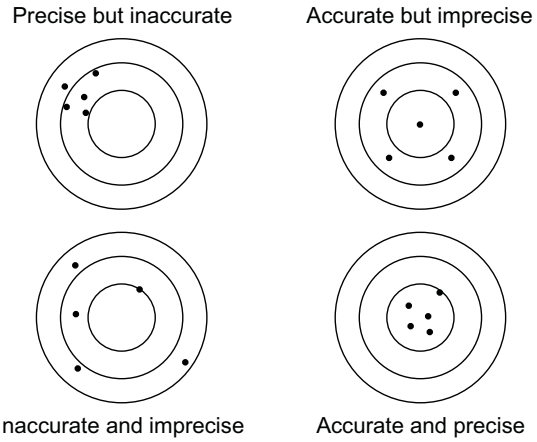

FIG. 2-11. Accuracy *vs*. precision.

isotopes in V-SMOW (water) are well known, they do not necessarily factor into the determination of $\delta^{18}O$. For ion microprobe analysis, the comparison becomes less direct as secondary standards must be calibrated by "conventional" techniques, typically fluorination or acid reaction combined with gas-source mass-spectrometry. The statistics of stable isotope analysis by SIMS are treated in detail by Fitzsimons *et al.* (2000).

The precision of SIMS analysis is generally limited by Poisson counting statistics (at low count rates, detector background may be a limitation). Thus, one standard deviation for a single analysis will not be better than $\pm N^{0.5}$ for N total counts; precision of ± 1‰ requires counting 10^6 atoms of ^{18}O and ± 0.1‰ requires 10^8 atoms. For $\delta^{18}O$, the number of ^{16}O atoms is also a factor, but with simultaneous analysis the total counts for ^{16}O are ~500x greater than for ^{18}O, and the uncertainty is much smaller and commonly ignored. Of course, a number of other factors can affect precision. Analytical error is more reliably evaluated from actual measurements than by theory.

Precision can be expressed as either the standard deviation of the mean (SD) or the standard error of the mean (SE). Each statistic has its appropriate use. The standard deviation describes the distribution of data about the mean. This is a reasonable proxy for the quality of a single spot-analysis by SIMS. The standard error is calculated as $SE = (SD/N^{0.5})$ where N is the number of observations. Thus, values of SE, in contrast to SD, typically get smaller as one analyzes more spots on a standard. SE is an indication of how well the mean for a population of data points is known and the likelihood that an additional analysis will change the mean. However, the SE of a group of

standard analyses is not a good measure of the quality of a single analysis.

As a further complication, both "internal" and "external" precision may be reported. For SIMS $\delta^{18}O$ measurements, the data for both ^{16}O and ^{18}O in a single spot are subdivided into a series of *n* cycles, and internal precision is based on the SE of the *n* comparisons. If a series of spots is analyzed, the external precision is the SD for those numbers. It is commonly thought that the external precision of multiple spot analyses should approach, but not be better than the internal precision. However, systematic errors can change this. For instance, the measured $^{18}O/^{16}O$ ratio in carbonate can vary significantly with depth during a single spot analysis, leading to a high internal error. However, this depth effect is reproducible from spot to spot and it is common to obtain external precision that is significantly better than would be predicted from internal precision. For this reason, internal precision may not be a useful measure of data quality. The mean square of weighted deviations (MSWD) is another measure, often used in geochronology that compares the measured SD of a data set to that predicted from the size of the population. A value of 1 indicates that the measured values match the statistics for Gaussian distribution, however this also ignores correlated effects.

The simplest and most direct measure of analytical precision is based on the spot-to-spot reproducibility of multiple analyses of different spots on a homogeneous standard. Since sample analyses need to be bracketed by standards, this provides a repeated measure of data quality during the analysis session. Values can be reported at 1, 2, or 3 SD depending on the desired confidence level. The SE is appropriate only for comparison of average values of multiple analyses.

Crystal Orientation Effects

Crystal orientation effects on the sputtered ion yields of single crystals have been an active field of study for the last 50 years (Robinson & Oen 1963). Channeling takes place when the incident ion beam is parallel to low index directions in the crystal lattice resulting in a reduced probability of ion–atom collisions and thus a lower sputtered yield. Channeling effects have also been found to influence the angular distribution of sputtered particles along low index directions (Wehner 1956). Further, preferential ejection of the sputtered species along low index directions has been attributed to focusing collision sequences where the ejection of surface atoms is due to momentum transport to the surface along closest packed rows of atoms (Silsbee 1957).

Channeling of the primary ion beam along specific planes in the crystal lattice of a mineral has long been proposed as a possible influence on SIMS instrument bias for isotope ratios. Lyon *et al.* (1998) reported a correlation of measured oxygen isotope ratio and crystallographic orientation of magnetite during ion microprobe analysis by Isolab 54. Values of $\delta^{18}O$ varied up to 10‰ upon rotation of a single crystal about [111] through a range of 290°. Huberty *et al.* (2009) investigated the crystallographic effect on bias using an IMS1280 and a sample mount with individual fragments of magnetite in random orientations. Electron backscatter diffraction (EBSD) by SEM was employed to determine the orientation of each grain. By rotation of the mount in the sample holder, the full range of possible orientations could be analyzed. The maximum variation of bias is ~4‰ (*vs*. 10‰ for Isolab) showing that instrumental parameters are important to determine the magnitude of this effect. The smallest bias was obtained when the incident Cs beam was parallel to low index directions, especially along <*hk*0>. These results suggest that it may be possible to minimize the orientation effect further or to make a correction.

For many other minerals, analysis of standard grains in random orientation at WiscSIMS proves that the magnitude of the orientation effect is less than spot-to-spot precision. Minerals for which crystallographic effects on bias have been shown to be less than ±0.5‰ for $\delta^{18}O$ include quartz, K-Na-Ca-feldspar, Mg-Fe ortho- and clinopyroxene, wollastonite, Fe-Ca-Al-Mg-Mn garnet, Mg-Fe olivine, zircon, chromite, $MgAl_2O_4$ spinel, and Ca-Mg-Fe carbonate.

X–Y Effects

Standardization monitors precision and stability of the instrument, and can be the basis of a correction for bias, but there are additional effects and careful standardization alone does not necessarily guarantee accuracy. It has long been suspected that small differences in sample and standard geometry can be significant (*e.g.*, Valley *et al.* 1998, Treble *et al.* 2007, Whitehouse & Nemchin 2009, Kita *et al.* 2009). These differences, herein referred to as X–Y effects, cause minor deflections of the secondary beam and can change the bias in isotope ratio. The IMS1280 compensates

for such differences with a manual Z-focus and by automatically adjusting secondary beam deflectors (DTFA) at the beginning of each analysis. Formerly, this correction was made crudely by hand, but even the improved computer controlled correction is imperfect. X–Y effects degrade precision for samples that are too far from the focusing axis, that have an inclined surface, or that have differences in height such as commonly result from polishing relief. For this reason, standards are mounted at WiscSIMS in the center of each sample and high precision analyses are attempted only within 5 mm of the center of the 25 mm round sample mount. This minimizes X–Y effects to sub 0.3‰-levels for $\delta^{18}O$ (2 SD, Kita *et al.* 2009). Topographic effects are more problematic, especially in samples that vary in hardness.

Figure 2-12 shows zircon grain fragments with relief of ~30 μm that commonly results when hard minerals are cast in softer epoxy and polished. Relief is also common on polished surfaces of rocks containing soft or easily plucked minerals such as carbonates or phyllosilicates. Relief can be monitored by use of a white light profilometer, which rapidly measures the elevation of the sample surface at sub-μm scale. Kita *et al.* (2009) analyzed $\delta^{18}O$ in chips of the homogeneous zircon standard, KIM-5, after a series of polishing steps that systematically reduced the polishing relief. A well polished mount with relief less than one micron yielded spot-to-spot precision of 0.3‰ (2 SD). However, the same zircon grains with more relief yielded less precise and less accurate results. The sample shown in Figure 3-12 produced analytical uncertainties of up to ±3‰ and average values are shifted in $\delta^{18}O$ (Fig. 2-13). These effects may also impact depth profiles for $\delta^{18}O$ and such studies should be evaluated by profiles into homogeneous materials.

Analysis near grain boundaries

Grain boundaries are of special interest in geological studies of growth zoning, alteration, and diffusion (Valley 2001, Desbois *et al.* 2007, Kelly

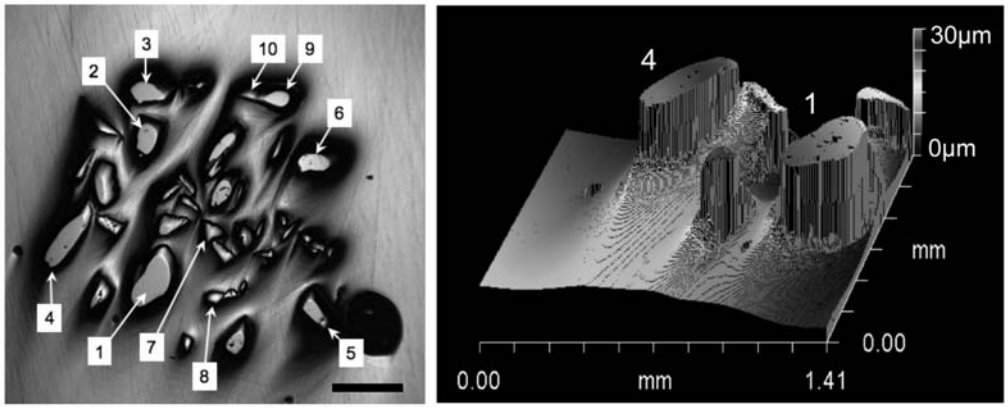

*FIG. 2-12. Zircon grains cast in epoxy showing smooth flat tops and ~30 micrometres of relief due to polishing. **Left:** Zircon grains in reflected light. (Scale = 500 μm). **Right:** Polishing relief measured by white light profilometer. Grains 1 and 4 are the same in both images (from Kita *et al.* 2009).

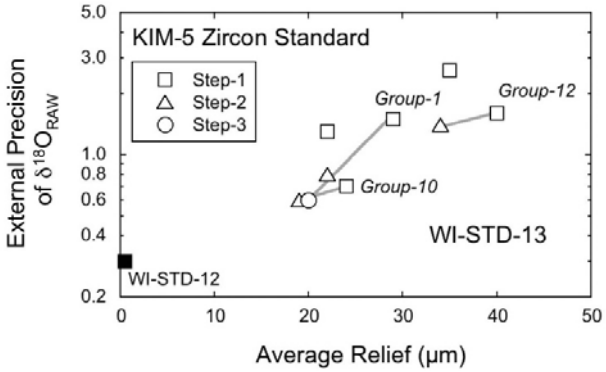

FIG. 2-13. Spot-to-spot reproducibility (2 SD) of SIMS measurements of $\delta^{18}O$ with 10 μm diameter spots in KIM-5 zircon standard grains. The amounts of polishing relief were reduced in three repolishing steps of the same grain mount, which has 13 groups of 100-500 μm chips of the KIM-5. Note that the reproducibility of analyses is shown on the Y-axis as a logarithmic scale. The filled square is from a second mount of KIM-5 with minimized relief (≤1 μm) analyzed during the same session (from Kita *et al.* 2009).

et al. 2007, Page *et al.* 2007a). However, the impact of relief on instrument bias is greatest for surfaces that are not normal to the secondary beam and especially near the edge of a grain. For many samples, reproducibility is improved by restricting analysis to the cores of grains. For studies of grain boundaries or objects that are too small to avoid regions close to the edge (Eiler *et al.* 2007, Bindeman *et al.* 2008, Kozdon *et al.* 2009) extra care should be taken to minimize relief. Figure 2-14 shows a grain of homogeneous diopside standard cast in epoxy and polished with a minimum of relief (< ~1 μm, Kita *et al.* 2009). Analyses of $\delta^{18}O$(raw) from within 20 μm of the grain boundary (average = 30.53 ± 0.09‰, 2 SE) are identical to analyses ~100 μm from the boundary (average = 30.58 ± 0.08‰) showing that there is no measurable effect for a smooth flat sample with low relief.

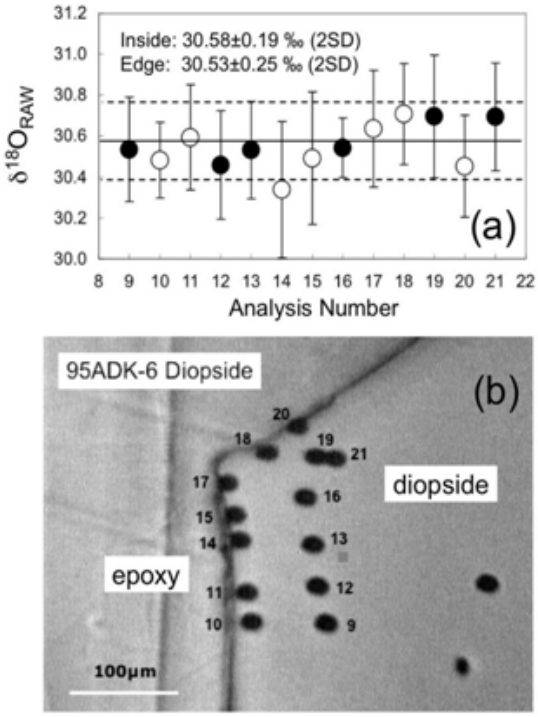

FIG. 2-14. Analyses of $\delta^{18}O$(raw) from the rim of homogeneous diopside, 95ADK-6, showing minimal polishing relief (< ~1 μm). **(a)** Analyses from within 20 μm of the nearest the grain boundary (open circles) and ~100 μm away (solid dots) are indistinguishable with spot-to-spot reproducibility of ±0.22‰ (2 SD) and 2 SE <0.09‰. **(b)** Reflected light image of the grain boundary between diopside and epoxy resin. The positions of the SIMS pits are shown with analysis number (from Kita *et al.* 2009).

QUARTZ OVERGROWTHS AND CEMENTS

Quartz and carbonate cements are ubiquitous in sedimentary rocks, control permeability in water and fossil fuel reservoirs, and record evidence of diagenetic history. Determining the timing, genesis, and geometry of cements is critical for extraction of natural resources, and for long-term sequestration of CO_2 and other industrial waste. There are several approaches to disaggregate quartz-cemented sandstone so that its constituent parts can be analyzed conventionally, however *in situ* analysis has shown such bulk samples to be mixtures not accurately reflecting the actual compositions (Graham *et al.* 1996). Ion microprobe analysis provides the means to resolve detrital grains *vs*. thin quartz overgrowth cements and to measure zoning among different generations of cement (Hervig *et al.* 1995, Graham *et al.* 1996, Williams *et al.* 1997a,b, Schieber *et al.* 2000, Lyon *et al.* 2000, Girard *et al.* 2001, Chen *et al.* 2001, Marchand *et al.* 2002, Alexandre *et al.* 2006, Kelly *et al.* 2007). Robert & Chaussidon (2006) correlated *in situ* analyses of $\delta^{18}O$ and $\delta^{30}Si$ in Precambrian chert to estimate Precambrian seawater temperatures. Carbonate cements are also well suited to *in situ* analysis (Riciputi *et al.* 1994, Mahon *et al.* 1998, Fayek *et al.* 2001); instrument bias can be corrected if chemical composition is determined for each spot by EMPA (Valley *et al.* 1997).

Mudstone

Mudstone is the most voluminous sedimentary rock type and the largest reservoir of high $\delta^{18}O$ material in the crust. The primary components are clay-size particles, including quartz that is generally thought to be detrital. Schieber *et al.* (2000) examined quartz silt grains from late Devonian shale of the eastern U.S. by CL imaging (Fig. 2-15) and ion microprobe analysis of $\delta^{18}O$. Grains texturally identified as detrital have $\delta^{18}O$ values averaging 9.4 ±3.0‰ (2 SD), consistent with igneous or metamorphic quartz (see also Aleon *et al.* 2002 for windblown aerosol quartz). Grains suggested to be quartz cement have much higher $\delta^{18}O$ values of 28.4 ± 2.0, confirming a low temperature diagenetic origin. Failure to recognize that up to 100% of the quartz in a mudstone formed *in situ* could lead to significant errors in interpretation of sedimentology, paleoproductivity, and biogeochemical cycling of silica (Schieber *et al.* 2000). Large amounts of high $\delta^{18}O$ diagenetic quartz would also suggest that variability of the $\delta^{18}O$ values of mudstones results in part from

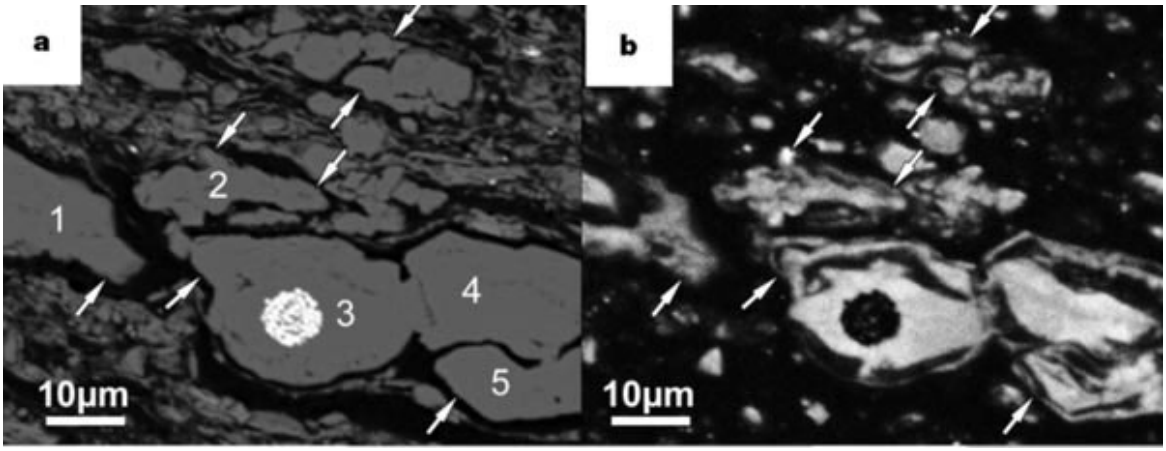

FIG. 2-15. Quartz grains in mudstone. **(a)** BSE image of quartz grains that are grey with uniform surfaces. **(b)** Cathodoluminescence (CL) image of the same area. Arrows show embayments and projections that suggest these quartz grains formed *in situ* as diagenetic cyst fills. Both larger and smaller grains show zoning in CL, further suggesting an *in situ* origin. Ion microprobe analysis shows that quartz silt has high $\delta^{18}O$ values, confirming the *in situ* diagenetic origin, and demonstrating almost complete absence of detrital quartz in this sample. Grain 3 contains a pyrite framboid (from Schieber *et al.* 2000).

differences in diagenesis and is not solely due to weathering.

St. Peter Sandstone

In the Ordovician St. Peter Sandstone of SW Wisconsin (Fig. 2-16), syntaxial quartz overgrowths are a minor component of poorly lithified rocks (Fig. 2-17). Because the lower Paleozoic sedimentary rocks of the Wisconsin Dome were never buried deeper than 1 km, the genesis of these optically continuous overgrowths has been uncertain (Graham *et al.* 1996, Chen *et al.* 2001). While pressure solution is extensive and causes thick overgrowths in samples that are deeply buried in the adjacent Michigan or Illinois basins, the shallow samples from SW Wisconsin show only trace evidence of pressure solution (arrow in Fig. 2-17) and other processes of overgrowth formation must be sought. It is widely thought that temperatures above 80°C are required to form

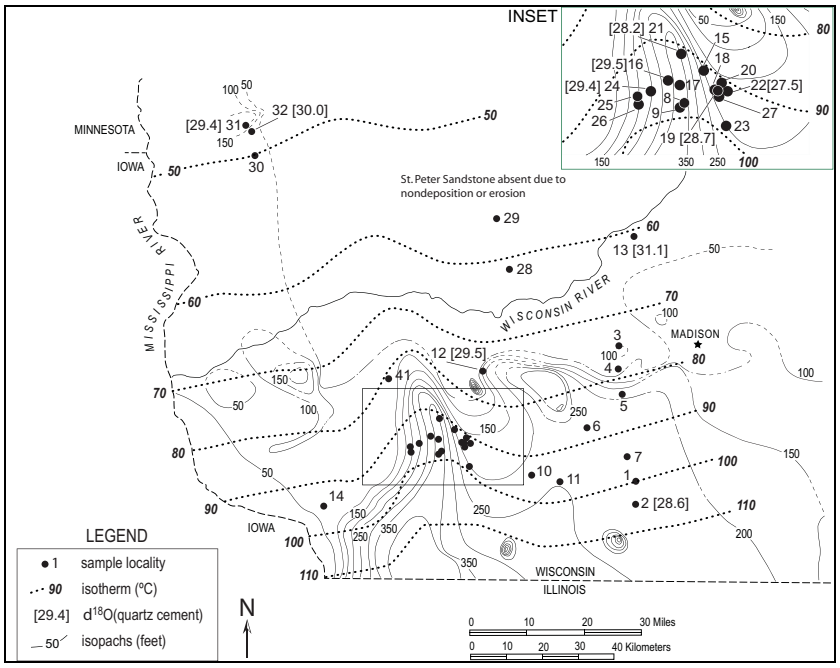

*FIG. 2-16. Isopachs of Ordovician St. Peter sandstone in SW Wisconsin. Deposits of the Upper Mississippi Valley Pb-Zn district are concentrated in dolomite above thicker sandstone domains, which are marked by the cluster of sample localities (filled dots) for which quartz overgrowths were studied by ion microprobe. Isotherms were modeled by Arnold *et al.* (1996) for heating of shallow sandstone by northward migrating Illinois Basin brines believed responsible for deposition of MVT base metals (from Kelly *et al.* 2007).

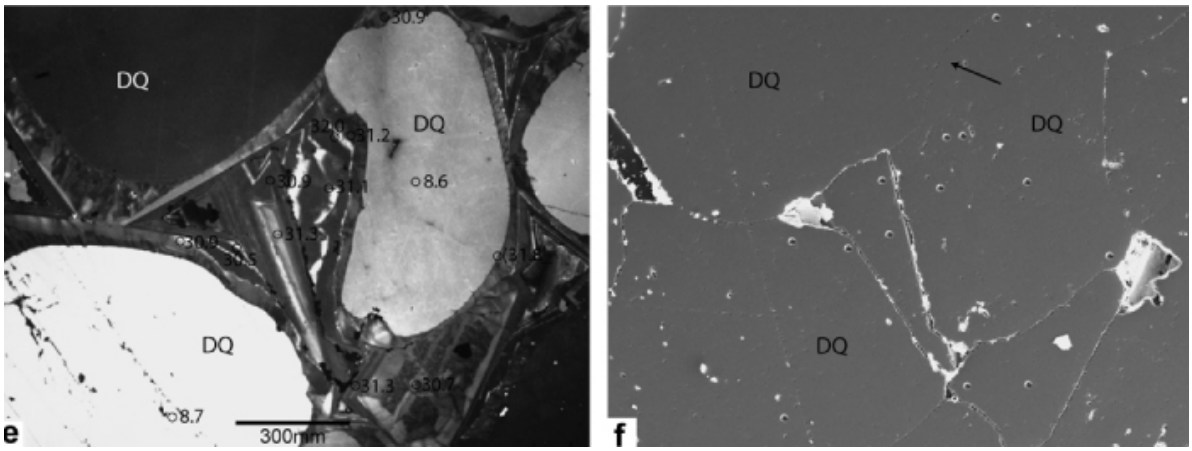

FIG. 2-17. Cathodoluminescence image (CL, left) showing complex quartz overgrowth textures and matching secondary electron images (SE, right). Ion microprobe pits are shown as circles in CL and as depressions in SE. DQ = cores of detrital quartz grains. Values of $\delta^{18}O$ are shown on CL image. Pore space is largely occluded by quartz cement as seen on right. An arrow points to minor pressure solution (compare SE and CL) that is not sufficient to generate cements. Scale bar = 300 μm (from Kelly *et al.* 2007).

quartz cement rather than opaline or fibrous silica, and burial depths in SW Wisconsin were never great enough to reach such temperatures at a normal geotherm. However, temperatures reached 100°C locally due to northward expulsion of ore-forming brines from the Illinois Basin into the Upper Mississippi Valley MVT–Pb–Zn District (Fig. 2-16). The St. Peter sandstone and underlying Cambrian sandstone units were aquifers for these brines and the ambient temperatures are estimated to have varied systematically from 110°C in the south to 50°C further north (Fig. 2-16, Arnold *et al.* 1996).

Did quartz overgrowths form during the MVT hydrothermal event and thus provide a record of regional fluid flow? Oxygen isotope ratios of the overgrowths provide a clear test of this hydrothermal model; variable temperatures of 110 to 50°C would cause $\delta^{18}O$(quartz) to change systematically by 9‰. Fig. 2-18 shows that $\delta^{18}O$ of detrital quartz cores (10.0 ±1.4‰, 1 SD) are distinct from quartz overgrowths (29.3±1.0‰, 1 SD) for 10 samples from SW Wisconsin. A small number of analysis pits with intermediate values were seen by post-analysis SEM imaging to have hit the boundaries of core and overgrowth. The constant value of $\delta^{18}O$(overgrowth) for samples distributed over a wide area indicates uniform conditions of

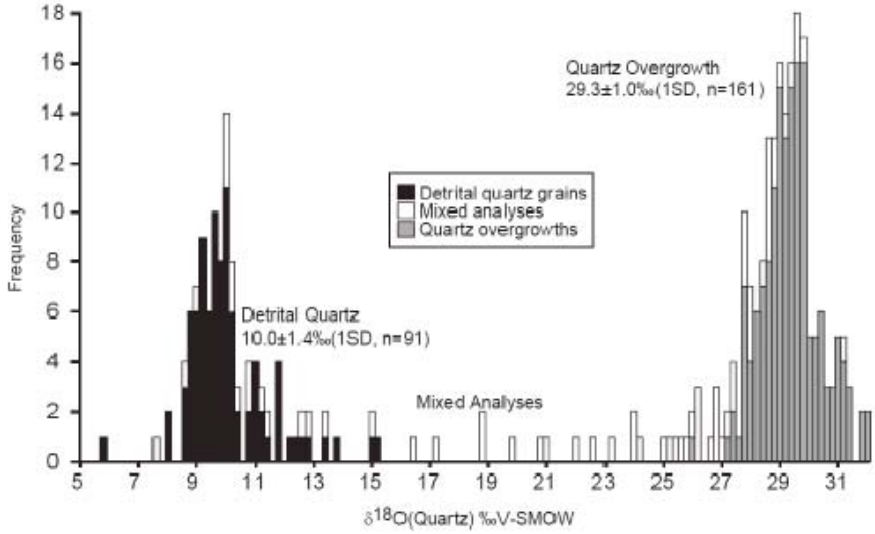

FIG. 2-18. Histogram showing the frequency of $\delta^{18}O$ for detrital quartz grains and quartz overgrowths in St. Peter sandstone measured from 10 μm spots at WiscSIMS. Mixed analyses hit overgrowth boundaries. All samples are from SW Wisconsin and SE Minnesota (from Kelly *et al.* 2007).

precipitation for all overgrowths and is not consistent with formation at variable temperatures during northward migration of Illinois Basin brines. Instead, the ion microprobe data suggest low temperature formation of overgrowths as silcrete. Apparently, syntaxial quartz can form at low temperatures (<40°C) in clean quartz arenite like the St. Peter Sandstone. In rocks containing clay minerals and glass, high degrees of supersaturation cause rapid precipitation of fibrous or hydrous silica. In contrast, clean quartz arenite is a nearly monomineralic rock, and slow equilibrium growth of quartz is possible at lower temperatures (Kelly *et al.* 2007).

FISH OTOLITHS

Fish otoliths are $CaCO_3$ ear stones, which record water conditions in daily growth bands (Fig. 2-19). Values of $\delta^{18}O$ respond to changes in temperature and indirectly to water chemistry (Campana 1999). Values of $\delta^{13}C$ are affected by temperature, diet, and dissolved inorganic carbonate, DIC. Weidel *et al.* (2007) studied 3 mm long otoliths from bluegill in Crampton Lake, Wisconsin, that underwent a 56-day experiment when $NaH^{13}CO_3$ was added to the lake to raise $\delta^{13}C$(DIC) in order to estimate the ratio of allochthonous to autochthonous nutrients (Pace *et al.* 2007). A rapid response of $\delta^{13}C$(otolith) to addition of this label shows that DIC is the dominant source of carbon in the otolith and not diet as previously thought (Weidel *et al.* 2007). In another study of nine larger otoliths from Pacific cod in the Gulf of Alaska, consistent 4‰ trends in $\delta^{18}O$ record a ~10-year migration history from shallow, warmer, possibly fresher (low $\delta^{18}O$), water to cold deeper water and back (Fig. 2-20). Thus, these otoliths are "flight recorders" of temperature and water composition through the life of the fish. Older otoliths at the same site have systematically higher "shallow water" $\delta^{18}O$ values consistent with lower temperatures during the Little Ice Age (A. Crowell & J. Valley, unpublished). The capability to measure such detailed stable isotope records presents as yet unexploited opportunities to decipher the provenance, migration history, diet, and age of fish, as well as paleoclimate.

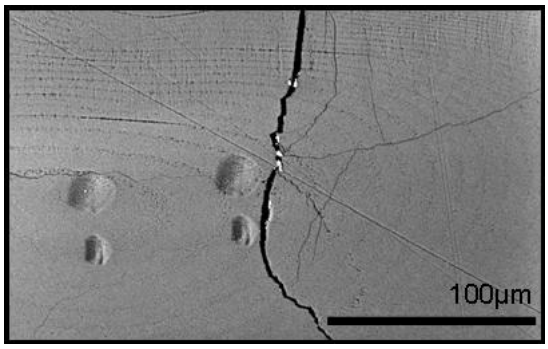

FIG. 2-19. SEM image of SIMS analysis pits for $\delta^{18}O$ (upper) and $\delta^{13}C$ (lower) in a Bluegill otolith from Crampton Lake, Wisconsin. Daily growth bands are resolved by single analyses (from Weidel *et al.* 2007).

FORAMINIFERA

Foraminifera are important calcifiers in the ocean, and their oxygen isotope ratios provide the most important and widely applied marine proxy of paleoclimate. However, because of small size and complexity, foraminifera present an analytical challenge. They do not necessarily precipitate their tests in equilibrium with seawater and the interpretation of paleoclimate requires a correction to data for vital effects. Fig. 2-21(left) shows the range of vital effects for $\delta^{18}O$ estimated for *N. pachyderma* (sin.) from conventional bulk analyses, expressed as [$\delta^{18}O$(foram) – $\delta^{18}O$(equilibrated calcite)] for the $\delta^{18}O$ and temperature of ambient seawater. Most of the paleoclimate record is based on analysis of pooled samples of many hand-picked organisms; some studies report data for single tests. It is implicitly assumed that these are homogeneous samples. However, foraminifera precipitate micrometre-scale layers during growth (Fig. 2-21, right) and some species precipitate calcite by more than one mechanism (Erez 2003). While it is common practice to apply a constant species-dependent vital effect to correct oxygen isotope ratios in foraminifera for paleoclimate and other applications, the range of values (Fig. 2-21, left) and complex internal structure (Fig. 2-21, right) suggest that foraminifera might be more complex. Only a handful of studies have investigated biogenic zoning of $\delta^{18}O$ by SIMS analysis of foraminifera (Rollion-Bard *et al.* 2008, Kozdon *et al.* 2009), corals (Rollion-Bard *et al.* 2004, 2008, Blamart *et al.* 2006), or conodonts (Trotter *et al.* 2008). The potential for new discoveries is high.

Kozdon *et al.* (2009) studied vital effects in *N. pachyderma* (sin.) collected live from the North Atlantic in net catches and shallowly buried in mud

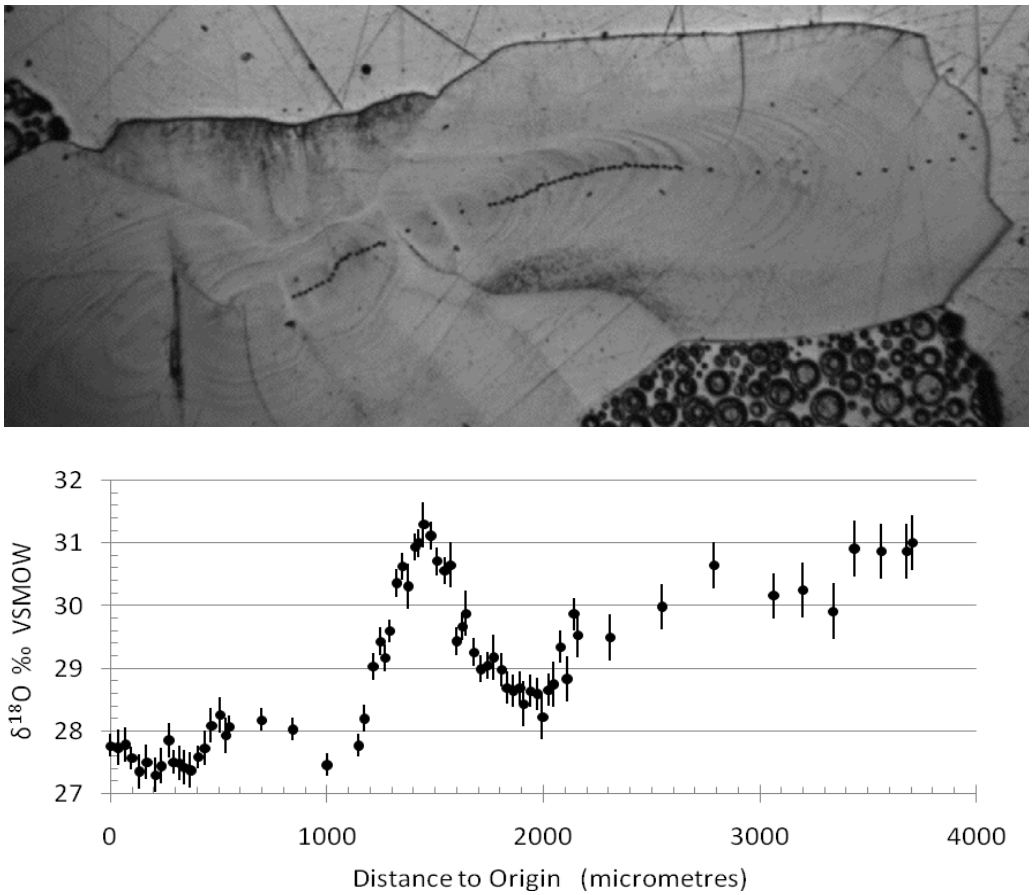

FIG. 2-20. **Upper:** SEM view of a Pacific cod otolith from Aialik Bay, Gulf of Alaska with 69 analyses spanning the ~10 year life of the fish. Field of view = 5 mm. **Lower:** Values of $\delta^{18}O$ vary by 4‰ due to movement from shallow, possibly freshened, waters (lower $\delta^{18}O$) to deeper colder water (high $\delta^{18}O$). Data are from A. Crowell and J. Valley (unpublished).

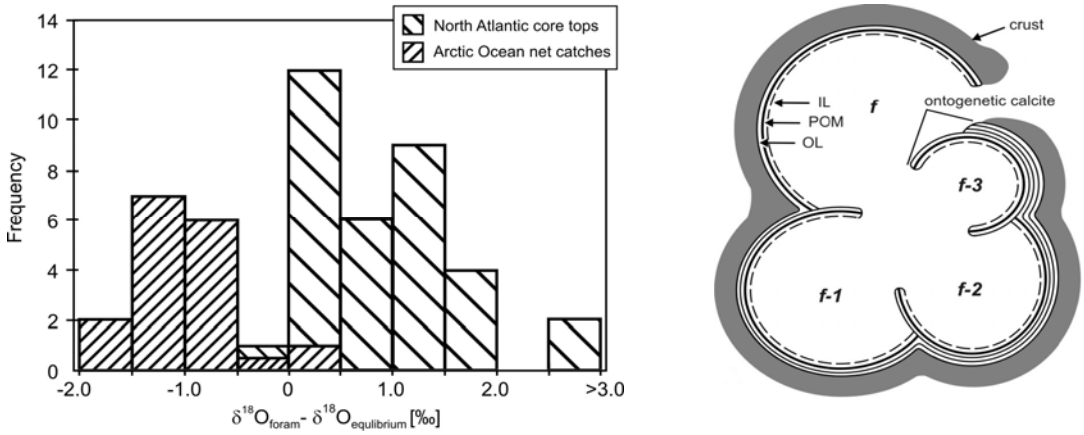

FIG. 2-21. **Left:** Histogram showing the range of vital effects in *N. pachyderma* (sin.) based on conventional bulk analyses. Values of $\delta^{18}O$(equilibrium) are calculated using the temperature and $\delta^{18}O$ of ambient seawater. **Right:** Schematic view of the *N. pachyderma* test (ca. 300μm dia.). Every time a new chamber is formed, the test is covered with a layer of calcite. The inner (IL) and outer (OL) calcareous layers are precipitated during the organism's ontogenetic development whereas the outer crust, which can contribute over 70% of the total test weight, is secreted near the end of life (from Kozdon *et al.* 2009).

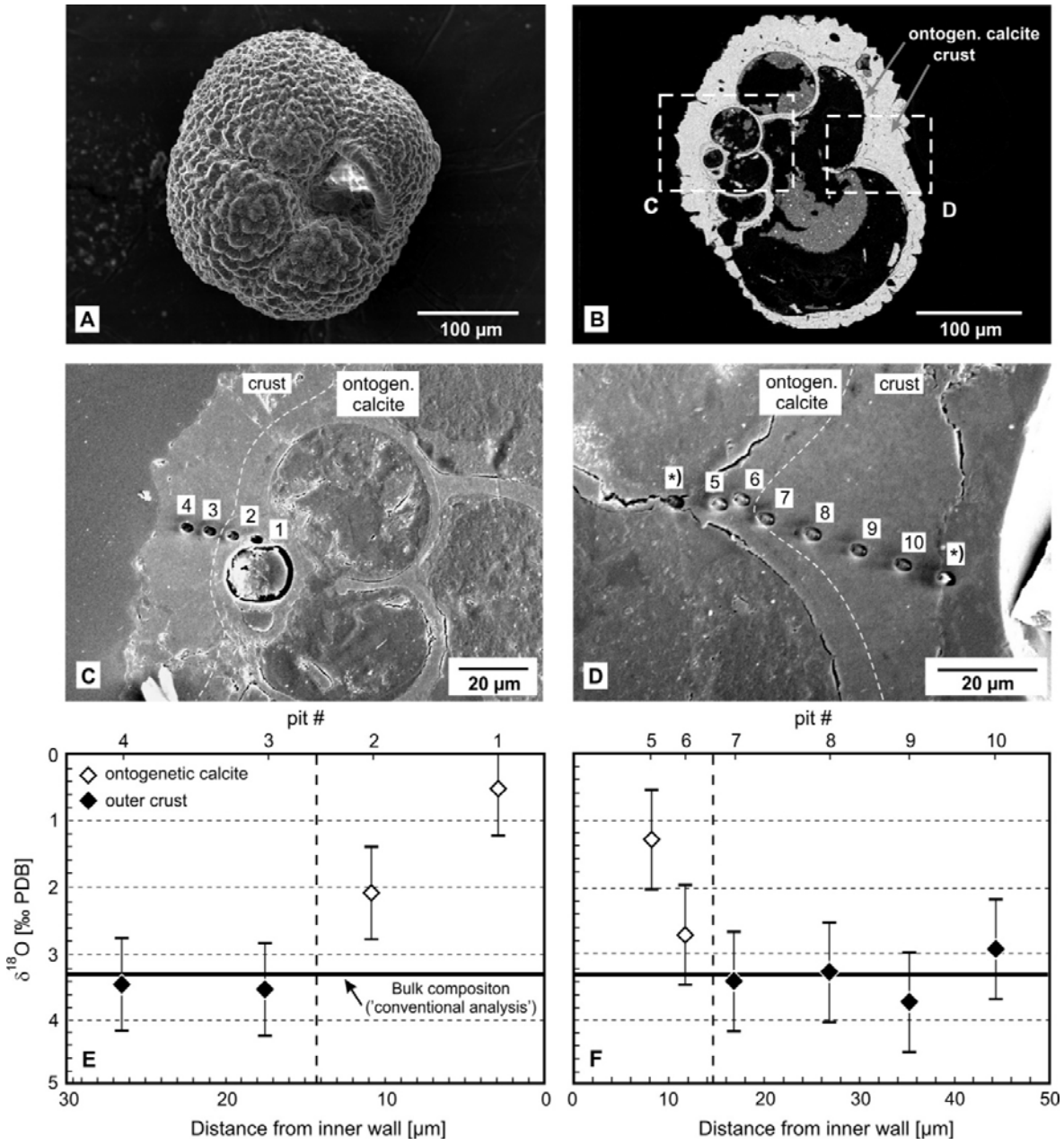

FIG. 2-22. **(A, B)** SEM images of an encrusted *N. pachyderma* test and a polished cross-section. Areas filled by epoxy are black in B, and dark grey in C and D. **(C, D)** SEM images of the gold-coated sample showing ion microprobe pits from traverses of early chambers and crust. Pits measure 2 x 3 µm. **(E, F)** Corresponding $\delta^{18}O$ values are arranged by distance from the inner chamber wall. Error bars are ±2 SD. Conventional bulk data (Simstich *et al.* 2003) represent analyses of multiple tests mixed together from the same size fraction (125-250 µm) as this sample (from Kozdon *et al.* 2009).

from the top of a piston core. Water chemistry and temperature of growth is known for these samples and diagenesis can be ruled out. Single tests ("shells") were cast in epoxy, polished to midsection, imaged by SEM, and analyzed for $\delta^{18}O$ by IMS1280 at WiscSIMS. Using a ~3 µm diameter beam, it was possible to make traverses of the walls of foraminifer tests with precision of ±0.7‰ (2 SD), which is sufficient to prove consistent zonation of 2–3‰ in $\delta^{18}O$ (Fig. 2-22). Significantly, these data show that *N. pachyderma* precipitates calcite by two different mechanisms and neither is in isotopic

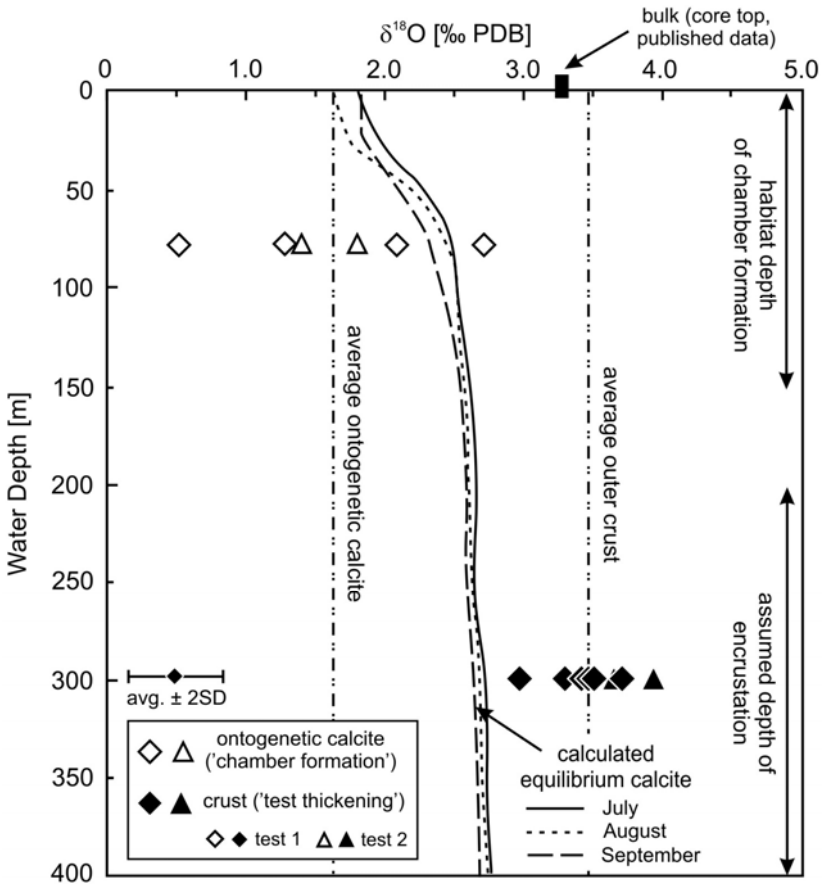

FIG. 2-23. Values of $\delta^{18}O$ from 2–6 μm spots in the ontogenetic calcite and outer crust from two individual tests of *N. pachyderma* (sin.) from the top of piston cores in North Atlantic sediments plotted against water depth and the calculated equilibrium $\delta^{18}O$(calcite) during the main planktonic bloom. Depth intervals for chamber formation and encrustation are based on plankton tow studies. Values of $\delta^{18}O$(crust) are similar to published 'whole test' data from bulk foraminiferal analysis, indicating a high degree of encrustation at this location (from Kozdon *et al.* 2009).

equilibrium with ambient seawater (Fig. 2-23). The inner ontogenetic calcite layers, precipitated during the growth of each new chamber, show a negative vital effect, while the crust, formed at the end of life, has a positive vital effect. Thus, there are two different vital effects with opposite signs that tend to cancel each other. The value of $\delta^{18}O$ obtained by a bulk analysis of one test is the average and could vary by up to 2‰ depending on the percentages of inner ontogenetic layers *vs*. crust. Failure to recognize this zonation could lead to incorrect conclusions. For instance, events that stress or alter the life cycle could be misinterpreted as temperature change.

SPELEOTHEMS

Speleothems are widely studied as a proxy of paleoclimate. Such carbonates are typically sampled by dental drilling at mm-scale, dated by U-series, and analyzed for $\delta^{18}O$ and $\delta^{13}C$ with the phosphoric acid technique. Recently, studies by ion microprobe have increased spatial resolution for oxygen isotope ratio to 20 μm (Kolodny *et al.* 2003, Treble *et al.* 2005, 2007, Fairchild *et al.* 2006) and to 10 μm (Orland *et al.* 2009).

Speleothems from Soreq Cave, Israel preserve a continuous isotopic record of the past 185,000 years (Bar-Matthews *et al.* 2003). Orland *et al.* (2009) imaged a stalagmite from Soreq Cave dated at 2.2 to 0.8 ka and analyzed $\delta^{18}O$ with a 10 μm spot at WiscSIMS. While previous 0.5 mm drill studies resolved decade to century scale climate variation, the ion microprobe analyses resolve seasonality with multiple spots within single years of speleothem growth. Figure 2-24 shows a section of the traverse dated at ~1.65 ka. This high-resolution record was measured in 10 mm cubes of sample cast in epoxy with calcite standard (Fig. 2-9). Before ion microprobe analysis, the polished sample was imaged by confocal laser fluorescent microscopy, which revealed concentric growth bands with gradational bright to dark fluorescence (Fig. 2-24). Oxygen isotope analysis demonstrates that these bands are annual and shows a consistent asymmetric pattern with lowest $\delta^{18}O$ at the beginning of each band (light-colored fluorescence, interpreted to be the annual wet season) grading upwards to higher values in dark calcite (interpreted

to be the annual dry season, Fig. 2-24). The difference in $\delta^{18}O$(calcite) between the lightest and darkest portion of each couplet, $\Delta^{18}O$(dark-light), is interpreted to reflect seasonality, with small $\Delta^{18}O$ values corresponding to dry years (Orland *et al.* 2009). This measure of seasonality correlates with estimates of annual rainfall based on $\delta^{18}O$(calcite) and with lake levels in the Dead Sea (Fig. 2-25). Taken together, these results indicate a long term drying of the climate, punctuated by droughts, from ca. 100 to 600 AD, which correlates with the period of decline and eventual defeat of the Roman and Byzantine empires in the Levant.

METAMORPHIC AND HYDROTHERMAL SYSTEMS

A number of classic questions in metamorphic petrology and mineral reaction kinetics can be studied by *in situ* analysis of stable isotope ratios. Oxygen isotope thermometry was one of the earliest applications of stable isotope geochemistry, however in metamorphic rocks thermometry has been plagued by difficulties and erroneous results (*e.g.*, Valley 2001). Just as petrologic thermometry only became viable once the electron microprobe was developed, isotope thermometry has been handicapped by the inability to make *in situ* measurements at the appropriate scale. Sub-millimetre scale heterogeneity of $\delta^{18}O$ can represent growth zoning preserved in minerals with slow oxygen diffusion, retrograde exchange in minerals with faster diffusion, or a variety of non-diffusive processes. The competing rates of diffusion and surface reaction are different for each mineral in a rock (Cole & Chakraborty 2001). In a purely diffusive system, minerals metamorphosed below their closure temperature for oxygen diffusion, such as garnet (Kohn *et al.* 1993, Kohn & Valley 1994, Jamtveit & Hervig 1994, Crowe *et al.* 2001, Vielzeuf *et al.* 2005b, Page *et al.* 2009), zircon (Peck *et al.* 2003, Page *et al.* 2007a, Lancaster *et al.* 2009), and monazite (Breecker & Sharp 2007), will preserve compositions from the time of crystallization and may preserve growth zoning of $\delta^{18}O$. Conversely, at temperatures above closure, minerals exchange with other "open" minerals and

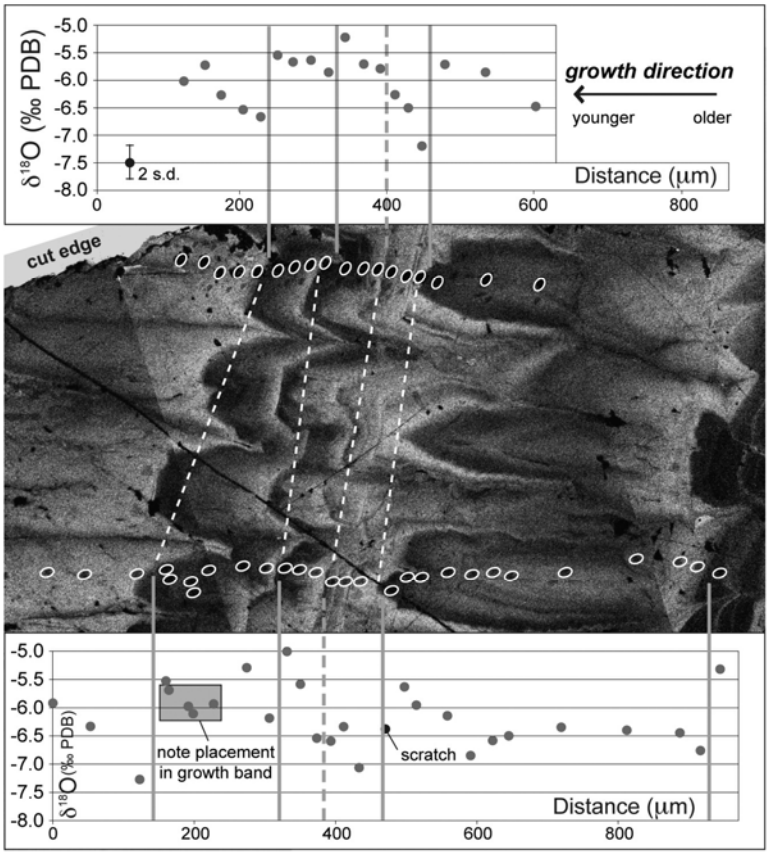

*FIG. 2-24. Fluorescent image of a 1 mm section of speleothem from Soreq Cave, Israel produced by laser confocal microscopy for several annual light-dark couplets dated *ca*. 1.65 ka. Ion microprobe analysis pits (IMS1280), 10 μm in diameter, are highlighted with ovals. Plots of two parallel 500-800 μm-long ion microprobe traverses show a good correlation of $\delta^{18}O$ (PDB) variation and growth bands. Growth is from right to left. Values of $\delta^{18}O$ show a consistent, saw-tooth asymmetry; they are lowest during the winter rainy season (bright fluorescence) and gradually increase during the dry season as fluorescence darkens (from Orland *et al.* 2009). Color version available at http://www.mineralogicalassociation.ca/index.php?p=160

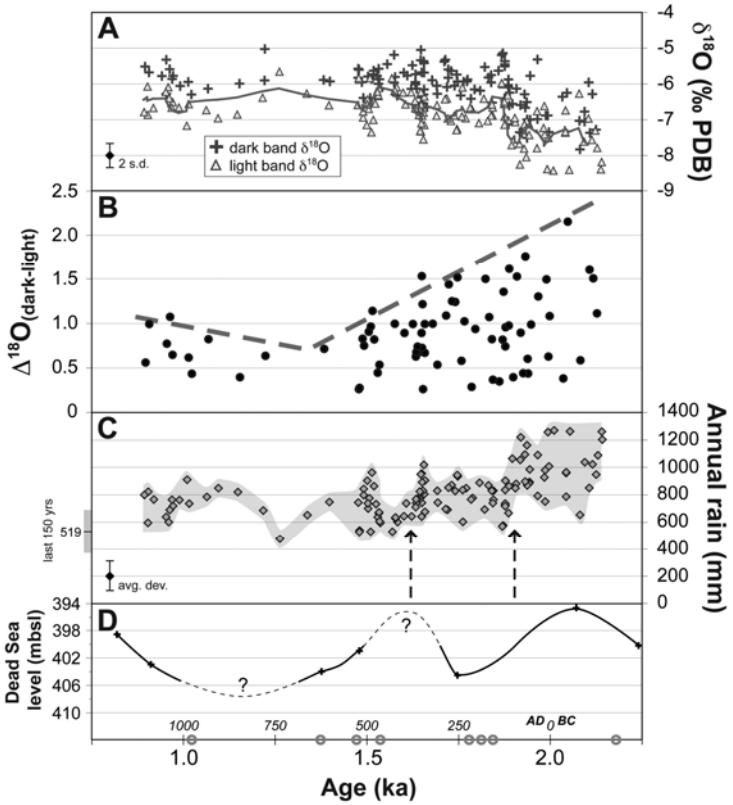

*FIG. 2-25. **(A)** Values $\delta^{18}O$(calcite) measured by ion microprobe for wet (light fluorescent band) and dry (dark band) season growth across a speleothem from Soreq Cave, Israel. Higher $\delta^{18}O$ values represent drier years and lower $\delta^{18}O$ values are wetter years. The line shows the general variability of $\delta^{18}O$ from 2.2–0.9 ka. **(B)** Values of $\Delta^{18}O_{dark\text{-}light}$ ($= \delta^{18}O_{dark\ cc} - \delta^{18}O_{light\ cc}$) for single annual bands show a decrease in maximum values of $\Delta^{18}O$ from 2.0–1.3 ka. **(C)** Estimates of annual precipitation (mm/y) calculated from the measured $\delta^{18}O$ of wet season calcite. Sharp decreases occur at ~1.9 and 1.6 ka (arrows). **(D)** Changes in lake level of the Dead Sea. Circles along the age-axis represent U-series dates for this sample (from Orland *et al.* 2009). Color version available at http://www.mineralogicalassociation.ca/index.php?p=160

any fluids. During cooling, such minerals are predicted to preserve diffusion profiles as a function of cooling rate (Eiler *et al.* 1993). However, a number of complexities are possible, including multiple heating events, localized recrystallization, micro-veining, and fast pathways for diffusion (Valley 2001, Watson & Baxter 2007). Microanalysis offers the possibility to distinguish such complex situations so that they may either be studied in detail, or avoided, according to the goals of a study (Fig. 2-26). Such studies will aid in the refinement of models of reactive metamorphic fluid flow that are based on stable isotope data and idealized assumptions about mineral exchange (Baumgartner & Valley 2001, Lüttge *et al.* 2004, Ague 2007, Watson & Baxter 2007, Bowman *et al.* 2009).

Bowman *et al.* (2009) studied layered marble near the contact of the Alta Stock in Little Cottonwood Canyon, Utah. Previous studies show that crystallization of periclase was driven by infiltration of water-rich fluids from the stock and that flow was concentrated in specific layers that are low in $\delta^{18}O$ (Cook & Bowman 2000). Sharp gradients in $\delta^{18}O$ (>6‰/10 cm, Fig. 2-27) are seen between these layers, but it was previously uncertain whether these gradients represent a metasomatic "front" or the "side" of a flow system, and if isotopic exchange was via volume diffusion in calcite or recrystallization. The ion microprobe data shown in Figure 2-27 test these questions. Individual crystals of calcite are not zoned in $\delta^{18}O$ indicating that marble was recrystallized during fluid flow parallel to layering. These Alta rocks show fundamentally different processes and scales of exchange than marble studied by Graham *et al.* (1998) from a polymetamorphosed contact aureole in the Hida Belt, Japan. The sample of Hida marble shows calcite with purple cathodoluminescence (CL) overprinted locally by yellow CL along grain boundaries, fractures, deformation lamellae, and replacement patches. The yellow CL domains are systematically lower in $\delta^{18}O$ by up to 15‰, with 200-300 μm wide gradients, which apparently formed by diffusion during infiltration of magmatic fluids. These differing conclusions illustrate important differences in process and support the use of reactive transport models that assume local equilibrium of fluids and calcite at Alta, but not at Hida.

A number of ion microprobe studies have documented sharp gradients in $\delta^{18}O$ due to hydro-

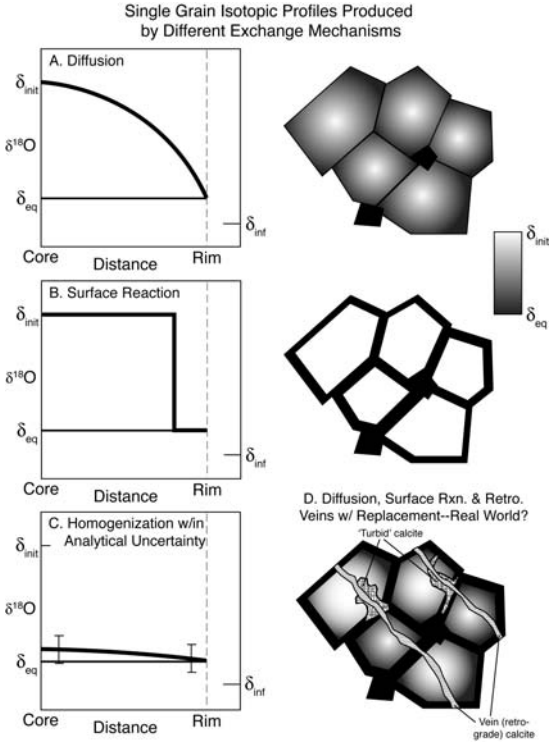

FIG. 2-26. Schematic profiles of $\delta^{18}O$ across a mineral grain that would result from exchange between the grain (δ_{init}) and an isotopically distinct grain-boundary fluid (δ_{inf}). **(A)** Diffusion only. **(B)** Surface Reaction (dissolution-reprecipitation) only. **(C)** Attainment of equilibrium (thin line, δ_{eq}) and equilibration to within analytical uncertainty (heavy line). Note that profiles could be composite, exhibiting effects of both diffusion and surface reaction, and that later events can be locally superimposed on the rock. *In situ* analysis is required to test these possibilities (from Bowman *et al.* 2009).

thermal alteration. Thin millimetre-scale amphibole veins in gabbro from a fast-spreading ocean ridge (Hess Deep) are bounded by sub-millimetre gradients of $\delta^{18}O$ in plagioclase and diffusion modeling suggests that they formed in less than 100 years (Coogan *et al.* 2007). Allan & Yardley (2007) compared cathodoluminescence imaging with analysis of fluid inclusions, trace elements and $\delta^{18}O$ in hydrothermal quartz from Mt. Leyshon, Australia. Oscillatory-zoned quartz grains vary systematically by up to 14‰ in $\delta^{18}O$ due to temperature changes from 650 to 280°C. Valley & Graham (1996) studied quartz from sub-volcanic Maol na Gainmhich granite, Isle of Skye, including one phenocryst that varies from magmatic values of $\delta^{18}O = +10$ to altered values of –3‰ over a distance of 400 μm due to crack-controlled infiltration of high temperature meteoric water. Mora *et al.* (1999) measured gradients up to 14‰ over 600 μm with $\delta^{18}O$ as low as –16‰ in feldspars of the Boehls Butte anorthosite also due to heated meteoric water. They inferred a chemical quench to oxygen diffusion due to rapid drying of retrograde fluids. Cole *et al.* (2004) also found gradients up to 15‰ within single crystals of plagioclase that were hydrothermally altered at Rico, Colorado. A coupled reaction–diffusion model suggests that high temperature fluids were active for 100–300 ka, while magma was present, and that circulation of 150–200°C waters continued for over a million years. These studies offer preliminary insight into a range of processes that regulate fluid flow, mineral exchange, and associated transfer of mass and heat preserved in the mineralogical record over very small length scales that without the ion microprobe would never have been observed.

GEM MINERALS

The genesis, mining locality, and trade routes of precious and semi-precious minerals is of interest for geological, historical and political reasons. Analysis by ion microprobe is preferred because of the small sample requirements (a 10 μm pit is invisible to the naked eye), and a number of studies have employed *in situ* oxygen isotope analysis to establish a "source fingerprint". Giuliani *et al.* (2000) studied $\delta^{18}O$ in emeralds from Roman to 18th century artifacts and found a 17‰ range in $\delta^{18}O$. They concluded that in antiquity emeralds from Pakistan and Egypt were traded by the Silk Route, and that after the 16th century, Colombian emeralds were traded across the Atlantic and Pacific. Likewise, *in situ* analysis of $\delta^{18}O$ combined with δD in turquoise differentiates among different mining districts and helped establish historical trade routes in pre-Columbian Mesoamerica (Fayek *et al.* 2002b).

A number of studies have shown that bulk values of $\delta^{18}O$ vary by up to 20‰ in rubies and sapphires, and thus $\delta^{18}O$ is an indicator of geological source (Giuliani *et al.* 2005, 2006, Zaw *et al.* 2006, Yui *et al.* 2005). While zoning of $\delta^{18}O$ is known from sapphire (Upton *et al.* 1999) and oxygen isotopes are readily analyzed by SIMS in corundum (Mariga *et al.* 2006), *in situ* analysis does not appear to have been applied yet to gem quality material.

Gem minerals are also studied for petrologic

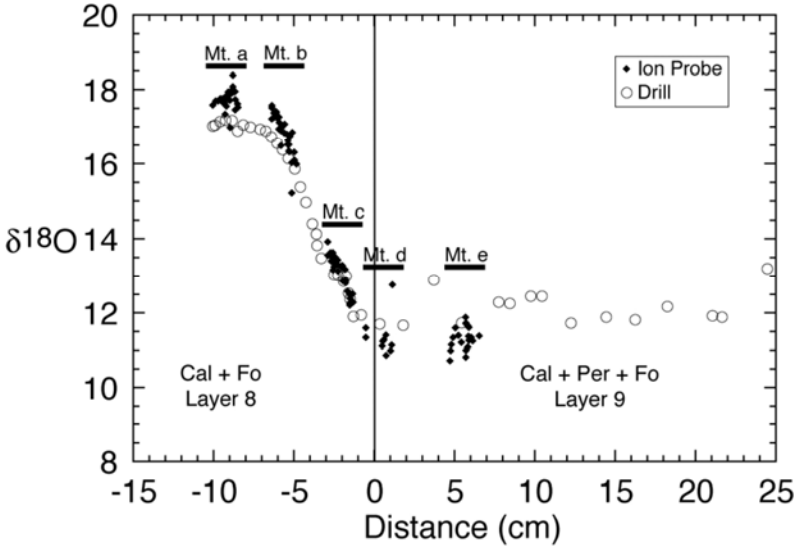

FIG. 2-27. Profile of $\delta^{18}O$(calcite) across the boundary of low $\delta^{18}O$ periclase-bearing marbles that were conduits for flow of magmatic fluids in the Alta Stock Aureole, Utah. Analyses by ion microprobe (solid diamonds, 10 μm spot) from 5 polished mounts (bars) show similar average values, but more variability, in comparison to larger samples obtained by dental drill (open circles, mm-scale) that inevitably mix larger domains, including late turbid calcite that is seen along grain boundaries (from Bowman *et al.* 2009).

reasons. Zoning of $\delta^{18}O$ varies with sequence of precipitation among different generations of jadeite that luminesce red, green, or blue by CL indicating multiple sources of jade-forming fluids during high pressure metamorphism (Sorenson *et al.* 2006). The composition of silicate inclusions within diamonds (DIs) varies by over 10‰ in $\delta^{18}O$. The highest $\delta^{18}O$ DIs are 50–100 μm coesite grains with $\delta^{18}O$ values up to 16.9‰, exceeding the highest value found in mantle xenoliths by up to 7‰ (Schulze *et al.* 2003). These high values are not in equilibrium with minerals of the host eclogite, yet the stability of coesite indicates that these unusual oxygen isotope compositions existed in the mantle and thus were armored by surrounding diamond. High $\delta^{18}O$ coesite DIs are found in highly zoned, low $\delta^{13}C$ eclogite diamonds, and a negative correlation of $\delta^{18}O$(coesite) and $\delta^{13}C$(diamond) indicates that subducted sediment is the ultimate source (Schulze *et al.* 2004).

ZIRCON

Zircon U-Pb geochronology provides the most robust and commonly applied ages in many Precambrian and younger terranes. *In situ* analysis of multiple geochemical systems in igneous and metamorphic zircon can directly link crystallization age to the compositions of coexisting minerals and melts, and provides constraints on the genesis and protoliths of host rocks. The ability to image growth zoning, inherited cores, and overgrowths (Figs. 2-28 and 2-35), as well as damaged domains and inclusions, facilitates the study of single zircon grains (Corfu *et al.* 2003, Valley 2003, Cavosie *et al.* 2006) and graphically demonstrates the importance of *in situ* analysis.

Because of the small volume of sample required for one ion microprobe analysis, multiple measurements can be made within single growth zones of a zircon to correlate age to other isotope systems ($\delta^{18}O$, $\delta^{7}Li$, εHf) or trace elements (REEs, Ti) (Cavosie *et al.* 2005, 2006, 2007, 2009, Booth *et al.* 2005, Martin *et al.* 2006, 2008, Kemp *et al.* 2006, 2007a, b, 2008, Hawkesworth & Kemp 2006a, b, Schmitt 2006, Schmitt *et al.* 2007, Bindeman *et al.* 2008, Page *et al.* 2007b, Trail *et al.* 2007, Schmitt & Hulen 2008, Fu *et al.* 2008, Moser *et al.* 2008, Appleby *et al.* 2008, Wilde *et al.* 2008, Ushikubo *et al.* 2008, Ickert *et al.* 2008, Cates & Mojzsis 2006, Pietranik *et al.* 2008, Harrison *et al.* 2008, Liu *et al.* 2009, Lancaster *et al.* 2009).

Other U-bearing minerals are more readily exchanged, allowing correlation of alteration events to *in situ* geochronology. Uraninite and coffinite are zoned at sub-millimetre scale with low values of $\delta^{18}O$ (to –33.9‰) due to low temperature interaction with meteoric water in the Cigar Lake deposit (Fayek *et al.* 2002a). Likewise, uraninite in shallow natural fission reactors at Oklo has lower $\delta^{18}O$ than the deeper reactor zones due to alteration by meteoric waters (Fayek *et al.* 2003). Monazite in hydrothermally altered sedimentary rocks of the Birch Creek contact aureole yields the same age and $\delta^{18}O$ as in the pluton, showing that they recrystallized, in contrast to unaltered detrital monazite in the same sedimentary rocks (Ayers *et al.* 2006).

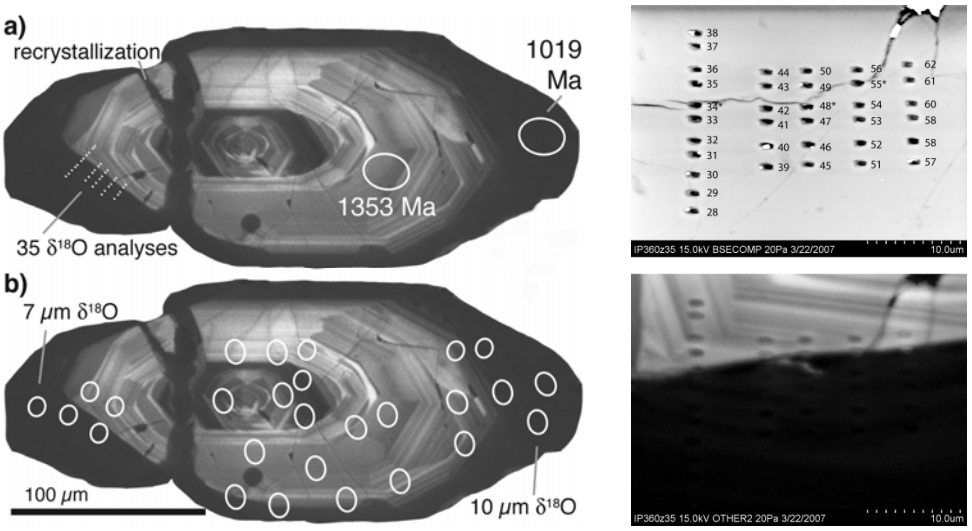

FIG. 2-28. Cathodoluminescence (CL) images of an Adirondack zircon showing bright oscillatory zoning in the core and darker CL in the rim. A dark recrystallized fracture cuts across the zircon. **(a)** Location of 30 μm U-Pb analysis pits by SHRIMP (Bickford *et al.* 2008) and sub-1 μm $\delta^{18}O$ pits by IMS1280. **(b)** Location and size of 10 μm and 7 μm oxygen isotope analyses by IMS1280. **(Right)** SEM and CL images of enlarged area of sub-1 μm pits from (A). See Fig. 2-6 for an enlarged view of two pits (from Page *et al.* 2007a).

$\delta^{18}O$ of Mantle-Derived Magmas

The $\delta^{18}O$ value of melts from the mantle is remarkably constant with only small outliers (Eiler 2001) and zircon in high temperature equilibrium with these compositions is likewise restricted in $\delta^{18}O$, averaging 5.3 ±0.6‰ (2 SD, Valley *et al.* 2005). Figure 2-29 shows the values of $\delta^{18}O$ for "mantle oxygen" in zircon from the Mid-Atlantic Ridge and kimberlite (Page *et al.* 2007b, Cavosie *et al.* 2009). The $\delta^{18}O$ values of zircon from the Moon have been measured (Whitehouse & Nemchin 2009) and are in good agreement with the compositions of Lunar basalt and gabbro (Wiechert *et al.* 2001, Spicuzza *et al.* 2007). The composition of mantle-derived olivine is nearly identical to this zircon, consistent with small fractionation at magmatic temperatures (Mattey *et al.* 1994, Eiler 2001). Zircon from evolved melts in the crust, if uncontaminated, is not greatly changed and commonly shares this same narrow range of "primitive" $\delta^{18}O$.

The fact that $\delta^{18}O$(zircon) values do not change appreciably during uncontaminated differentiation may seem surprising given that the $\delta^{18}O$ values of magmas can increase by 1 to 1.5‰ during fractional crystallization from mafic to felsic compositions. However, such increases in $\delta^{18}O$(magma) are caused by removal of mafic minerals that are lower in $\delta^{18}O$ than the melt, leaving the magma higher in $\delta^{18}O$ and enriched in quartzofeldspathic components. The changing chemistry of the melt causes $\Delta^{18}O$(magma–zircon) to increase at approximately the same rate as $\delta^{18}O$(magma), and thus $\delta^{18}O$(zircon) is unaffected. Valley (2003) discussed this process and summarized the equilibrium fractionation of oxygen isotopes between zircon and other minerals. Lackey *et al.* (2008) presented a relation for estimating the fractionation of zircon vs. melt:

$$\Delta^{18}O(\text{magma-zircon}) \approx 0.0612(\text{wt.\% } SiO_2, \text{ magma or WR}) - 2.50‰$$

There is a small temperature effect on fractionation at magmatic temperatures. However, the effect on values of $\Delta^{18}O$(magma-zircon) is especially small because zircon is intermediate in fractionating $\delta^{18}O$ among common rock-forming minerals; at equilibrium it is lower in $\delta^{18}O$ than quartz and feldspar and higher than magnetite and olivine (Valley 2003). Thus, values of $\delta^{18}O$(zircon) are closer to values of the melt than $\delta^{18}O$(quartz or feldspar) and are insensitive to changes in temperature. Bindeman & Valley (2002) demonstrated the small range of $\delta^{18}O$(zircon) values for temperature changes from ~700 to 800°C in the Bishop Tuff magma chamber (Fig. 2-30). At higher temperatures, this effect is even smaller.

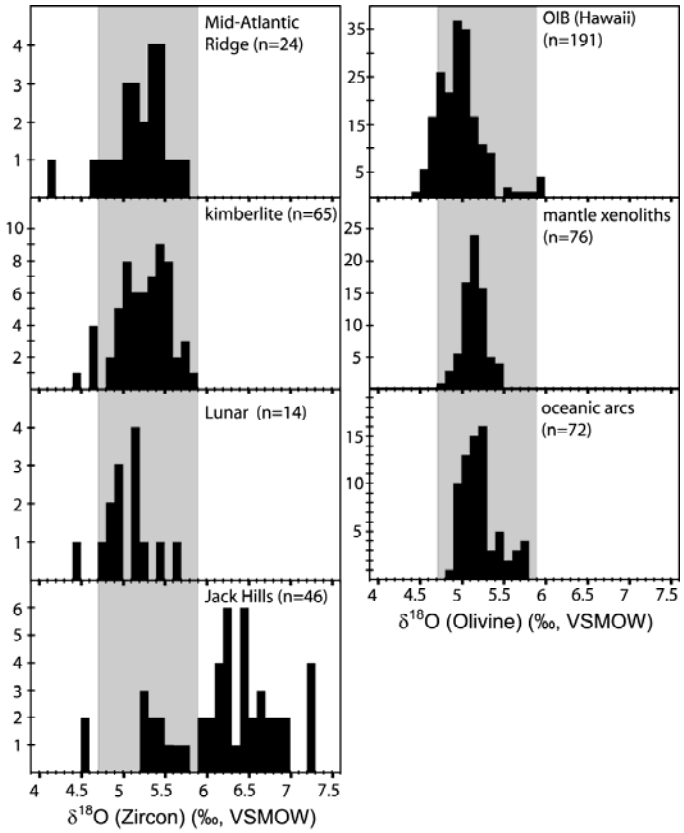

FIG. 2-29. Histogram of $\delta^{18}O$ values for igneous zircon and olivine from primitive sources on Earth and the Moon. The shaded field at $\delta^{18}O$ = 4.7 to 5.9‰ encompasses primitive or mantle values of $\delta^{18}O$(zircon) = 5.3 ±0.6‰ (from Cavosie *et al.* 2009 and references therein).

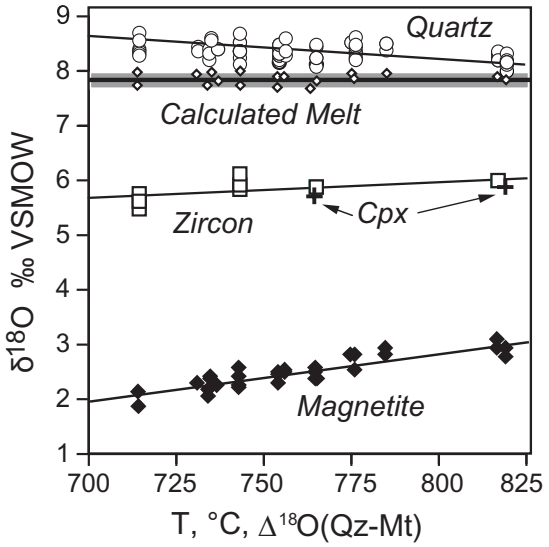

FIG. 2-30. Measured values of $\delta^{18}O$ (laser fluorination) for zircon, quartz, clinopyroxene, and magnetite in the Bishop Tuff plotted against magmatic temperature. Melt compositions are calculated. Values of $\delta^{18}O$(zircon) are relatively insensitive to changes in pre-eruptive temperature, even though quartz and magnetite vary by up to 1‰ (from Bindeman & Valley 2002).

Oxygen Diffusion and Exchange in Zircon

Zircon is highly retentive of chemical and isotopic composition due to its refractory character and extremely slow diffusion for most elements (Cherniak & Watson 2003, Peck *et al.* 2003, Page *et al.* 2007a). Both experiments and empirical studies indicate that closure temperature for oxygen isotope exchange is above 800°C for "dry" conditions. Sharp gradients in $\delta^{18}O$ within single zircon grains (Fig. 2-31) show that values are generally unaffected during amphibolite, granulite, and eclogite facies metamorphism, and at least some anatexis (Page *et al.* 2007a). In contrast, zircons that are discordant in age may be unaffected in $\delta^{18}O$, but in many instances have been shown not to be reliable in preserving magmatic values of $\delta^{18}O$ (Valley *et al.* 1994, Valley 2003, Booth *et al.* 2005, Nemchin *et al.* 2006, Cavosie *et al.* 2005, 2007). It has also been proposed that crystal-plastic deformation of zircon, which can be seen optically in thin section or by electron backscatter diffraction (EBSD), creates fast pathways for diffusion and facilitates Pb, REE, and oxygen isotope exchange (Reddy *et al.* 2006, Timms *et al.* 2008). However, detailed analysis of many

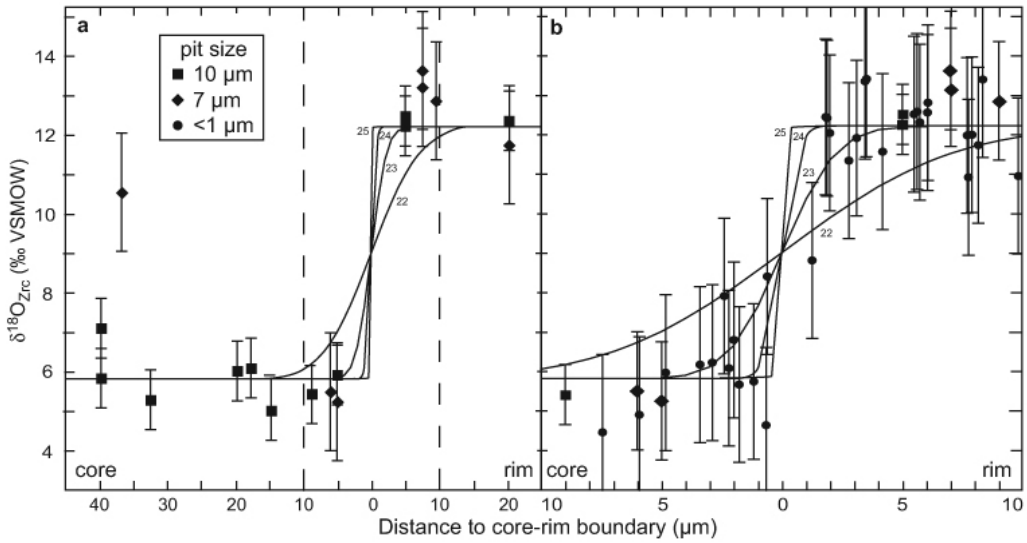

*FIG. 2-31. Oxygen isotope profile measured at WiscSIMS in the zoned zircon from Fig. 2-28. Error bars are 2 SD for the zircon standard. Data from 10, 7, and sub-1µm pits show a sharp increase in $\delta^{18}O$ from the core to the rim. Two spots with elevated $\delta^{18}O$ from the core may represent an earlier generation of zircon. Calculated diffusion profiles are for an isothermal period of 50 Myr and diffusion coefficients of 10^{-22} to 10^{-25} cm^2s^{-1}. The sub-1µm spot data are best fit by D = $10^{-23.5}$ cm^2s^{-1} at 750°C (from Page *et al.* 2007a). Color at http://www.mineralogicalassociation.ca/index.php?p=160

crystals, including some that are clearly deformed, has thus far failed to identify an otherwise unaltered zircon that is zoned due to this process. Other internal checks against alteration include: imaging, age concordance, trace element pattern, internal zoning, and fractionation relative to coexisting phases (Valley 2003). Thus, values of $\delta^{18}O$ are preserved and (with care) reliably interpreted in many zircon grains even when coexisting minerals have been reset by high-grade metamorphism and deformation, intense hydrothermal alteration, or melting. Zircon offers a means to distinguish magmatic compositions from reequilibration or post-magmatic alteration, a common problem for igneous rocks.

Hydrothermal and Metamorphic Zircon

Direct precipitation of zircon from a hydrothermal fluid has been proposed in many studies. If correct, such zircon is important for providing age information of events that are typically difficult to date such as ore deposition and metamorphism. Likewise, if unrecognized, hydrothermal zircon could lead to errors of interpretation. Fu *et al.* (2009) analyzed zircon that had previously been interpreted as hydrothermal from the Gidginbung Au-Ag deposit, Lachlan Orogen, Australia and found that values of $\delta^{18}O$ were constant and mantle-like at 5.4 ±0.9‰ (2 SD), and that Ti, REEs, Hf isotopes, and CL zoning were all best explained by crystallization of zircon from a magma. Likewise, Cavosie *et al.* (2009) examined zircon from young oxide gabbro bodies and highly altered "veins" in serpentinite from the Mid-Atlantic Ridge, and found that the zircon is homogeneous with mantle-like values of $\delta^{18}O$ (5.3 ± 0.8‰ 2 SD), and magmatic CL zoning and REE profiles. Hydrothermal zircon in this environment is predicted to have $\delta^{18}O$ more than 5‰ lower than the measured values. Thus all analyzed zircon is interpreted as igneous and the "veins" appear to be very thin, altered dikes. While there is no reason to doubt the existence of hydrothermal zircon and convincing reports exist, these results suggest that zircon should be tested by detailed geochemistry and imaging before it is assumed to be hydrothermal.

Zircon commonly forms in high-grade metamorphic rocks as new crystals, overgrowths, or replacement. It is common to date zircon in order to establish the timing of metamorphism and to correlate age with estimates of pressure and temperature. However, the zircon-forming reaction can be driven by metasomatism, crystallization of anatectic melts, unmixing of Zr from igneous minerals like ilmenite, or breakdown reactions of metamorphic minerals such as garnet. Thus the timing of zircon growth cannot be assumed to

coincide with the thermal peak of metamorphism. *In situ* analysis of the oxygen isotope ratio is a useful adjunct for interpretation of *in situ* geochronology of metamorphic zircon. Combined with CL imaging, it is possible to test equilibration between zircon and other petrologically significant minerals such as garnet. This is necessary in order to use zircon ages to calibrate the chronology or P–T–t path of a rock (Harley & Kelly 2007, Moser *et al.* 2008, Lancaster *et al.* 2009).

Crustal Recycling

The oxygen isotope ratio of igneous zircon is sensitive to differences in the source and contamination of magmas (Valley 2003). Crustal recycling can be recognized from magmatic values of $\delta^{18}O$(zircon), especially if crustal components were weathered or hydrothermally altered before they became incorporated into magmas. In many plutonic environments, this process is basically one of cannibalism, new magmas remelt earlier co-magmatic rocks of similar chemistry, and the only geochemical evidence will come from isotopes and elements that are altered. Hydrothermal alteration can change the $\delta^{18}O$ of a rock on a time scale of tens to thousands of years, while heavy isotope systems such as Sr, Nd, and Hf require many millions of years to become distinctive by radiogenic in-growth. Thus, if country rocks are igneous and young at the time of remelting, $\delta^{18}O$ may be the only geochemical signature of that interaction. While this distinction might seem moot to a geochemist, the implications are significant for other processes such as heat transport.

Shallow hydrothermal alteration affects vast amounts of crust and is especially prevalent in sub-volcanic environments. Exchange with heated meteoric waters commonly results in low $\delta^{18}O$ values for felsic extrusive and intrusive rocks, but whether this interaction creates low $\delta^{18}O$ magmas has been controversial (see Taylor 1986). The best evidence to resolve this question comes from analysis of zircon that, once crystallized, is unaffected by hydrothermal alteration.

The Yellowstone volcanic field exposes voluminous rhyolite tuff and flows, erupted over the past 2 m.y., including three major caldera-forming eruptions (100–2000 km^3) and many that are smaller. Bindeman & Valley (2001) showed that quartz and zircon are in oxygen isotopic equilibrium for many of the rhyolite units at Yellowstone, but that profound disequilibrium exists for low $\delta^{18}O$ intra-caldera flows that erupted shortly after large caldera-forming eruptions. The conclusions of the 2001 study were based on bulk analysis of $\delta^{18}O$ in zircon concentrates and have been reinvestigated with *in situ* analysis. Bindeman *et al.* (2008) found that individual zircon grains have inherited cores with diverse values of $\delta^{18}O$, that rims can be either higher or lower in $\delta^{18}O$, and that zoning in $\delta^{18}O$ resulted largely from dissolution and crystallization of zircon, rather than diffusion. These results suggest that isolated domains and unexposed intrusive units existed within what had been inferred to be a single magma body. This conclusion contrasts with earlier models where a long-lived magma chamber is periodically tapped. Instead, Bindeman *et al.* (2008) concluded that silicic magmatism proceeded via rapid, shallow-level remelting of earlier erupted and hydrothermally altered Yellowstone crust, driven by on-going intrusion of basaltic magma. Similar complex zoning and low $\delta^{18}O$ values are seen by ion microprobe analysis of zircon from the Cougar Point Tuff, an earlier rhyolite (12.4-10.5 Ma) from the Snake River Plain, showing that mafic intrusions from the Yellowstone hot spot have created voluminous low $\delta^{18}O$ rhyolite magmas (Cathey *et al.* 2007). Apparently, continuous mafic magmas ponding in focused areas of continental crust provide ideal conditions for the successive cycles of intrusion, melting, hydrothermal alteration, and remelting, necessary to form low $\delta^{18}O$ felsic magmas.

Deep penetration of seawater and associated hydrothermal alteration have been documented for oceanic crust at spreading centers. Oxygen isotope ratios record the intensity of alteration and temperature. At high temperatures, values of $\delta^{18}O$(rock) can drop from 6 to below 4‰, while at low temperatures, values exceed 10‰ in highly altered rocks (see Eiler 2001). In this environment, it might be expected that both high and low $\delta^{18}O$ magmas would be produced by remelting of altered basaltic wallrocks. Zircon is found in a number of lithologies from modern spreading centers, however values of $\delta^{18}O$(zircon) show the same narrow range of values found in other primitive reservoirs. Igneous zircon from gabbro and serpentinite from the Mid-Atlantic Ridge averages 5.3 ±0.8‰ (2 SD, Cavosie *et al.* 2009). One large, 10 mm long, zircon grain from an oxide gabbro on the Indian Ridge was analyzed 44 times at WiscSIMS because its ductile deformation was proposed to facilitate chemical alteration (see Fig. 2 in Reddy *et al.* 2006), however

$\delta^{18}O$ values are homogeneous and identical to unaltered zircon (average = 5.28 ± 0.34‰ 2 SD; 2 SE = 0.05‰, Wilde & Valley, unpublished). Likewise, igneous zircon from 24 samples of plagiogranite, Fe-Ti oxide gabbro and veins in serpentinite show mantle-like values of 5.17 ± 0.50‰ (n = 140, 2 SD, Grimes & Valley, unpublished). Why are the effects of hydrothermal alteration and remelting, that are prominent at Yellowstone, not seen in $\delta^{18}O$(zircon) values of magmas from mid-ocean ridges? Possible answers to this question include: 1) zircon-bearing magmas at spreading centers may be direct differentiates from the mantle and remelting is not important, 2) alteration drives $\delta^{18}O$ of wallrocks to both higher and lower values and the average effect is small, or 3) only a relatively small sample set has been analyzed. Correlated *in situ* analysis of age, $\delta^{18}O$, and trace elements in such zircon will provide critical new evidence to resolve this question.

Magmatism in convergent margins is generally believed to be dominated by partial melting of metasomatized peridotite in the overlying mantle wedge, but arc magmas can also result from melting of the slab itself and the importance of slab melting is controversial. Oxygen isotopes are useful to recognize slab melts because of the involvement of high $\delta^{18}O$ sediment, but magmatic $\delta^{18}O$ must be distinguished from subsolidus alteration. Samples of trapped melt inclusions (now glass) within phenocrysts can be armored from subsolidus exchange (Eiler *et al.* 1998, 2007, Gurenko *et al.* 2001, Hauri 2002, Gurenko & Chaussidon 2002, Bouvier *et al*. 2008). For instance, hydrous melt inclusions within olivine from peridotite xenoliths in basaltic andesite of Batan Island were analyzed and found to preserve magmatic values of $\delta^{18}O$, and trace, minor, and major element composition. The glass inclusions are broadly dacitic with $\delta^{18}O = 6.45 \pm 0.51$‰ indicating that they resulted from low-degree melting of metasomatized peridotite rather than subducted ocean crust, and suggesting that some adakite-like magmas may have a similar origin (Eiler *et al.* 2007).

Maturation of the Crust Through Time

Valley *et al.* (2005) reported $\delta^{18}O$ and U–Pb ages for magmatic zircon from 1200 rocks that vary in age from 4.4 Ga to Recent (Fig. 2-32). Taken as a whole, there are no systematic differences observed for ion microprobe data from individual zircon grains *vs*. laser fluorination analyses of bulk samples comprising hundreds of zircon grains. These results show a remarkable consistency throughout the Archean; values for terranes on five continents range from the mantle value to mildly elevated in $\delta^{18}O$, *ca*. 4.7 to 7.5‰. Soon after the end of the Archean, higher $\delta^{18}O$ zircon becomes increasingly common; by 1.5 Ga, many zircon grains yield values in the range of 8 to 10‰, which would be in equilibrium with whole rock $\delta^{18}O$ values of 9 to 12‰. Such elevated oxygen isotope ratios indicate recycling of sedimentary rocks into magma by assimilation or wholesale melting. Clearly, conditions were different in the Archean, both in the rates and style of tectonic processes responsible for melting of crust, and in the availability of high $\delta^{18}O$ supracrustal materials, especially clay-rich mud rocks (Valley *et al.* 2005). During the Proterozoic, the average $\delta^{18}O$ of magmatic zircon increased as the crust matured and high $\delta^{18}O$ material was recycled into magmas.

Archean Magmas and Early Earth

The uniformly primitive to mildly elevated Archean values of $\delta^{18}O$(zircon), 4.7 to 7.5‰, extend to the oldest terrestrial zircon known. This ~3‰ range of $\delta^{18}O$ values is relatively small when viewed in the context of all magmas in Figure 2-32, however it is still significantly expanded relative to the ~1‰ range of zircon from mantle-derived magmas and other primitive sources, 4.7 to 5.9‰ (5.3 ±0.6‰) (Fig. 2-29). The values above 6.3‰ (*i.e*., distinctly higher than 5.9‰, considering analytical uncertainty conservatively at 0.4‰) are best explained by low temperature aqueous alteration of rock and sediment on the surface of Earth followed by burial and melting to form high $\delta^{18}O$ magmas from which zircon crystallized. The exact details of burial and melting are controversial. Some researchers favor modern-style tectonics, subduction, and mantle melting, while others envision processes such as plumes, calderas, and impacts, with melting in the crust. Regardless of process, such mildly elevated values of $\delta^{18}O$ indicate a supracrustal input and cannot form at high mantle temperatures where oxygen isotope fractionations are very small. Figure 2-32 shows $\delta^{18}O$ values measured on five different ion microprobes for detrital zircon older than 3.9 Ga from the Jack Hills, Australia in comparison to values measured in bulk samples by laser fluorination (Peck *et al.* 2001, Wilde *et al.* 2001,

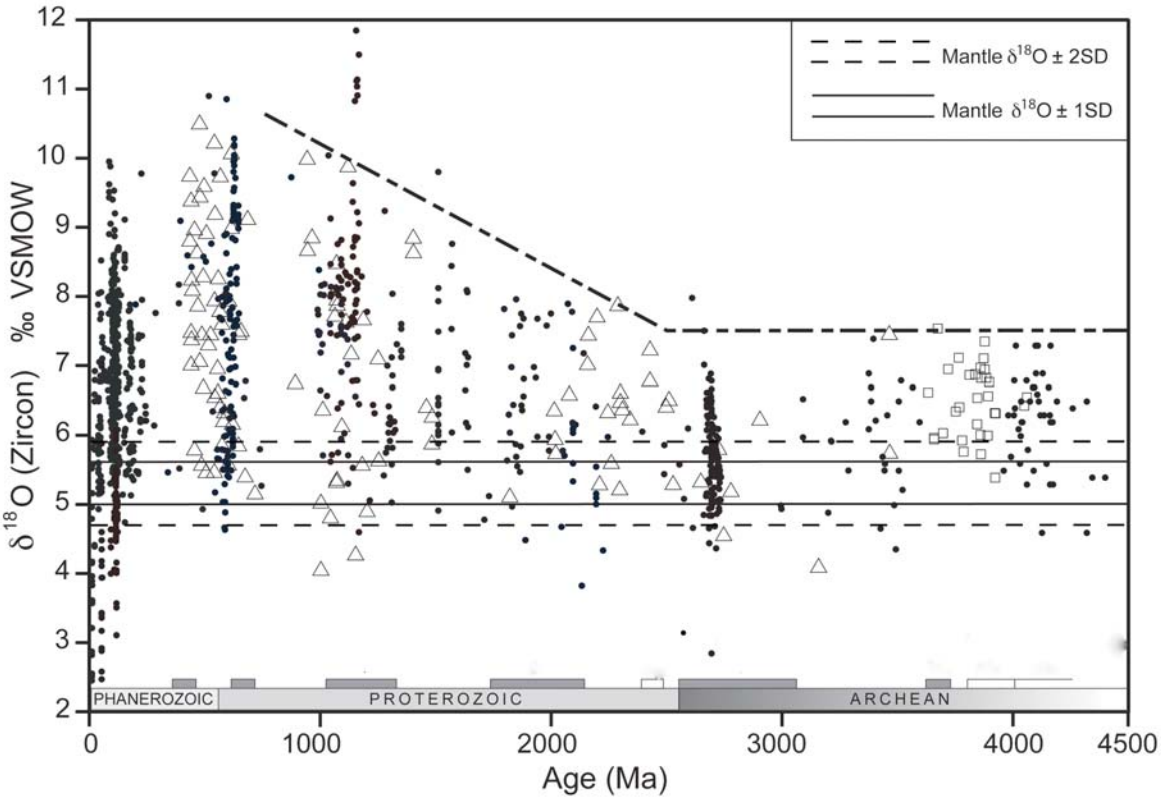

FIG. 2-32. Values of $\delta^{18}O$ for igneous zircon from 4.4 Ga to recent. The composition of zircon in high-temperature equilibrium with mantle $\delta^{18}O$ averages 5.3 ±0.6 (2 SD). Sources of data: dots, Valley *et al.* 2005; triangles and squares, Kemp *et al.* 2006, Wilde *et al.* 2008. Values of $\delta^{18}O$(zircon) range from mantle-like to mildly elevated in the Archean. Values of $\delta^{18}O$ above 7.5‰ reflect increased recycling of high $\delta^{18}O$ crustal material on the post-Archean Earth.

Mojzsis *et al.* 2001, Cavosie *et al.* 2005, Nemchin *et al.* 2006, Trail *et al.* 2007). In addition, oxygen 3-isotope analysis at WiscSIMS shows values of $\Delta^{17}O = 0‰$ confirming the terrestrial origin of this ancient (4.4 to 4 Ga) zircon (see Fig. 2-39). The few values of $\delta^{18}O$ above 7.5‰ in Figure 2-33 were originally interpreted as coming from S-type granite magmas (Mojzsis *et al.* 2001), but are no longer interpreted as igneous (Valley *et al.* 2006, Trail *et al.* 2007). All studies have found a significantnumber of zircon grains with $\delta^{18}O$ above the mantle-equilibrated range of 5.3 ±0.6‰. While several studies have emphasized the complex nature of such zircon and the possibility that some $\delta^{18}O$ values reflect post-magmatic processes (Cavosie *et al.* 2005, Nemchin *et al.* 2006, Valley *et al.* 2006), a large number of samples show concentric CL zoning, concordant ages, and normal trace element compositions (Fig. 2-1). It is difficult to imagine a process whereby the oxygen of a zircon, which is tetrahedrally coordinated and strongly bonded to silicon, could be completely exchanged by diffusion while the Pb, which resides in non-ionic sites caused by radiation damage, is preserved. Thus concordant U-Pb ages provide a good criterion that specific domains of a zircon are unaltered. However, U and Th content and radiation damage can be zoned in zircon, and this test requires correlation of the analysis spots. There is no evidence that the mildly elevated values of $\delta^{18}O$ in the pre-4 Ga zircon samples result solely from younger subsolidus exchange, weathering or alteration of the zircon grains themselves, and thus the compositions of these zircon "time-capsules" are robust evidence of conditions on the Early Earth.

Values of $\delta^{18}O$ above the mantle composition extend as early as 4.325 Ga (Fig. 2-34), suggesting that the surface of Earth was cool enough to condense liquid water at this time and that hotter "Hadean" conditions ended before 4.3 Ga. The existence of liquid water and thus oceans at this time is also suggested by high [Li] of 10–70 ppm

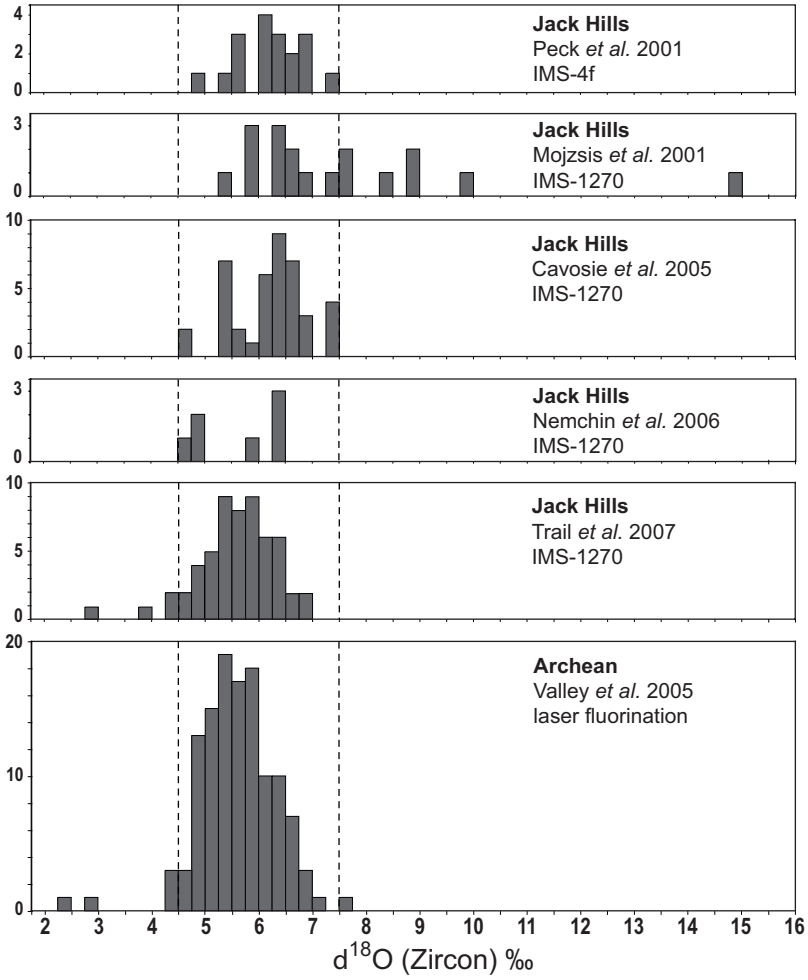

FIG. 2-33. Comparison of values of $\delta^{18}O$ measured by SIMS for detrital > 3.9 Ga zircon from the Jack Hills, Australia, and by laser fluorination for other Archean igneous zircon.

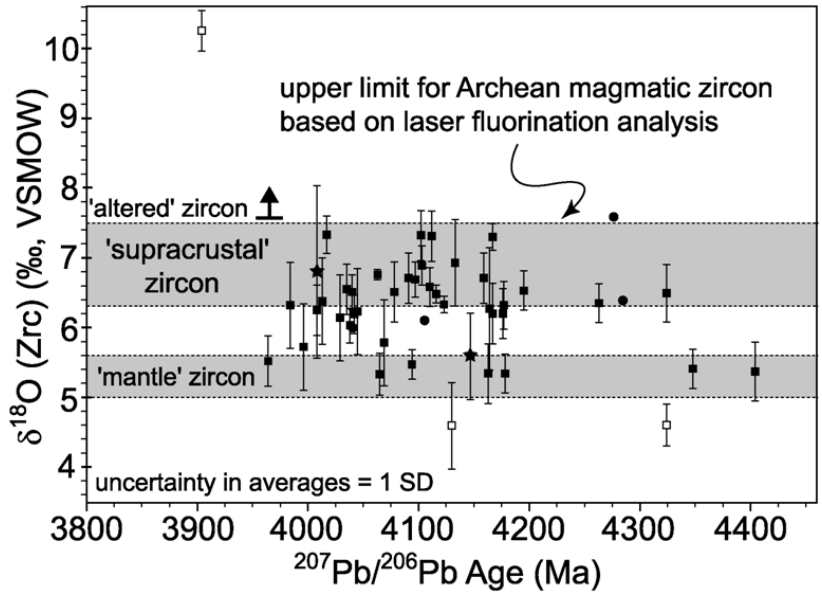

FIG. 2-34. Average $\delta^{18}O$ *vs*. age for Early Archean zircon. Solid squares are zircon analyses preserving magmatic $\delta^{18}O$ (Cavosie *et al.* 2005). Open squares are altered zircon grains. The 'mantle' zircon field is plotted with 1 SD limits, 5.3 ±0.3‰ (Valley *et al.* 1998). The 'supracrustal' field indicates a range in magmatic $\delta^{18}O$(zircon) that is elevated relative to equilibrium with mantle melts (from Cavosie *et al.* 2007).

and low δ^7Li values of 0 to –10‰ in zircon grains as old as 4.3 Ga (Ushikubo *et al.* 2008). Heavy weathering on early Earth is consistent with sauna-like temperatures and a CO_2-rich atmosphere that would have created thick saprolite horizons and destroyed igneous rocks exposed on the surface, possibly explaining the absence of known rocks older than 4 Ga. Alternatively, in the absence of greenhouse gases, Snowball Earth conditions may have prevailed under a fainter young Sun (Zahnle 2006). Either way, liquid water existed in geothermal regions and weathering and low temperature alteration was common. Possibly, secluded pools evolved, confined by ice or land that provided unusual habitats for the first life.

Zircon as the Record of the Kapuskasing Orogen

Moser *et al.* (2008) described the genesis of neo-Archean lithosphere recorded in zircon from the Kapuskasing Uplift of the Superior Province. Ion microprobe analysis was used to correlate U-Pb age and δ^{18}O (Fig. 2-35). Four periods are recognized between 2.9 and 2.5 Ga: creation of primitive to evolved crust (2870–2670 Ma); rapid uplift, arc unroofing, erosion of detrital zircon, and burial of sediments to the lower crust (2670–2660 Ma); prolonged high temperature metamorphism (2660–2580 Ma); and Huronian continental rifting and magma intra-plating (< 2510 Ma). Thus single zircon grains can preserve evidence of multiple prolonged tectonic events.

Hafnium, U-Pb, and Oxygen

In combination with laser-ablation ICP-MS, other geochemical systems such as Lu-Hf can be correlated to SIMS data for δ^{18}O and age (Kemp *et al.* 2006, 2007a, 2008, Hawkesworth & Kemp 2006a, 2006b, Hawkesworth *et al.* 2006, Valley *et al.* 2006, Bolhar *et al.* 2008, Harrison *et al.* 2008, Pietranik *et al.* 2008).

Kemp *et al.* (2007) studied zircon from three suites of hornblende-bearing "I-type" granite from the Lachlan Fold Belt, eastern Australia. The common interpretation of the Lachlan I-type and S-type granite plutons, based in part on whole rock δ^{18}O, is that protoliths were igneous and sedimentary rocks, respectively (O'Neil & Chappell 1977, Chappell & White 2004). However, the new data show that I-type granite zircon has elevated δ^{18}O and that protoliths contained from 25 to 60% metasedimentary material (Fig. 2-36). The combination of *in situ* data for δ^{18}O, U-Pb, and Hf suggests a revised view of the genesis of these rocks, starting with a low δ^{18}O (5–6‰), probably mantle-derived, parent magma, and proceeding through anatexis of the deep crust, emplacement of magmas in the mid-crust, and then zircon growth synchronous with assimilation and fractional crystallization (AFC). Zoning of δ^{18}O in some zircon records magmatic evolution during AFC. Thus the I-type granite bodies are reinterpreted as largely sedimentary in origin, but representing a component of evolved primitive magmas and growth of the crust (Kemp *et al.* 2007a).

METEORITES: OXYGEN THREE-ISOTOPES

The fractionation of oxygen isotopes follows mass-dependent processes in most planetary environments. Thus, on Earth, there is generally no need to analyze ^{17}O, the "forgotten isotope" (but see Bao *et al.* 2000). This arises because both equilibrium and kinetic isotope fractionations are linearly proportional to $\Delta M/M$, and any chemical process that fractionates $^{18}O/^{16}O$ by a given amount will fractionate $^{17}O/^{16}O$ by one-half of that amount. Thus, data fall along a Terrestrial Fractionation Line (TFL) that has a slope of approximately 0.52 in plots of δ^{18}O *vs*. δ^{17}O (McKeegan & Leshin 2001, Miller 2002).

In contrast to Earth and the Moon, oxygen three-isotope analysis of meteorites has been common since Clayton *et al.* (1973) discovered compositions of carbonaceous meteorites that proved the importance of Mass-Independent Fractionations (MIF). Apparently, material was mixed during formation of the Earth-Moon system, homogenizing any pre-existing MIFs, but these differences are preserved in other bodies. The most precise oxygen three-isotope data are made by conventional laser-fluorination techniques, but ion microprobe analysis is increasingly important for meteoritic samples that may contain fine-scale zoning or heterogeneity (McKeegan & Leshin 2001, Kita *et al.* 2004, Krot *et al.* 2006, Nakamura *et al.* 2008).

Oxygen three-isotopes in various primitive meteorites record the variety of materials formed in the earliest solar system and constrain the processes that fractionated oxygen isotopes (Clayton & Mayeda 1996; see also McKeegan & Leshin 2001, Clayton 2007). Improved precision of ±0.3‰ for δ^{17}O and Δ^{17}O for 15μm spots (Kita *et al.* 2007a, 2009), *vs*. ~2‰ in earlier ion microprobe studies, resolves mass-dependent fractionation processes, superimposed on mass-independent trends (Fig. 2-37). High precision, *in situ* analysis with spot

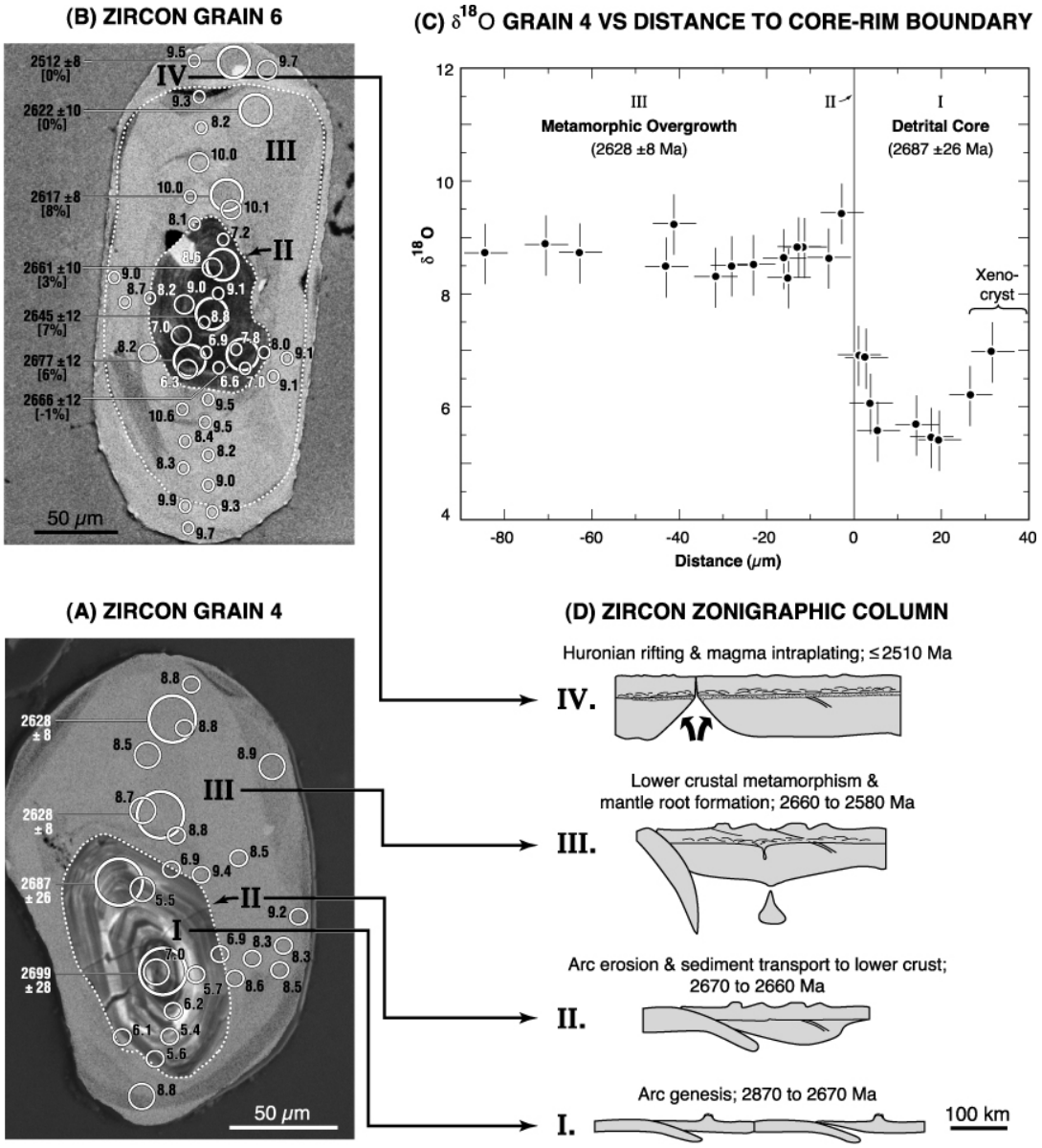

FIG. 2-35. **(A, B)** CL images of Archean zircon from the Kapuskasing Uplift showing ion microprobe spots and values of U-Pb age and $\delta^{18}O$. Zircon 6 shows patchy re-setting of age to metamorphic values and domain enrichment of $\delta^{18}O$ associated with darkening/disruption of CL. **(C)** Primary $\delta^{18}O$ values from magmatic core and metamorphic rim of zircon 4. **(D)** Stages of continental plate creation and local destruction as recorded in zircon zoning (from Moser *et al.* 2008).

sizes as small as 1 μm can resolve composite samples and zoning that was previously unknown. A more complete discussion of this topic is in chapter 1 of this volume. Therefore, examples are presented here that illustrate the new capabilities.

Stardust

The NASA Stardust mission returned sub-micrometre to 10 micrometre-scale particles from comet Wild 2, which contain high temperature minerals similar to those in primitive meteorites (McKeegan *et al.* 2006). The possibility of chondritic material in a comet is surprising because they are thought to form in the inner Solar Nebula, while comets contain material formed in cold interstellar regions of the Kuiper Belt.

Nakamura *et al.* (2008) sectioned four 10 to 40 μm chondrule-like particles from comet Wild 2 containing olivine, pyroxene and metal by microtome, and analyzed for oxygen three-isotopes

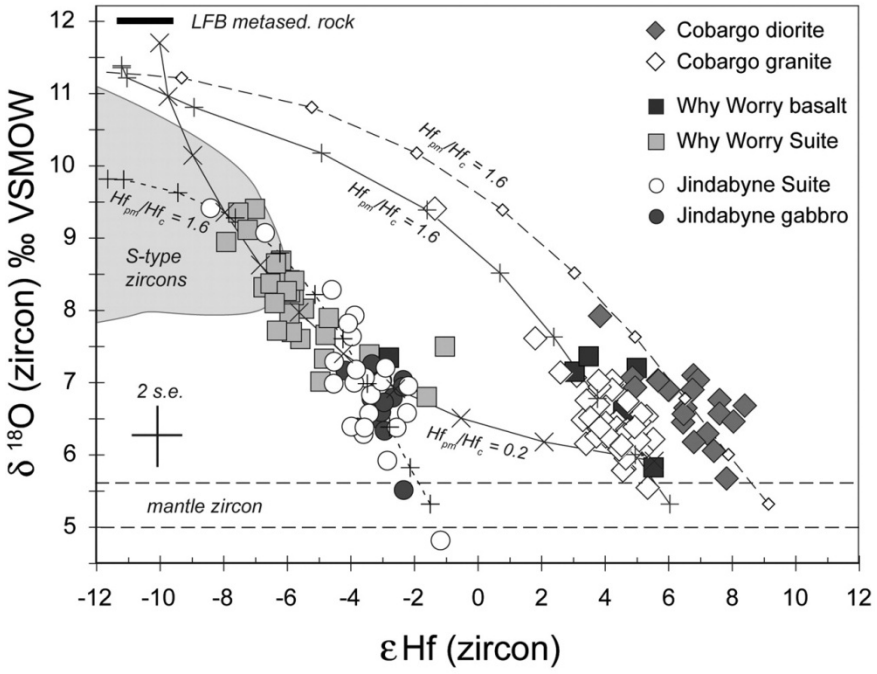

FIG. 2-36. Values of $\delta^{18}O$ *vs.* εHf for zircon from hornblende granite (I-type) in comparison to zircon in S-type granitic and metasedimentary rocks from the Lachlan Fold Belt (LFB). Curves model AFC, assimilation and fractional crystallization, of the magma for different ratios of Hf in the parent magma and in the crust (from Kemp *et al.* 2007a).

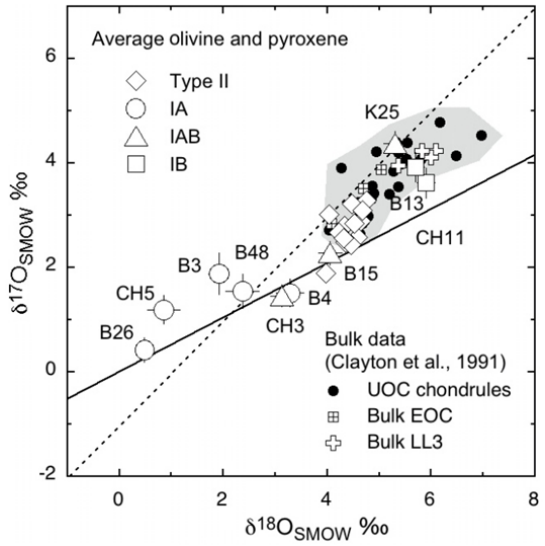

FIG. 2-37. Oxygen three-isotope plot of olivine and pyroxene measured by SIMS (from Kita *et al.* 2006).

in 2 μm and in 1 μm diameter spots at WiscSIMS (Fig. 2-38C). In the largest particle, two 5–10 μm grains of olivine were resolved by X-ray imaging (Fig. 2-38B), and analyzed 4 to 10 times each for oxygen three-isotopes. The oxygen isotope ratios of these samples are chondrule-like and fall along the CCAM line with the lowest values approaching the composition of the Sun (Fig. 2-38D). Furthermore, the compositions of these two adjacent olivine grains (Fig. 2-38B) are distinctly different. These results suggest formation in the inner Solar Nebula and transport to the outer Solar System by X-wind or outward flow in the mid-plane (Nakamura *et al.* 2008).

Martian Meteorites

The only solid samples of Mars available for analysis on Earth are 57 samples from 34 meteorites classified as the SNC group (shergottite, nakhlite, Chassigny) with a cumulative mass of 91 kg. All SNCs are thought to come from the same planet and individual meteorites within this group have ages and rare gas compositions that suggest they formed on Mars. The most important unifying characteristic of the SNC group of meteorites is that they all plot along a mass-dependent fractionation line with a slope of 0.52 in $\delta^{18}O$ *vs.* $\delta^{17}O$ that parallels the terrestrial fractionation line, but is offset by 0.3‰ (*i.e.*, $\Delta^{17}O = +0.3$, Clayton & Mayeda 1996, Franchi *et al.* 1999, Spicuzza *et al.* 2007).

The ALH84001 meteorite is the most famous of the Martian clan because of thin 50–100 μm diameter rosettes of late, radial fibrous, concentrically zoned carbonate that were proposed to harbor evidence for microbial life on Mars (McKay *et al.* 1996). Every aspect of this proposal has been disputed, some would say refuted. For instance, the origin of the carbonates themselves has been proposed to be terrestrial contamination (Kopp

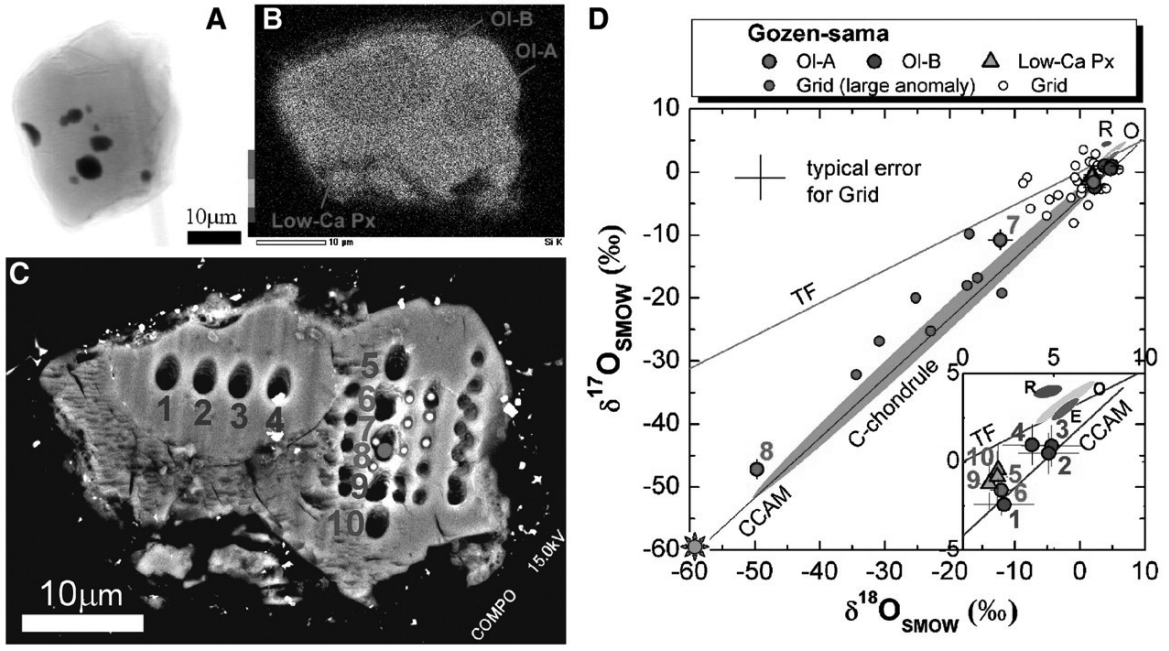

FIG. 2-38. Cross-section of a particle from comet Wild 2. **(A)** Transmitted X-ray image showing inclusions of Fe-Ni metal. **(B)** X-ray map of Si showing two olivine grains within low Ca pyroxene (rotated 90° from A). **(C)** BSE image of (B) showing ten 2-μm diameter analysis pits and 36 1-μm pits. **(D)** Values of $\delta^{18}O$ vs. $\delta^{17}O$ for 2 μm pits (large dots) and 1 μm pits (small dots) measured at WiscSIMS. Values of $\delta^{18}O$ and $\delta^{17}O$ from 2 μm pits are precise at ±1.3‰ (2 SD) and smaller pits are ±4.1‰. The star at lower left shows the composition of the Sun (McKeegan *et al.* 2008) (from Nakamura *et al.* 2008).

& Humayun 2003). This conclusion is consistent with evidence from other meteorites, found in Antarctic ice (CM Chondrites), that have been demonstrated to contain terrestrial carbonates (Tyra *et al.* 2007) and measurements showing that much of the organic matter in ALH84001 is of terrestrial origin (Jull *et al.* 1998). If the carbonates in ALH84001 are terrestrial, this would disprove any link to extraterrestrial life and this possibility has been tested by SIMS analysis.

Several ion microprobe studies of carbonates in ALH84001 have shown that the rosettes are zoned by *ca*. 25‰ in $\delta^{18}O$, and that $\delta^{18}O$ correlates to X(Mg) of the carbonate (Valley *et al.* 1997, Leshin *et al.* 1998, Eiler *et al.* 2002, Saxton *et al.* 1998, Holland *et al.* 2005). In contrast, phosphates in this meteorite are relatively constant with $\delta^{18}O$ = 3 to 6‰ (Greenwood *et al.* 2003). Eiler *et al.* (2002) showed that a second type of carbonate (clots) can be distinguished from the rosettes in this meteorite based on textures, chemical composition and $\delta^{18}O$. They proposed that rosettes formed at low temperatures (<180°C) and that the clots are shock-melted rosettes.

Analysis of $\delta^{18}O$ alone cannot rule out terrestrial contamination for some component of the carbonates in ALH84001, which are complexly zoned, fractured, and formed at different times. However, analysis of oxygen three-isotopes in the different generations of carbonate can resolve this issue because of the distinctive difference in $\Delta^{17}O$ of Earth *vs*. Mars. Ion microprobe analysis shows that both the carbonate rosettes and clots have $\Delta^{17}O$ ~0.8‰ (Fig. 2-39, Valley *et al.* 2007), confirming analysis of bulk carbonate powder that shows $\Delta^{17}O$ = 0.8 (Farquhar *et al.* 1998) *vs*. 0.32‰ for host orthopyroxene (Clayton & Mayeda 1996, Franchi *et al.* 1999, Spicuzza *et al.* 2007). Taken together, these results prove that all of the major generations of carbonate in ALH84001 are extraterrestrial in genesis and come from the same planet. Furthermore, the difference in $\Delta^{17}O$ (0.8 for carbonate *vs*. 0.3‰ for bulk silicate Mars) shows that the carbonates were not in oxygen isotope equilibrium with the silicate crust of Mars (Farquhar *et al.* 1998). On Earth, the atmosphere and crust actively exchange oxygen (and have similar $\Delta^{17}O$) via the oceans and ocean ridge hydrothermal processes, but in the absence of tectonics and an ocean, such exchange does not happen on Mars.

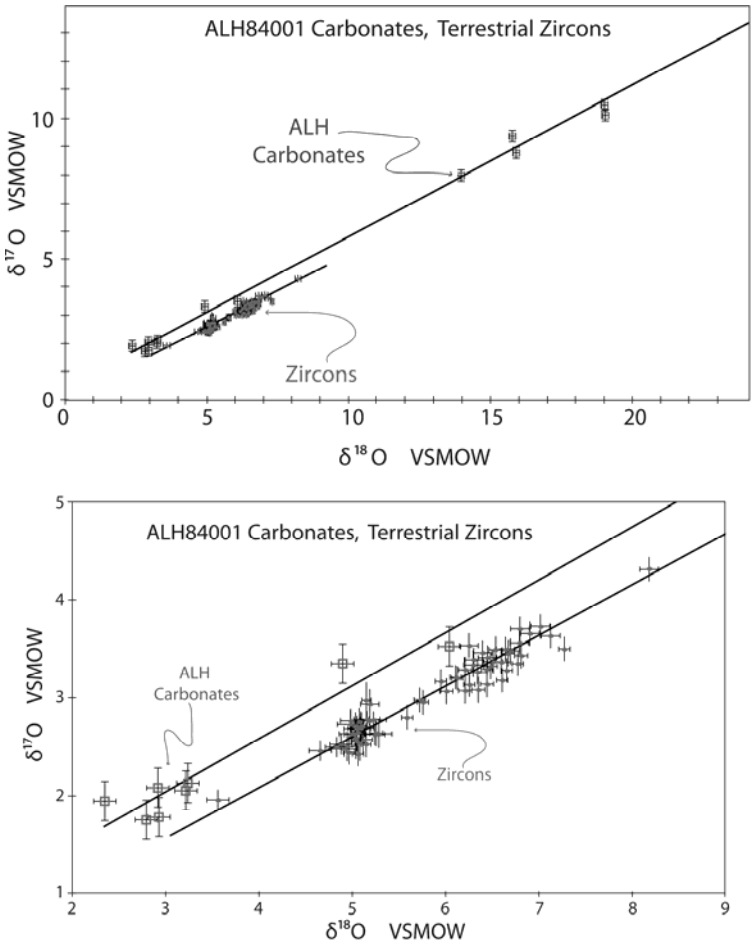

*FIG. 2-39. *In situ* oxygen three-isotope analyses of carbonates from the Martian meteorite, ALH84001, and terrestrial zircon by ion microprobe. Both data sets plot on mass-dependent fractionation lines, but all components of the ALH carbonates are offset at $\Delta^{17}O \approx 0.8‰$ (Valley *et al.* 2007), relative to Earth ($\Delta^{17}O = 0‰$) proving a non-terrestrial origin and suggesting exchange with an atmosphere on Mars that was not equilibrated with the Martian silicate crust (Farquhar *et al.* 1998). The terrestrial zircon analyses show no resolvable difference in $\Delta^{17}O$ between ~0.1 Ga mantle megacrysts from kimberlite and 4.4 to 4 Ga detrital zircon. Color available at http://www.mineralogicalassociation.ca/index.php?p=160

WHAT NEXT?

The past decade has seen dramatic improvements in instrumentation for *in situ* isotope analysis and new studies are just starting to appear that employ these tools. This paper reviews progress for just one element, oxygen, the most common element in the crust and the most heavily studied stable isotope system. We think that some of the lessons learned in oxygen isotope studies will be useful in development of other isotope systems. The quality of analytical results can depend on attention to detail. Experimental and theoretical calibrations of equilibrium fractionation factors and of the kinetics of isotope exchange are critical to interpretation of natural data. *In situ* analysis can aid in interpreting experimental products and also creates greater need for new experiments, especially of diffusion rates and reaction kinetics. *In situ* analysis also creates new demand for homogeneous standards of minerals, glasses, and compounds.

In coming years, the ion microprobe will be applied in many new areas and to reevaluate classic studies. Already, some conventional wisdom has been changed; but will the ion microprobe become the analytical tool of choice? We think the answer is: sometimes. The "conventional" and "*in situ*" techniques are complimentary. The better accuracy and precision of conventional gas source mass spectrometers will always be important for large homogeneous materials. In some situations, even with a heterogeneous sample, a single average composition is most useful. Likewise, the cost and complexity of operating an ion microprobe is a factor. Some *in situ* studies will show that materials are homogeneous and nothing new is to be learned at high magnification. Such materials will likely continue to be analyzed at the millimetre scale. However for other studies, including many reviewed here, the ion microprobe reveals new information leading to fundamental insights that could not be obtained in any other way. There is no end in sight for the fun and excitement of these studies.

ACKNOWLEDGEMENTS

The authors thank J. Bowman, A. Cavosie, A. Crowell, B. Fu, C. Grimes, P. Heck, J. Huberty, R. Kozdon, P. Lancaster, D. Moser, I. Orland, F. Z. Page, W. Peck, B. Rusk, M. Spicuzza, S. Wilde, and T. Ushikubo for helpful conversations, and use of unpublished or in press data and figures. M. Diman and A. Valley assisted in drafting, and M. Spicuzza aided in preparation of this manuscript. We also thank A. Cavosie, D. Cole, R. Kozdon, D. Miller, K. Muehlenbachs, I. Orland, F. Z. Page for helpful reviews of this paper, and M. Fayek for editing this volume. WiscSIMS is partly supported by NSF-EAR (0319230, 0744079), DOE (93ER14389), and the NASA Astrobiology Institute.

REFERENCES

AGUE, J.J. (2007): Models of permeability contrasts in subduction zone mélange: Implications for gradients in fluid fluxes, Syros and Tinos Islands, Greece. *Chem. Geol*. **239**, 217-227.

ALÉON, J., CHAUSSIDON, M., MARTY, B., SCHUTZ, L. & JAENICKE, R. (2002): Oxygen isotopes in single micrometer-sized quartz grains: Tracing the source of Saharan dust over long-distance atmospheric transport. *Geochim. Cosmochim. Acta* **66**, 3351-3365.

ALEXANDRE, A., BASILE-DOELSCH, I., SONZOGNI, C., SYLVESTRE, F., PARRON, C., MEUNIER, J.-D. & COLIN, F. (2006): Oxygen isotope analyses of fine silica grains using laser-extraction technique: Comparison with oxygen isotope data obtained from ion microprobe analyses and application to quartzite and silcrete cement investigation. *Geochim. Cosmochim. Acta* **70**, 2827-2835.

ALLAN, M.M. & YARDLEY, B.W.D. (2007): Tracking meteoric infiltration into a magmatic-hydrothermal system: A cathodoluminescence, oxygen isotope and trace element study of quartz from Mt. Leyshon, Australia. *Chem. Geol*. **240**, 343-360.

AMBROSE, S. & KATZENBERG, M.A. (*eds*.) (2000): Biogeochemical Approaches to Paleodietary Analysis. Adv in Archaeol. and Mus. Sci. **5**, Kluwer Academic, New York.

APPLEBY, S.K., GRAHAM, C.M., GILLESPIE, M.R., HINTON, R.W. & OLIVER, G.J.H. (2008): A cryptic record of magma mixing in diorites revealed by high-precision SIMS oxygen isotope analysis of zircons. *Earth Planet. Sci. Lett*. **269**, 105-117.

ARNOLD, B.W., BAHR, J.M. & FANTUCCI, R. (1996): Paleohydrogeology of the Upper Mississippi Valley zinc-lead district. *In* Carbonate-hosted Lead-zinc Deposits (D. Sangster, *ed*.). Soc. Econ. Geol. **4**, pp. 378-389.

AYERS, J.C., LOFLIN, M., MILLER, C.F., BARTON, M.D. & COATH, C.D. (2006): In situ oxygen isotope analysis of monazite as a monitor of fluid infiltration during contact metamorphism: Birch Creek Pluton aureole, White Mountains, eastern California. *Geology*, **34**, 653-656.

BAO, H., THIEMENS, M.H., FARQUHAR, J., CAMPBELL, D.A., LEE, C.C., HEINE, K. & LOOPE, D.B. (2000): Anomalous ^{17}O compositions in massive sulphate deposits on the Earth. *Nature* **406**, 176-178.

BAR-MATTHEWS, M., AYALON, A., GILMOUR, M., MATTHEWS, A. & HAWKESWORTH, C.J. (2003): Sea-land oxygen isotopic relationships from planktonic foraminifera and speleothems in the Eastern Mediterranean region and their implication for paleorainfall during interglacial intervals. *Geochim. Cosmochim. Acta* **67,** 3181-3199.

BAUMGARTNER, L.P. & VALLEY, J.W. (2001): Stable Isotope Transport and Contact Metamorphic Fluid Flow: *In* Stable Isotope Geochemistry, *Rev. Min. & Geochem*. (J.W. Valley & D.R. Cole, *eds*.) **43**, 415-468.

BICKFORD, M.E., MCLELLAND, J.M., SELLECK, B.W., HILL, B.M. & HEUMANN, M.J. (2008): Timing of anatexis in the eastern Adirondack Highlands: Implications for tectonic evolution during *ca*. 1050 Ma Ottawan orogenesis. *Geol. Soc. Am. Bull.* **120**, 950-961.

BINDEMAN, I.N. & VALLEY, J.W. (2001): Low $\delta^{18}O$ rhyolites from Yellowstone: magmatic evolution based on analysis of zircons and individual phenocrysts. *J. Petrol*. **42**,1491-1517.

BINDEMAN, I.N. & VALLEY, J.W. (2002): Oxygen isotope study of the Long Valley magma system, California: isotope thermometry and convection in large silicic magma bodies. *Contr. Min. Petrol*. **144**, 185-205.

BINDEMAN, I.N., FU, B., KITA, N.T. & VALLEY, J.W. (2008): Origin and evolution of silicic magmatism at Yellowstone based on ion microprobe analysis of isotopically zoned zircons. *J. Petrol*. **49**, 163-193.

BLAMART, D., ROLLION-BARD, C., CUIF, J.-P. & JUILLET-LECLERC, A., LUTRINGER, A., VAN WEERING, T.C.E. & HENRIET, J.-P. (2006): C and O isotopes in a deep-sea coral (*Lophelia pertusa*) related to skeletal microstructure. *In* Cold-water corals and ecosystems (A. Freiwald & J.M. Roberts, *eds*.) Springer, 1005-1020.

BOLHAR, R., WEAVER, S.D., WHITEHOUSE, M.J., PALIN, J.M., WOODHEAD, J.D. & COLE, J.W. (2008): Sources and evolution of arc magmas inferred from coupled O and Hf isotope systematics of plutonic zircons from the Cretaceous Separation Point Suite (New Zealand). *Earth Planet. Sci. Lett*. **268**, 312-324.

BOOTH, A.L., KOLODNY, Y., CHAMBERLAIN, C.P., MCWILLIAMS, M., SCHMITT, A.K. & WOODEN, J. (2005): Oxygen isotopic composition and U-Pb discordance in zircon. *Geochim. Cosmochim. Acta* **69**, 4895-4905.

BOUVIER, A.-S., MÉTRICH, N., DELOULE, E. (2008) Slab-derived Fluids in Magma Sources of St-Vincent (Lesser Antilles Arc): Volatile and Light Element Imprints, *J. Petrol*. **49**, 8, 1427-1448.

BOWMAN J.R., VALLEY J.W. & KITA N.T. (2009): Mechanisms of oxygen isotopic exchange and isotopic evolution of $^{18}O/^{16}O$-depleted periclase zone marbles in the Alta aureole, Utah: Insights from ion microprobe analysis of calcite. *Contr. Min. Petrol.* **157**, 77-93.

BREECKER, D.O. & SHARP, D.Z. (2007): A monazite oxygen isotope thermometer. *Am. Mineral*. **92**, 1561-1572.

CAMPANA, S.E. (1999): Chemistry and composition of fish otoliths: pathways, mechanisms, and applications. *Mar. Ecol. Prog. Ser*. **188**, 263–297.

CATES, N.L. & MOJZSIS, S.J. (2006): Chemical and isotopic evidence for widespread Eoarchean metasedimentary enclaves in southern West Greenland. *Geochim. Cosmochim. Acta* **70**, 4229-4257.

CATHEY, H.E., NASH, B.P., VALLEY, J.W., KITA, N.T., USHIKUBO, T. & SPICUZZA, M.J. (2007): Pervasive and persistent large-volume, low $\delta^{18}O$ silicic magma generation at the Yellowstone hotspot: 12.7- 10.5 Ma: Ion microprobe analysis of zircons in the Cougar Point tuff. *Eos Trans. AGU*, **88**(52) Fall Meet. Suppl., Abstract V51C-0708.

CAVOSIE, A.J., KITA, N.T. & VALLEY, J.W. (2009): Magmatic zircons from the Mid-Atlantic Ridge: Primitive oxygen isotope signature. *Am. Mineral*. (in press).

CAVOSIE, A.J., VALLEY, J.W. & WILDE, S.A. (2005): Magmatic $\delta^{18}O$ in 4400-3900 Ma detrital zircons: A record of the alteration and recycling of crust in the Early Archean. *Earth Plan. Sci. Lett*. **235**, 663-681.

CAVOSIE, A.J., VALLEY, J.W. & WILDE, S.A. (2007): The oldest terrestrial mineral record: A review of 4400 to 4000 Ma detrital zircons from the Jack Hills, Western Australia. *In* Earth's Oldest Rocks. (M.J. van Kranendonk, R.H. Smithies & V.C. Bennett, eds.) *Devel. Precam. Geol*. **15**, 91-111.

CAVOSIE, A.J., VALLEY, J.W. & WILDE, S.A. (2006): Correlated microanalysis of zircon: Trace element, $\delta^{18}O$, and U-Th-Pb isotopic constraints on the igneous origin of complex >3900 Ma detrital grains. *Geochim. Cosmochim. Acta* **70**, 5601-5616.

CHAPPELL, B.W. & WHITE, J.R. (2004): Two contrasting granite types: 25 years later. *Austral. Jour. Earth Sci.* **48**, 489-499.

CHEN, Z., RICIPUTI, L.R., MORA, C.I. & FISHMAN, N.S. (2001): Regional fluid migration in the Illinois basin: Evidence from in situ oxygen isotope analysis of authigenic K-feldspar and quartz from the Mount Simon Sandstone. *Geology*. **29**, 1067-1070.

CHERNIAK, D.J. & WATSON, E.B. (2003): Diffusion in zircon. *In* Zircon. Reviews in Mineralogy & Geochemistry (J.H. Hanchar & P.W.O Hoskin, eds.) **53**, 113-144.

CLARK, I.D. & FRITZ, P. (1997): Environmental isotopes in hydrogeology. Lewis Publ., New York: 328 p.

CLAYTON, R.N. (2007): Isotopes: From Earth to the Solar System. *Annual Rev. Earth Planet. Sci*. **35**, 1-19.

CLAYTON, R.N. & MAYEDA, T.K. (1996): Oxygen isotope studies of achondrites. *Geochim. Cosmochim. Acta* **60**, 1999-2017.

CLAYTON, R.N., GROSSMAN, L. & MAYEDA, T.K. (1973): A component of primitive nuclear composition in carbonaceous meteorites. *Science* **182**, 485-488.

COLE, D.R., & CHAKRABORTY, S. (2001): Rates and mechanisms of kinetics of isotopic exchange in homogeneous and heterogeneous systems. *In* Stable Isotope Geochemistry, Rev. in Min. and Geochem. (J.W. Valley & D.R. Cole, *eds*.) **43**, 83–223.

COLE, D.R., LARSON, P.B., RICIPUTI, L.R. & MORA, C.I. (2004): Oxygen isotope zoning profiles in hydrothermally altered feldspars: Estimating the duration of water-rock interaction. *Geology* **32**, 29-32.

COOGAN, L.A., MANNING, C.E. & WILSON, R.N. (2007): Oxygen isotope evidence for short-lived high-temperature fluid flow in the lower oceanic crust at fast-spreading ridges. *Earth Planet. Sci.* **260**, 524-536.

COOK, S.J. & BOWMAN, J.R. (2000): Mineralogical evidence for fluid-rock interaction accompanying prograde contact metamorphism of siliceous dolomites: Alta Stock Aureole, Utah, USA. *Jour. of Petrology*, **41**, 739-757.

CORFU, F., HANCHAR, J.M., HOSKIN, P.W.O. & KINNY, P. (2003): Atlas of zircon textures. *In* Zircon. Reviews in Mineralogy & Geochemistry (J.H. Hanchar & P.W.O Hoskin, eds.) **53**, 469-500.

CRISS, R.R. (1999): Principles of stable isotope distribution. Oxford Press, 254p.

CROWE, D.E., RICIPUTI, L.R., BEZENEK, S. & IGNATIEV, A. (2001): Oxygen isotope and trace element zoning in hydrothermal garnets: windows into large-scale fluid-flow behavior. *Geology* **29**, 479-482.

DE GROOT, P.A., *ed*. (2004): *Handbook of stable isotope analytical techniques*. Vol. 1, Elsevier.

DESBOIS, G., INGRIN, J., KITA, N.T., VALLEY, J.W. & DELOULE, E. (2007): New constraints on metamorphic history of Adirondack diopsides (NY, USA): Al and $\delta^{18}O$ profiles. *Am. Mineral*. **93**, 453-459.

DOWNES, H., MITTLEFEHLDT, D.W., KITA, N.T. & VALLEY, J.W. (2008) Evidence from polymict ureilite meteorites for a disrupted and re-accreted single ureilite parent asteroid gardened by several distinct impactors. *Geochim. Cosmochim. Acta* **72**, 4825-4844.

EILER, J.M. (2001): Oxygen isotope variations of basaltic lavas and upper mantle rocks. *In* Stable Isotope Geochemistry, Rev. in Min. and Geochem. (J.W. Valley & D.R. Cole, eds.) **43**, 319-364.

EILER, J.M., GRAHAM, C. & VALLEY, J.W. (1997): SIMS analysis of oxygen isotopes: matrix effects in complex minerals and glasses. *Chem. Geol*. **138**, 221-244.

EILER, J.M., MCINNES, B., VALLEY, J.W., GRAHAM, C.M. & STOLPER, E.M. (1998): Oxygen isotope evidence for slab-derived fluids in the sub-arc mantle. *Nature* **393**, 777-781.

EILER, J.M., SCHIANO, P., VALLEY, J.W., KITA, N.T. & STOLPER, E.M. (2007): Oxygen-isotope and trace element constraints on the origins of silica-rich melts in the sub-arc mantle. G^3: *Geochem. Geophys. Geosyst*. **8**, #9, 21p, DOI:10.1029/2006GC001503.

EILER, J.M., VALLEY, J.W. & BAUMGARTNER, L.P. (1993): A new look at stable isotope thermometry. *Geochim. Cosmochim. Acta* **57**, 2571-2583.

EILER, J.M., VALLEY, J.W., GRAHAM, C.M. & FOURNELLE, J. (2002): Two populations of carbonate in ALH84001: Geochemical evidence for discrimination and genesis. *Geochim. Cosmochim. Acta* **66**,1285-1303.

EREZ, J. (2003); The source of ions for biomineralization in foraminifera and their implications for paleoceanographic proxies. *In* Biomineralization, Rev. in Min. and Geochem. (P.M. Dove, J.J. De Yoreo & S. Weiner, *eds*.) **54**, 115-149.

FAIRCHILD, I.J., SMITH, C.L., BAKER, A., FULLER, L., SPOTL, C., MATTEY, D. & MCDERMOTT, F. (2006): Modification and preservation of environmental signals in speleothems. *Earth Sci. Rev*. **75**, 105-153.

FARQUHAR, J., THIEMENS, M.H. & JACKSON, T. (1998): Atmosphere-surface interactions on Mars:

$D^{17}O$ measurements of carbonate from ALH 84001. *Science* **280**, 1580-1582.

FAYEK, M., HARRISON, T.M., GROVE, M., MCKEEGAN, K.D., COATH, C.D. & BOLES, J.R. (2001): *In situ* stable isotopic evidence for protracted and complex carbonate cementation in a petroleum reservoir, North Coles Levee, San Joaquin Basin, California, U.S.A. *J. Sed. Res*. **71**, 444-458.

FAYAK, M., HARRISON, T.M., EWING, R.C., GROVE, M. & COATH, C.D. (2002a): O and Pb isotopic analyses of uranium minerals by ion microprobe and U-Pb ages from the Cigar Lake deposit. *Chem. Geol*., **185**, 205-225.

FAYEK, M., RICIPUTI, L.R., MILFORD, H.E. & MATHIEN, F.J. (2002b): Sourcing turquoise using O and H isotopes. *Geol. Soc. Amer. Abstr with Prog.* **39** (6), p. 396.

FAYEK, M., UTSUNOMIYA, S., EWING, R.C., RICIPUTI, L.R. & JENSEN, K.A. (2003): Oxygen isotopic composition of nano-scale uraninite at the Oklo-Okélobondo natural fission reactors, Gabon. *Amer. Mineral*. **88**, 1583-1590.

FITZSIMONS, I.C.W., HARTE, B. & CLARK, R.M. (2000): SIMS stable isotope measurement: counting statistics and analytical precision. *Mineral. Mag*. **64**, 59-83.

FRANCHI, I.A., WRIGHT, I.P., SEXTON, A.S. & PILLINGER, C.T. (1999): The oxygen-isotopic composition of Earth and Mars. *Meterorit. Planet. Sci.* **34**, 657-661.

FU, B., PAGE F.Z., CAVOSIE, A.J., FOURNELLE, J., KITA, N.T., LACKEY, J.S., WILDE, S.A. & VALLEY, J.W. (2008): Ti-in-zircon thermometry: applications and limitations. *Contr. Min. Petrol*. **156**, 197-215.

FU B., MERNAGH T.P., KITA N.T., KEMP A.I.S., VALLEY J.W. (2009): Distinguishing magmatic zircon from hydrothermal zircon: a case study from the Gidginbung high-sulphidation Au-Ag-(Cu) deposit, SE Australia. *Chem. Geol.* **259**, 131-142. doi:10.1016/j.chemgeo.2008.10.035

GILETTI, B.J., SEMET, M.P. & YUND, R.A. (1978): Studies in diffusion: III, Oxygen and feldspars, an ion microprobe determination. *Geochim. Cosmochim. Acta* **42**, 45-57.

GIRARD, J.-P., MUNZ, I.A., JOHANSEN, J., HILL, S. & CANHAM, A. (2001): Conditions and timing of quartz cementation in Brent reservoirs, Hild Field, North Sea: constraints from fluid inclusions and SIMS oxygen isotope analysis. *Chem Geol*. **176**, 73-92.

GIULIANI, G., CHAUSSIDON, M., SCHUBNEL, H.J., PIAT, D.H., ROLLION, B.C., FRANCE-LANORD, C., GIARD, D. & RONDEAU, B. (2000): Oxygen isotopes and emerald trade routes since antiquity. *Science* **287**, 631-633.

GIULIANI, G., FALLICK, A.E., GARNIER, V., FRANCE-LANORD, C., OHNENSTETTER, D. & SCHWARZ, D. (2005): Oxygen isotope composition as a tracer for the origins of rubies and sapphires. *Geology* **33**, 249-252.

GIULIANI, G., FALLICK, A., RAKOTONDRAZAFY, M. OHNENSTETTER, D., ANDRIAMAMONJU, A., RALANTOARISON, T., RAKOTOSAMIZANANY, S., RAZANATSEHENO, M., OFFANT, Y., GARNIER, V., DUNAIGRE, C., SCHWARZ, D., MERCIER, A., RATRIMO, V. & RALISON, B. (2006): Oxygen isotope systematics of gem corundum deposits in Madagascar: relevance for their geological origin. *Mineral. Deposita* **42**, 251-270.

GNASER, H. & HUTCHEON, I.D. (1988): Preferential Emission of Lighter Isotopes in the Initial-Stage of Sputtering. *Surf. Sci.* **195**, 499-512.

GRAHAM, C.M., VALLEY, J.W., EILER, J.M. & WADA, H. (1998): Timescales and mechanisms of fluid infiltration in a marble: an ion microprobe study. *Contrib. Mineral Petrol.* **132**, 371-389.

GRAHAM, C.M., VALLEY, J.W. & WINTER, B.L. (1996): Ion microprobe analysis of $^{18}O/^{16}O$ in authigenic and detrital quartz in St. Peter sandstone, Michigan Basin and Wisconsin Arch, USA: Contrasting diagenetic histories. *Geochim. Cosmochim. Acta* **24**. 5101-5116.

GREENWOOD, J.P., BLAKE, R.E. & COATH, C.D. (2003): Ion microprobe measurements of $^{18}O/^{16}O$ ratios of phosphate minerals in the Martian meteorites ALH84001 and Los Angeles. *Geochim. Cosmochim. Acta* **67**, 2289-2298.

GRIFFITHS, H. (1998): Stable isotopes: Integration of biological ecological and geochemical processes. Bios Scientific Publishers, Oxford, UK: 438 p.

GURENKO, A.A. & CHAUSSIDON, M. (2002): Oxygen isotope variations in primitive tholeiites of Iceland: evidence from a SIMS study of glass inclusions, olivine phenocrysts and pillow rim glasses. *Earth Planet. Sci. Lett*. **205**, 63-79.

GURENKO, A.A., CHAUSSIDON, M. & SCHMINCKE, H.U. (2001): Magma ascent and contamination beneath one intraplate volcano; evidence from S and O isotopes in glass inclusions and their host clinopyroxenes from Miocene basaltic hyaloclastites southwest of Gran Canaria (Canary Islands). *Geochim. Cosmochim. Acta* **65**, 4359-4374.

HARLEY, S.L. & KELLY, N.M. (2007): The impact of zircon-garnet REE distribution on the interpretation of zircon U-Pb ages in complex high-grade terrains: an example from the Rauer Islands, East Antarctica. *Chem. Geol*., **241**, 62-87.

HARRISON, T.M., SCHMITT, A.K., MCCULLOCH, M.T. & LOVERA, O.M. (2008): Early ($\geq$4.5 Ga) formation of terrestrial crust: Lu-Hf, $\delta^{18}O$, and Ti thermometry results for Hadean zircons. *Earth Plan. Sci. Lett*. **268**, 476-486.

HAURI, E. (2002): SIMS analysis of volatiles in silicate glasses, 2: isotopes and abundances in Hawaiian melt inclusions. *Chem. Geol*. **183**, 115-141.

HAWKESWORTH, C.J. & KEMP, A.I.S. (2006a): Evolution of the continental crust. *Nature* **443**, 811-817.

HAWKESWORTH, C.J. & KEMP, A.I.S. (2006b): Using hafnium and oxygen isotopes in zircons to unravel the record of crustal evolution. *Chem. Geol*. **226**, 144–162, doi:10.1016/j.chemgeo. 2005.09.018.

HERVIG, R.L., WILLIAMS, L.B., KIRKLAND, I.K. & LONGSTAFFE, F.J. (1995): Oxygen isotope microanalyses of diagenetic quartz: possible low temperature occlusion of pores. *Geochim. Cosmochim. Acta* **59**, 2537-2543.

HERVIG, R.L., WILLIAMS, P., THOMAS, R.M., SCHAUER, S.N. & STEELE, I.M., (1992): Microanalysis of oxygen isotopes in insulators by secondary ion mass spectrometry. *Intern. J. of Mass Spectrom. and Ion Proc*. **120**, 45-63.

HINTON, R.W. (1995): Ion microprobe analysis in geology. *In* Microprobe techniques in Earth sciences. (P.J. Potts, J.J. Bowles, & S.J.B. Reed, eds.) Chapman and Hall, 235-289.

HOEFS, J. (2004): Stable Isotope Geochemistry, 5th ed. Springer, Berlin. 201pp.

HOLLAND, G., SAXTON, J.M., LYON, I.C. & TURNER, G. (2005): Negative $\delta^{18}O$ values in Allan Hills 84001 carbonate: Possible evidence for water precipitation on Mars. *Geochim. Cosmochim. Acta* **69**, 1359-1369.

HUBERTY, J.M., KITA, N.T., HECK, P.R., KOZDON, R., FOURNELLE, J.H., XU, H., VALLEY, J.W. (2009) Crystal orientation effects on bias of $\delta^{18}O$ in magnetite by SIMS. Goldsch. Conf., in press.

ICKERT, R.B., HEISS, J., WILLIAMS, I.S., IRELAND, T.R., LANC, P., SCHRAM, N., FOSTER, J.J. & CLEMENT, S.W. (2008): Determining high precision, in situ, oxygen isotope ratios with a *SHRIMP II*: Analyses of MPI-DING silicate glass reference materials and zircon from contrasting granites. *Chem. Geol*. **257**, 461-474.

IRELAND, T. (1995): Ion microprobe mass spectrometry: techniques and applications in cosmochemistry, geochemistry, and geochronology. *In* Advances in analytical geochemistry, (M. Hyman & M.W. Rowe, *eds*.). JAI Press 2, 1-118.

IRELAND, T. & WILLIAMS, I.S. (2003): Considerations in zircon geochronology by SIMS. *Rev. in Min. Geochem*. **53**, 215-242.

JAMTVEIT, B. & HERVIG, R.L. (1994): Constraints on transport and kinetics in hydrothermal systems from zoned garnet crystals. *Science* **263**, 505-508.

JOHNSON, C.M., BEARD, B.L. & ALBAREDE, F. (2004): Geochemistry of Non-traditional Stable Isotopes. *Rev. in Min. Geochem.* **55**. 454 p.

JULL, A.J.T., COURTNEY, C., JEFFREY, D.A. & BECK J.W. (1998): Isotopic evidence for a terrestrial source of organic compounds found in Martian meteorites Allan Hills 84001 and Elephant Moraine 79001. *Science* **279**, 366-369.

KELLY, J.L., FU, B., KITA, N.T. & VALLEY, J.W. (2007): Optically continuous silcrete cements of the St. Peter Sandstone: Oxygen isotope analysis by ion microprobe and laser fluorination. *Geochim. Cosmochim. Acta*. **71**, 3812-3832.

KEMP, A.I.S., HAWKESWORTH, C.J., PATERSON, B.A. & KINNY, P.D. (2006): Episodic growth and the Gondwana Supercontinent from hafnium and oxygen isotopes in zircon. *Nature*, **439**, 580–583, doi: 10.1038/nature04505.

KEMP, A.I.S., HAWKESWORTH, C.J., FOSTER, G.L., PATERSON, B.A., WOODHEAD, J.D., HERGT, J.M., GRAY, C.M. & WHITEHOUSE, M.J. (2007a): Magmatic and crustal differentiation history of granitic rocks from Hf-O isotopes in zircon. *Science,* **315**, 980-983.

KEMP, A.I.S., SHIMURA, E. & HAWKESWORTH C.J. (2007b): Linking granulites, silicic magmatism, and crustal growth in arcs: Ion microprobe (zircon) U-Pb ages from the Hidaka metamorphic belt, Japan. *Geology* **35**, 807-810.

KEMP, A.I.S., HAWKESWORTH, C.J., PATERSON, B.A., FOSTER, G.L., KINNY, P.D. & WHITEHOUSE, M.J. (2008): Exploring the plutonic-volcanic link: a zircon U-Pb, Lu-Hf, and oxygen isotope study of paired volcanic and granitic units from southeastern Australia. *Trans. Royal. Soc. Edinburgh: Earth Sci*. **97**, 337-355.

KENDALL, C. & MCDONNELL, J.J. (1998): *Isotope tracers in catchment hydrology*. Elsevier Science BV, Amsterdam: 839 p.

KITA, N.T., IKEDA, Y., TOGASHI, S., LIU, Y.Z., MORISHITA, Y. & WEISBERG, M.K., (2004): Origin of ureilites inferred from a SIMS oxygen isotopic and trace element study of clasts in the Dar al Gani 319 polymict ureilite. *Geochim. Cosmochim. Acta*, **68**, 4213-4235.

KITA, N.T., NAGAHARA, H., TACHIBANA, S. & VALLEY, J.W. (2006): The systematic oxygen isotopic variations among chondrules from the least equilibrated ordinary chondrites: New ion microprobe study. *Lun. Plan. Sci. Conf.*, **37**, abstr. #1496.

KITA, N.T., NAGAHARA, H., TACHIBANA, S., FOURNELLE, J.H. & VALLEY, J.W. (2007a): Oxygen isotopic compositions of chondrule classes in Semarkona (LL3.0): Search for ^{16}O-depleted components in chondrules. *Lunar Planet. Sci. Conf. 38*, abstr. #1791.

KITA, N.T., USHIKUBO, T., FU, B., SPICUZZA, M.J. & VALLEY, J.W. (2007b): Analytical developments on oxygen three isotope analyses using a new generation ion microprobe IMS-1280. *Lunar Planet. Sci. Conf. 38,* abstr. #1981.

KITA, N.T., KIMURA, M., USHIKUBO, T. & VALLEY, J.W. (2008): Oxygen isotope systematics of chondrules from the least equilibrated H chondrite. *Lunar Planet. Sci. Conf. 39*, Abstr. #2059.

KITA, N.T., USHIKUBO, T., FU, B. & VALLEY J.W. (2009): High precision SIMS oxygen isotope analyses and the effect of sample topography, *Chem. Geol*., doi:10.1016/j.chemgeo.2009.02.012

KOHN, M.J. & VALLEY, J.W. (1994): Oxygen Isotope Constraints on Metamorphic Fluid Flow, Townshend Dam, Vermont, USA. *Geochim. Cosmochim. Acta* **58**, 5551-5566.

KOHN, M.J., VALLEY, J.W., ELSENHEIMER, D., & SPICUZZA, M. (1993) Oxygen Isotope Zoning in Garnet and Staurolite: Evidence for Closed System Mineral Growth During Regional Metamorphism. *Amer. Mineral*. 78, 988-1001.

KOLODNY, Y., BAR-MATTHEWS, M., AYALON, A. & MCKEEGAN, K.D. (2003): A high spatial resolution δ^{18}O profile of a speleothem using an ion microprobe. *Chem. Geol*. **197,** 21–28.

KOPP, R.E. & HUMAYUN, M. (2003): Kinetic model of carbonate dissolution in Martian meteorite ALH84001. *Geochim. Cosmochim. Acta* **67**, 3247-3256.

KOZDON, R., USHIKUBO, T., KITA, N.T. & VALLEY, J.W. (2009): Intratest oxygen isotope variability in planktonic foraminifera: New insights from in situ measurements by ion microprobe. *Chem. Geol*., **258**, 327-337.

KROT, A.N., YURIMOTO, H., MCKEEGAN, K.D., LESHIN, L., CHAUSSIDON, M., LIBOUREL, G., YOSHITAKE, M., HUSS, G.R., GUAN, Y. & ZANDA, B. (2006): Oxygen isotopic compositions of chondrules: Implications for evolution of oxygen isotopic reservoirs in the inner solar nebula. *Chemie der Erde - Geochemistry* **66**, 249-276.

LACKEY, J.S., VALLEY, J.W., CHEN, J.H. & STOCKLI, D.F. (2008): Dynamic Magma Systems, Crustal Recycling, and Alteration in the Central Sierra Nevada Batholith: The Oxygen Isotope Record. *J Petrol*. Doi:10.1093/petrology/egn030, **49**,1397-1426.

LANCASTER, P.J., FU, B., PAGE, F.Z., KITA, N.T., BICKFORD, M.E., HILL, B.M., MCLELLAND, J.M.

& VALLEY, J.W. (2009): Genesis of metapelitic migmatites in the Adirondack Mts., New York, *J. Meta. Geol*. **27**, 41-54.

LESHIN, L.A., MCKEEGAN, K.D., CARPENTER, P.K. & HARVEY, R.P. (1998): Oxygen isotopic constraints on the genesis of carbonates from Martian meteorite ALH 84001. *Geochim. Cosmochim*. *Acta* **62**, 3-13.

LIU, D., WILDE, S.A, WAN, Y., WANG, S., VALLEY, J.W., KITA, N.T., DONG, C., XIE, H., YANG, C., ZHANG, Y. & GAO, L. (2009): Combined U-Pb, hafnium and oxygen isotope analysis of zircons from metaigneous rocks in the southern North China Craton reveal multiple events in the Late Mesoarchean-Early Neoarchean. *Chem. Geol*. doi:10.1016/j.chemgeo.2008.10.041

LORIN, J.C., HAVETTE, A. & SLODZIAN, G. (1981): Isotope effect in secondary ion emission. *In* SIMS III, (A. Benninghoven, J. Giber, J. László, M. Riedel, & H.W. Werner, eds). 115-123.

LÜTTGE, A., BOLTON, E.W. & RYE, D.M. (2004): A kinetic model of metamorphism: An application to siliceous dolomites, *Contr. Min. Pet*., DOI: 10.1007 / s00410-003-0520-8, **146**, 546 - 565.

LYON, I.C., SAXTON, J.M. & CORNAH, S.J. (1998): Isotopic fractionation in secondary ionization mass spectrometry: crystallographic orientation effects in magnetite. *Intl. J. Mass Spectrom. Ion Proc.* **172**, 115-122.

LYON, I.C., BURLEY, S.D., MCKEEVER, P.J., SAXTON, J.M. & MACAULAY, C. (2000): Oxygen isotope analysis of authigenic quartz in sandstones; a comparison of ion microprobe and conventional analytical techniques. *In* Quartz cementation in sandstones (R.H. Worden & S. Morad, eds.) Spec. Pub. Internatl. Assoc. Sediment. **29**, 299-316.

MAHON, K.I., HARRISON, T.M. & MCKEEGAN, K.D. (1998): The thermal and cementation histories of a sandstone petroleum reservoir, Elk Hills, California: Part 2, *In situ* oxygen and carbon isotopic results. *Chem. Geol*. **152**, 257-271.

MARCHAND, A.M.E., MACAULAY, C.I., HASZELDINE, R.S. & FALLICK, A.E. (2002): Pore water evolution in oilfield sandstones: constraints from oxygen isotope microanalyses of quartz cement. *Chem Geol*. **191**, 285-304.

MARIGA, J., RIPLEY, E.M., LI, C., MCKEEGAN, K.D., SCHMIDT, A. & GROOVE, M. (2006): Oxygen isotopic disequilibrium in plagioclase-corundum-hercynite xenoliths from the Voisey's Bay Intrusion, Labrador, Canada. *Earth Planet. Sci.* **248**, 263-275.

MARTIN, L., DUCHENE, S., DELOULE, E. & VANDER HAEGHE, O. (2006): The isotopic composition of zircon and garnet: A record of the metamorphic history of Naxos, Greece. *Lithos* **87**, 174-192.

MARTIN, L.A.J., DUCHENE, S., DELOULE, E. & VANDERHAEGHE, O. (2008): Mobility of trace elements and oxygen in zircon during metamorphism: Consequences for geochemical tracing. *Earth Planet. Sci. Lett*. **267**, 161-174.

MATTEY, D., LOWRY, D. & MACPHERSON, C. (1994): Oxygen isotope composition of mantle peridotite. *Earth and Plan. Sci. Lett.* **128**, 231-241.

MCKAY, D.S., GIBSON, E.K., THOMAS-KEPRTA, K.L., VALI, H., ROMANEK, C.S., CLEMETT, S.J., CHILLIER, X.D.F., MAECHLING, C.R. & ZARE, R.N. (1996): Search for past life on Mars: Possible relict biogenic activity in martian meteorite ALH84001. *Science* **273**, 924-930.

MCKEEGAN, K.D. (1987): Oxygen isotopes in refractory stratospheric dust particles: proof of extraterrestrial origin. *Science* **237**, 1468-1471.

MCKEEGAN, K.D. & LESHIN, L.A. (2001): Stable isotope variations in extraterrestrial materials, *In* Stable Isotope Geochemistry, Rev. in Min. and Geochem. (J.W. Valley & D.R. Cole, eds.) **43**, 279–311.

MCKEEGAN, K.D. & 46 OTHERS (2006): Isotopic compositions of cometary matter returned by Stardust. *Science* **314**, 1724-1728.

MCKEEGAN K.D., JARZEBINSKI, G., MAO, P.H., COATH, C.D., KUNIHIRO, T., WIENS, R., ALLTON, J., CALLAWAY, M., RODRIGUEZ, M. & BURNETT, D.S. (2008): A first look at oxygen in a genesis concentrator sample. *Lunar Planet. Sci. Conf.* ***39***, abstr. #2020.

MILLER, M.F. (2002): Isotopic fractionation and the quantification of ^{17}O anomalies in the oxygen three-isotope system: an appraisal and geochemical significance. *Geochim. Cosmochim. Acta* **66**, 1881-1889.

MOJZSIS, S.J., HARRISON, T.M. & PIDGEON, R.T. (2001): Oxygen-isotope evidence from ancient zircons for liquid water at the Earth's surface 4,300 Myr ago. *Nature* **409**, 178-181.

MORA, C.I., RICIPUTI, L.R. & COLE, D.R. (1999): Short-lived oxygen diffusion during hot, deep-seated meteoric alteration of anorthosite. *Science* **286**, 2323-2325.

MOSER, D.E., BOWMAN, J.R., WOODEN, J., VALLEY, J.W., MAZDAB, F. & KITA, N. (2008): Creation of a Continent recorded in zircon zoning. *Geology* **36**, 239-242.

NAKAMURA, T., NOGUCHI, T., TSUCHIYAMA, A., USHIKUBO, T., KITA, N.T., VALLEY, J.W., ZOLENSKY, M.E., KAKAZU, Y., SAKAMOTO, K., MASHIO, E, UESUGI, K. & NAKANO, T. (2008): Chondrule-like objects in short-period comet 81P/Wild 2. *Science* **321**, 1664-1667.

NEMCHIN, A.A., PIDGEON, R.T. & WHITEHOUSE, M.J. (2006): Re-evaluation of the origin and evolution of >4.2Ga zircons from the Jack Hills metasedimentary rocks. *Earth Planet. Sci. Lett*. **244**, 218-233.

NIER, A.O. (1947): A mass spectrometer for isotope and gas analysis. *Review of Sci. Instr*. **18**, 398-411.

O'NEIL, J.R. (1986) Terminology and Standards. *In* "Stable Isotope in High Temperature Geological Processes", J.W. Valley, J.R. O'Neil, & H.P. Taylor, *eds*.) *Mineral. Soc. .Am. Rev. in Mineralogy* **16**, 561-570.

O'NEIL, J.R. & CHAPPELL, B.W. (1977): Oxygen and hydrogen isotope relations in the Berridale batholith. *Jour. Geochem. Soc. London* **133**, 559-571.

ORLAND, I.J., BAR-MATTHEWS, M., KITA, N.T., AYALON, A., MATTHEWS, A. & VALLEY, J.W. (2009): Climate deterioration in the Eastern Mediterranean as revealed by ion microprobe analysis of a speleothem that grew from 2.2 to 0.9 ka in Soreq Cave, Israel. . *Quat. Res*. **71**, 27-35.

PACE, M.L, CARPENTER, S.R. COLE, J.J., COLOSO, J.J., KITCHELL, J.R., HODGSON, J.R., MIDDELBURG, J.J., PRESTON, N.D., SOLOMON, C.T. & WEIDEL, B.C. (2007): Does terrestrial organic carbon subsidize the food web in a clear-water lake? *Limnol. Oceanogr.* **52**, 2177-2189.

PAGE, F.Z., USHIKUBO, T., KITA, N.T., RICIPUTI, L.R. & VALLEY, J.W. (2007a): High precision oxygen isotope analysis of picogram samples reveals 2-μm gradients and slow diffusion in zircon. *Am. Mineral*. **92**, 1772-1775.

PAGE, F.Z., FU, B., KITA MARTIN, L., DUCHENE, S., DELOULE, E. & VANDERHAEGHE, N.T., FOURNELLE, J., SPICUZZA, M.J., SCHULZE, D.J., VILJOEN, V., BASEI, M.A.S. & VALLEY, J.W. (2007b): Zircons from kimberlites: New insights from oxygen isotopes, trace elements, and Ti in zircon thermometry. *Geochim. Cosmochim. Acta* **71**, 3887-3903.

PAGE, F.Z., KITA, N.T. & VALLEY, J.W. (2009): Ion microprobe analysis of oxygen isotopes in garnets of complex chemistry. *Chem. Geol*. (in review).

PECK, W.H., VALLEY, J.W., WILDE, S.A. & GRAHAM, C.M. (2001): Oxygen isotope ratios and rare earth elements in 3.3 to 4.4 Ga zircons: Ion microprobe evidence for high $\delta^{18}O$ continental crust and oceans in the Early Archean. *Geochim. Cosmochim. Acta* **65**, 4215-4229.

PECK, W.H., VALLEY, J.W. & GRAHAM, C.M. (2003): Slow oxygen diffusion rates in igneous zircons from metamorphic rocks. *Am. Mineral*. **88**, 1003-1014.

PIETRANIK, A.B., HAWKESWORTH, C.J., STOREY, C.D., KEMP, T.I., SIRCOMBE, K.N., WHITEHOUSE, M.J. & BLEEKER, W. (2008): Episodic, mafic crust formation from 4.5 to 2.8 Ga: New evidence from detrital zircons, Slave craton, Canada. *Geology*, **36**, 875–878, doi: 10.1130/G24861A.1.

REDDY, S.M., TIMMS, N.E., TRIMBY, P., KINNY, P.D., BUCHAN, C., BLAKE, K. (2006): Crystal plastic deformation of zircon: A defect in the assumption of chemical robustness. *Geology* **34**, 257-260.

RICIPUTI, L.R. & PATERSON, B.A. (1994): High spatial-resolution measurement of O isotope ratios in silicates and carbonates by ion microprobe. *Am. Mineral*. **79**, 1227-1230.

RICIPUTI, L.R., MACHEL, H.G. & COLE, D.R. (1994): An ion microprobe study of diagenetic carbonates in the Devonian Nisku Formation of Alberta, Canada. *Jour. Sed. Res*. **A64**, 115-127.

RICIPUTI, L.R., PATERSON, B.A. & RIPPERDAN, R.L. (1998): Measurement of light stable isotope ratios by SIMS: Matrix effects for oxygen, carbon, and sulfur isotopes in minerals. *Internl. J. Mass. Spec*. **178**, 81-112.

ROBERT, F. & CHAUSSIDON, M. (2006) A paleotemperature curve for the Precambrian oceans based on silicon isotopes in cherts. *Nature* **443**, 969- 972.

ROBINSON, M.T. & OEN, O.S. (1963): Computer Studies of the Slowing Down of Energetic Atoms in Crystals, *Phys. Rev*. **132**, 6, 2385-2398.

ROLLION-BARD, C., BLAMART, D., CUIF, J.P. & JUILLET-LECLERC, A. (2004): Microanalysis of C and O isotopes of azooxanthellate and zooxanthellate corals by ion microprobe. *Coral Reefs*, **22**, 405-415.

ROLLION-BARD, C., EREZ, J. & ZILBERMAN, T. (2008): Intra-shell oxygen isotope ratios in the benthic foraminifera genus *Amphistegina* and the influence of seawater carbonate chemistry and temperature on this ratio. *Geochim. Cosmochim. Acta* **72**, 6006-6014.

RUSK, B., HOFSTRA, A., LEACH, D., LOWERS, H., KOENIG, A., VALLEY, J.W. & KITA, N.T. (2007): Combined cathodoluminescence, oxygen isotopes, and trace element study of vein quartz from several hydrothermal ore deposits. *Geol. Soc. Amer. Abstr w prog*. **39** (6) p. 396.

SAXTON, J.M., LYON, I.C. & TURNER, G. (1998): Correlated chemical and isotopic zoning in carbonates in Martian meteorite ALH84001. *Earth Planet. Sci.* **160**, 811-822.

SCHIEBER, J., KRINSLEY, D. & RICIPUTI, L. (2000): Diagenetic origin of quartz silt in mudstones and implications for silica cycling: *Nature* **406**, 981-985.

SCHMITT, A.K. (2006): Laacher See revisited: High-spatial-resolution zircon dating indicates rapid formation of a zoned magma chamber. *Geology* **34**, 597-600.

SCHMITT, A.K. & HULEN, J.B. (2008): Buried rhyolites within the active, high-temperature Salton Sea geothermal system. *Jour. Volc. Geotherm. Res*. **178**, 708-718.

SCHMITT, A.K., MARKS, M.A.W., NESBOR, H.D. & MARKEL, G. (2007): The onset and origin of differentiated Rhine Graben volcanism based on U-Pb ages and oxygen isotopic composition of zircon. *Eur J. Mineral*. **19**, 849-857.

SCHULZE, D.J., HARTE, B., VALLEY, J.W., BRENAN, J.M. & CHANNER, D.M.R. (2003): Extreme crustal oxygen isotope signatures preserved in coesite in diamond. *Nature* **423**, 68-70.

SCHULZE, D.J., HARTE, B., VALLEY, J.W. & CHANNER, D.M.D. (2004): Evidence of subduction and crust-mantle mixing from a single diamond. *Lithos*. **77**, 349-358

SCHUHMACHER, M., FERNANDES, F. & DE CHAMBOST, E. (2004): Achieving high reproducibility isotope ratios with the Cameca IMS 1270 in the multicollection mode. *Applied Sur. Sci.* **231-232**, 878-882.

SHARP, Z. (2007): Principles of Stable Isotope Geochemistry. Prentice Hall. 344 p.

SHIMIZU, N. & HART, S.R. (1982): Applications of the ion microprobe to geochemistry and cosmochemistry. *Ann. Rev. Earth Planet. Sci*. **10**, 483-526.

SILSBEE, R.H. (1957): Focusing in Collision Problems in Solids, *J. Applied Phys*. **28**, 1246-1250.

SLODZIAN, G. (1980): Microanalyzers using secondary ion emission: advances in electronics and electron physics. *In* Advances in Electronics and Electron Physics (A. Septier ed.), *Academic Press **138***, 1-44.

SLODZIAN, G. (1982): Dependence of ionization yields upon elemental composition: isotopic variations. *In* Secondary ion mass spectrometry, (A. Benninghoven, J. Giber, J. László, M. Riedel & H.W. Werner, eds.). *SIMS III*, 115-123.

SLODZIAN, G. (2004): Challenges in localized high precision isotope analysis by SIMS. *Applied Surf. Sci***. 231-232**, 2-12.

SLODZIAN, G., CHAINTREAU, M., DENNEBOUY, R. & ROUSSE, G. (2001): Precise in situ measurements of isotopic abundances with pulse counting of sputtered ions, *Eur. J. Applied Physics* **14**, 19 – 232.

SORENSEN, S., HARLOW, G.E. & RUMBLE, D.R., III (2006): The origin of jadeitite-forming subduction-zone fluids: CL-guided SIMS

oxygen-isotope and trace-element evidence. *Am. Mineral*. **91**, 979-996.

SPICUZZA, M.J., DAY, J.M.D., TAYLOR, L.A., VALLEY, J.W. (2007): Oxygen Isotope constraints on the origin and differentiation of the Moon. *Ear. Plan. Sci. Lett.* **253**, 254-265.

TIMMS, N.E., REDDY, S.M, KINNY, P.D., MOSER, D.E., NEMCHIN, A., EVANS, K., CLARK, C., HAMILTON, P.J. (2008): The effects of crystal plastic deformation on zircon geochemical systems. *Trans. Am. Geophys. Un. Abst.* MR21C-02.

TRAIL, D., MOJZSIS, S.J., HARRISON, T.M., SCHMITT, A.K., WATSON, E.B. & YOUNG, E.D. (2007): Constraints on Hadean zircon protoliths from oxygen isotopes, Ti-thermometry, and rare earth elements. *Geochem. Geophys. Geosystems* 8:6. Doi:10.1029/2006GC001449.

TREBLE, P.C., CHAPPELL, J., GAGAN, M.K., MCKEEGAN, K.D. & HARRISON, T.M. (2005): *In situ* measurement of seasonal $\delta^{18}O$ variations and analysis of isotopic trends in a modern speleothems from Australia. *Earth Plan. Sci. Lett*. **233**, 17-32.

TREBLE, P.C., SCHMITT, A.K., EDWARDS, R.L., MCKEEGAN, K.D., HARRISON, T.M., GROVE, M., CHEN, H. & WANG, Y.J. (2007): High resolution SIMS $\delta^{18}O$ analyses of Hulu Cave speleothem at the time of Heinrich event 1. *Chem. Geol.* **238,** 197-212.

TROTTER, J.A., WILLIAMS, I.S., BARNES, C.R., LECUYER, C. & NICOLL, R.S. (2008): Did cooling oceans trigger Ordovician biodiversification? Evidence from conodont thermometry. *Science* **321**, 550-554.

TYRA, M.A., FARQUHAR, J., WING, B.A., BENEDIX, G.K., JULL, A.J.T., JACKSON, T. & THIEMENS, M.H. (2007): Terrestrial alteration of carbonate in a suite of Antarctic CM chondrites: Evidence from oxygen and carbon isotopes. *Geochim. Cosmochim. Acta* **71**, 782-795.

UNKOVICH, M.J., PATE, J., MCNEILL, A. & GIBBS, J. (2001): Stable isotope techniques in the study of biological processes and functioning of ecosystems. Kluwer, Dordrecht: 289 p.

UPTON, B.G.J., HINTON, R.W., ASPEN, P., FINCH, A. & VALLEY, J.W. (1999): Megacrysts and associated xenoliths: Evidence for migration of geochemically enriched melts in the upper mantle beneath Scotland. *J. Petrol*., **40**, 6, 935-956.

USHIKUBO, T., KITA, N.T., CAVOSIE, A.J., WILDE, S.A., RUDNICK, R.L. & VALLEY, J.W. (2008): Lithium in Jack Hills zircons: Evidence for extensive weathering of Earth's earliest crust. *Ear. Plan. Sci. Lett*. **272**, 666-676.

VALLEY, J.W. (2001): Stable isotope thermometry at high temperatures. *In* Stable Isotope Geochemistry, Rev. in Min. and Geochem. (J.W. Valley & D.R. Cole, eds.) **43**, 365-414.

VALLEY, J.W. (2003): Oxygen isotopes in zircon. *In* Zircon, Rev. in Min. and Geochem. (J.M. Hanchar & P.W.O Hoskin, eds.). **53**, 343-385.

VALLEY, J.W. & COLE, D.R. (2001): Stable isotope geochemistry. Rev. in Mineral., Vol. 43: 662 p.

VALLEY, J.W. & GRAHAM, C.M. (1991): Ion microprobe analysis of oxygen isotope ratios in metamorphic magnetite-diffusion reequilibration and implications for thermal history. *Contr. Mineral. Petrol.* **109**, 38-52.

VALLEY, J.W. & GRAHAM, C.M. (1996): Ion microprobe analysis of oxygen isotope ratios in quartz from Skye granite: healed micro-cracks, fluid flow, and hydrothermal exchange. *Contr. Mineral. Petrol.* **124**, 225-234.

VALLEY, J.W., CHIARENZELLI, J., & MCLELLAND, J.M. (1994): Oxygen Isotope Geochemistry of Zircon. *Earth. Planet. Sci. Letts.* **126**, 187-206.

VALLEY, J.W., EILER, J.M., GRAHAM, C.M., GIBSON, E.K., ROMANEK, C.S. & STOLPER, E.M. (1997): Low temperature carbonates in the Martian meteorite, ALH84001. *Science* **275**, 1633-1638.

VALLEY, J.W., GRAHAM, C.M., HARTE, B., KINNY, P. & EILER, J.M. (1998): Ion microprobe analysis of oxygen, carbon, and hydrogen isotope ratios. In: McKibben, M.A., *et al.* (eds), Soc. Econ. Geol. Rev. in Econ. Geol. 7, 73-98.

VALLEY, J.W., LACKEY, J.S., CAVOSIE, A.J., CLECHENKO, C.C., SPICUZZA, M.J., BASEI, M.A.S., BINDEMAN, I.N., FERREIRA, V.P., SIAL, A.N., KING, E.M., PECK, W.H., SINHA, A.K. & WEI, C.S. (2005): 4.4 billion years of crustal maturation: Oxygen isotopes in magmatic zircon. *Contr. Mineral. Petrol*. **150**, 561–580, doi: 10.1007/s00410-005-0025-8.

VALLEY, J.W., CAVOSIE, A.J., FU, B., PECK, W.H. & WILDE, S.A. (2006): Comment on "Heterogeneous Hadean Hafnium: Evidence of Continental Growth at 4.4 to 4.5 Ga". *Science* **312**, 1139a.

VALLEY, J.W., USHIKUBO, T. & KITA, N.T. (2007): *In situ* Analysis of Three Oxygen Isotopes and OH in ALH 84001: Further Evidence of Two Generations of Carbonates. *Lunar Planet. Sci. Conf*. **38**, abstr. #1147.

VIELZEUF, D., CHAMPENOIS M., VALLEY J.W., BRUNET F. & DEVIDAL J.L. (2005a): SIMS analysis of oxygen isotopes: Matrix effects in Fe-Mg-Ca garnets. *Chem. Geol*. **223**, 208-226.

VIELZEUF, D., VESCHAMBRE, M. & BRUNET, F. (2005b): Oxygen isotope heterogeneities and diffusion profile in composite metamorphic-magmatic garnets from the Pyrenees. *Am. Mineral.* **90**, 463-472.

WEHNER, G.K. (1956): Controlled Sputtering of Metals by Low-Energy Hg Ions, Phys. Rev. **102**, 3, 690-704.

WATSON, E.B. & BAXTER, E.F. (2007): Diffusion in solid-earth systems. *Ear. Plan. Sci. Lett.* **253**: 307-327.

WEIDEL, B.C., USHIKUBO, T., CARPENTER, S.R., KITA, N.T., COLE, J.J., KITCHELL, J.F., PACE, M.L. & VALLEY, J.W. (2007): Diary of a bluegill (*Lempomis macrochirus*): daily $\delta^{13}C$ and $\delta^{18}O$ records in otoliths by ion microprobe. *Can. J. Fish. Aquat. Sci*. **64**, 1641-1645

WHITEHOUSE, M.J. & NEMCHIN, A.A. (2009): High precision, high accuracy measurement of oxygen isotopes in a large lunar zircon by SIMS. *Chem. Geol*. **261**: 31-41.

WIECHERT, U., HALLIDAY, A.N., LEE, D.-C., SNYDER, G.A., TAYLOR, L.A. & RUMBLE, D. (2001): Oxygen isotopes and the Moon forming giant impact. *Science* **284**, 345-348.

WILDE, S.A., VALLEY, J.W., PECK, W.H. & GRAHAM, C.M. (2001): Evidence from detrital zircons for the Existence of continental crust and oceans on the Earth 4.4 Gyr ago. *Nature* **409**, 175-178.

WILDE, S.A., VALLEY, J.W., KITA, N.T., CAVOSIE, A.J. & LIU, D. (2008): SHRIMP U-Pb and CAMECA 1280 oxygen isotope results from ancient detrital zircons in the Caozhuang quartzite, Eastern Hebei, N. China Craton: Evidence for crustal reworking 3.8 Ga ago. *Am. J. Sci*. **308**, 185–199, doi: 10.2475/03.2008.01.

WILLIAMS, L.B., HERVIG, R.L. & BJORLYKKE, K.. (1997a): New evidence for the origin of quartz cements in hydrocarbon reservoirs revealed by oxygen isotope microanalyses. *Geochim. Cosmochim. Acta* **61**, 2529-2538.

WILLIAMS, L.B., HERVIG, R.L. & DUTTON, S.P. (1997b): Constraints on paleofluid compositions in the Travis Peak Formation, East Texas: evidence from microanalyses of oxygen isotopes in diagenetic quartz. *In* Basin-wide diagenetic patterns: integrated petrologic, geochemical, and hydrologic considerations. (I.P. Montanez, J.M. Gregg & K. Shelton, eds.), *SEPM* **57**, 269-279.

YUI, T.-F., WU, C.-M., LIMTRAKUN, P., SRICHARN, W. & BOONSOONG, A. (2005): Oxygen isotope studies on placer sapphire and ruby in the Chanthaburi-Trat alkali basaltic gemfield, Thailand. *Lithos* **86**, 197-211.

ZAHNLE, K.J. (2006): Earth's earliest atmosphere. *Elements* **2**, 217-222.

ZAW, K., SUTHERLAND, F.L., DELLAPASQUA, F., RYAN, C.G., YUI, T.-F., MERNAGH, T.P. & DUNCAN, D. (2006): Contrasts in gem corundum characteristics, eastern Australian basaltic fields: trace elements, fluid/melt inclusions and oxygen isotopes. *Mineral. Mag*. **70**, 669-687.

ZINNER, E. (1989): Isotopic measurements with the ion microprobe. *In* New frontiers in stable isotopic research: laser probes, ion probes, and small-sample analysis (W.C. Shanks, III & R.E. Criss, eds.), U.S. Geol. Survey. Bull. 1890, 145–162.